

AD-A106 059

PRATT AND WHITNEY AIRCRAFT GROUP WEST PALM BEACH FL 8--ETC F/O 21/5
OPTIMIZATION OF COMPRESSOR VANE AND BLEED SETTINGS.(U)

JUN 81 J E BARBEROGLIO, J O SONG

F33615-79-C-2013

UNCLASSIFIED

PWA-FR-14487

AFWAL-TR-81-2046

NL

1 of 1
200 059



END
DATE
FILMED
47-81
DTIC

18 11
AFWAL TR-81-2046

AD A106059

OPTIMIZATION OF COMPRESSOR VANE AND BLEED SETTINGS.

12
LEVEL 1

10
J. E. Garberoglio / J. O. Song / W. L. Boudreaux
Pratt & Whitney Aircraft Group
Government Products Division
West Palm Beach, Florida 33402

14 PUP-FR-1441

12 83

11 Jun 1981

PTIC
ELECTE
OCT 23 1981
D



FILE COPY

9
F2211-77-0-112
FINAL REPORT, PERIOD 15 MAY 1979 - 15 MAY 1981

10 2247 / 10 31
Approved for public release; distribution unlimited

Aero Propulsion Laboratory
Wright Aeronautical Laboratories
Air Force Systems Command
Wright-Patterson Air Force Base, Ohio 45433

242

22

NOTICE

When Government drawings, specifications, or other data are used for any purpose other than in connection with a definitely related Government procurement operation, the United States Government thereby incurs no responsibility nor any obligation whatsoever; and the fact that the government may have formulated, furnished, or in any way supplied the said drawings, specifications, or other data, is not to be regarded by implication or otherwise as in any manner licensing the holder or any other person or corporation, or conveying any rights or permission to manufacture, use, or sell any patented invention that may in any way be related thereto.

This report has been reviewed by the Office of Public Affairs (ASD/PA) and is releasable to the National Technical Information Service (NTIS). At NTIS, it will be available to the general public, including foreign nations.

This technical report has been reviewed and is approved for publication.



DR. ARTHUR J. WENNERSTROM, GS-15
Chief, Compressor Research Group



WALKER H. MITCHELL, GS-15
Chief, Technology Branch

FOR THE COMMANDER



H. I. BUSH
Acting Director
Turbine Engine Division

If your address has changed, if you wish to be removed from our mailing list, or if the addressee is no longer employed by your organization, please notify AFWAL/POTX, W-PAFB, OH 45433 to help us maintain a current mailing list.

Copies of this report should not be returned unless return is required by security considerations, contractual obligations, or notice on a specific document.

REPORT DOCUMENTATION PAGE		READ INSTRUCTIONS BEFORE COMPLETING FORM
1. Report Number AFWAL-TR 81-2046	2. Govt Accession No. AD-A106059	3. Recipient's Catalog Number
4. Title (and Subtitle) OPTIMIZATION OF COMPRESSOR VANE AND BLEED SETTINGS		5. Type of Report & Period Covered Final, May 1979 — May 1981
		6. Performing Org. Report Number FR-14487
7. Author(s) J. E. Garberoglio, J. O. Song, and W. L. Boudreaux		8. Contract or Grant Number(s) F33615-79-C-2013
9. Performing Organization Name and Address United Technologies Corporation Pratt & Whitney Aircraft Group Government Products Division P.O. Box 2691, West Palm Beach, FL 33402		10. Program Element, Project, Task Area & Work Unit Numbers Project 2307, Task S1, Work Unit 36
11. Controlling Office Name and Address Aero Propulsion Laboratory (AFWAL/POTX) AF Wright Aeronautical Laboratories, AFSC Wright-Patterson AFB, Ohio 45433		12. Report Date June 1981
		13. Number of Pages 83
14. Monitoring Agency Name & Address (if different from Controlling Office)		15. Security Class. (of this report) Unclassified
		15a. Declassification/Downgrading Schedule
16. Distribution Statement (of this Report) Approved for public release; distribution unlimited.		
17. Distribution Statement (of the abstract entered in Block 20, if different from Report)		
18. Supplementary Notes		
19. Key Words (Continue on reverse side if necessary and identify by block number) Compressor Optimization Adiabatic Efficiency Optimization Methods Stall Variable Stators Variable Bleed		
20. Abstract (Continue on reverse side if necessary and identify by block number) This report evaluates optimization methods for their effectiveness in relating multistage axial compressor test data to the decision to vary a selected vane or bleed to reach a predetermined performance goal. Compressor simulations were used in a comparative evaluation and each method was judged on the basis of the number of tests required to achieve an optimum performance goal. The influence of measurement errors and finite vane travel were also prime considerations. Based on this evaluation, the COPES/CONMIN approximate optimization technique was chosen most suitable.		

FOREWORD

The Pratt & Whitney Aircraft Government Products Division of the United Technologies Corporation has prepared this final report in compliance with Sequence No. 2 of the Contract Data Requirements List attached to Contract F33615-79-C-2013, "Research on Software for Optimization of Vane and Bleed Settings In Multistage Axial Compressors."

The work reported herein was performed during the period from 15 May 1979 through 15 May 1981. This work is identified with Air Force Project Number 2307, Task S1, Work Unit 36. Captain Efren Strain is the Air Force Program Manager.

The authors wish to thank Professor G. N. Vanderplaats of the U. S. Naval Postgraduate School for helpful discussions on the approximate optimization method included in this report.

Accession For	
NTIS GRA&I	<input checked="checked" type="checkbox"/>
DTIC TAB	<input type="checkbox"/>
Unannounced	<input type="checkbox"/>
Justification	
By	
Distribution/	
Availability Codes	
and/or	
Dist	Special
A	

TABLE OF CONTENTS

<i>Section</i>	<i>Page</i>
I INTRODUCTION.....	1
II BACKGROUND OF THE PROBLEM.....	2
III OPTIMIZATION GOALS.....	6
1. Performance Goals.....	6
2. Aeromechanical Constraints.....	11
3. Overall Decision Logic.....	11
IV COMPRESSOR OPTIMIZATION METHODS.....	22
V LOCAL UNCONSTRAINED OPTIMIZATION TECHNIQUES.....	24
1. Multivariate Search Algorithms.....	24
2. Multivariate Search Specifics.....	26
3. Evaluation of Multivariate Search Algorithms.....	30
4. Practical Implementation.....	34
VI LOCAL CONSTRAINED OPTIMIZATION TECHNIQUES.....	42
VII GLOBAL OPTIMIZATION METHODS.....	46
1. Aird Method.....	46
2. Box-Wilson Method.....	46
VIII COPES/CONMIN APPROXIMATE OPTIMIZATION.....	50
1. Numerical Results — Quadratic Surface.....	53
2. Numerical Results — Compressor Simulation.....	64
IX CONCLUSIONS.....	74
REFERENCES.....	75

LIST OF ILLUSTRATIONS

Figure		Page
1	Points Required for High-Speed Efficiency Optimization.....	3
2	Time Required for High-Speed Efficiency Optimization in Actual Hours....	3
3	Total Number of Points for High-Speed Surge Optimization.....	5
4	Actual Number of Hours for High-Speed Surge Optimization.....	5
5	Performance Map To Illustrate Stall Margin Definitions.....	9
6	Random Logarithmic Decrement Warning.....	13
7	Mistuning Danger.....	13
8	Example 1 Illustrating the Necessity of Closed Loop Control.....	14
9	Example 2 Illustrating the Necessity of Closed Loop Control.....	15
10	Simplified Decision Logic.....	16
11a	Detailed Decision Logic (Part 1).....	17
11b	Detailed Decision Logic (Part 2).....	18
12	Effect of Constraints on Vane Angle Selection.....	20
13	Optimization Approaches.....	22
14	The Optimization Process.....	25
15	Generation of Conjugate Directions in Powell's Algorithm.....	26
16	Multistage Compressor Calculation.....	31
17	Performance Map of Model Characteristics.....	32
18	Behavior of Hooke-Jeeves Algorithm with Starting Values of $\alpha_1 = -3.0$ Deg and $\alpha_2 = -0.5$ Deg.....	35
19	Behavior of Hooke-Jeeves Algorithm with Starting Values of $\alpha_1 = 0$ Deg and $\alpha_2 = 0$ Deg.....	36
20	Behavior of Rosenbrock Algorithm with Starting Values of $\alpha_1 = 0$ Deg and $\alpha_2 = 0$ Deg.....	37
21	Behavior of Powell Algorithm with Starting Values of $\alpha_1 = 0$ Deg and $\alpha_2 =$ 0 Deg.....	38
22	Performance of CONMIN on Constrained Optimization Goal 4.....	43

ILLUSTRATIONS (Continued)

<i>Figure</i>		<i>Page</i>
23	Performance of Constrained Optimization Goal 4 Using an Indirect Approach.....	44
24	Global Polyalgorithm Consists of a Local Optimization Scheme and a Global Search Method.....	47
25	Comparison of Points Required for High-Speed Efficiency Optimization.....	52
26	Performance of COPES/CONMIN for Constrained Optimization Using Starting Schedule A.....	54
27	Influence of Measurement Error on the Performance of COPES/CONMIN for Constrained Optimization Using Starting Schedule A.....	56
28	Performance of COPES/CONMIN for Constrained Optimization Using Starting Schedule B.....	58
29	Performance of COPES/CONMIN for Constrained Optimization Using Starting Schedule C.....	59
30	Performance of COPES/CONMIN for Unconstrained Optimization Using Starting Schedule A.....	60
31	Influence of Measurement Error on the Performance of COPES/CONMIN for Unconstrained Optimization Using Starting Schedule A.....	61
32	Performance of COPES/CONMIN for Unconstrained Optimization Using Starting Schedule B.....	62
33	Performance of COPES/CONMIN for Unconstrained Optimization Using Starting Schedule C.....	63
34	Compressor Model Performance Map.....	65
35	Efficiency and Stall Margin Variation with Variable Vane 1.....	66
36	Efficiency and Stall Margin Variation with Variable Vane 2.....	67
37	Efficiency and Stall Margin Variation with Variable Vane 3.....	68
38	Efficiency and Stall Margin Variation with Variable Vane 4.....	69

LIST OF TABLES

<i>Table</i>		<i>Page</i>
1	Matrix of Optimization Goals.....	7
2	Stall Margin Definitions.....	10
3	Structural Integrity Instrumentation.....	12
4	Comparison of Optimization Approaches.....	23
5	Evaluation of Multivariate Search Techniques (Starting Values: $\alpha_1 = -3$ deg, $\alpha_2 = -0.5$ deg).....	33
6	Evaluation of Multivariate Search Techniques (Starting Values: $\alpha_1 = 0$ deg, $\alpha_2 = 0$ deg).....	39
7	Results of Global Search Method.....	48
8	Results of a Box-Wilson Full Factorial Experiment.....	48
9	Initial Test Points — Schedule A.....	53
10	Measurement Error.....	55
11	Initial Test Points — Schedule B.....	57
12	Initial Test Points — Schedule C.....	57
13	Optimum Vane Angles When $SM \geq 0$	64
14	Summary of Optimization Examples Solved.....	70
15	Vane Travel Limits.....	71
16	Measurement Errors for Example 5.....	72

SECTION I INTRODUCTION

Gas turbine engines for jet aircraft must maintain high performance over a wide range of flight conditions. Thus, many of the components in these engines incorporate variable-geometry configurations and bleed systems to meet the requirements of changing environments. The fan and the compressor normally contain a combination of variable-vane rows and bleeds to accomplish this objective. Hence, optimization of variable vanes and bleeds or selection of the best vane and bleed schedule plays a very important role in compression system development. During initial development, most compressors are built with all vane rows variable, even though only a few rows may be variable in the final design configuration. Optimization objectives vary from configuration to configuration. However, typical examples of parameters requiring optimization include overall efficiency, surge margin, airflow, and pressure ratio.

Current optimization techniques generally consist of running a matrix of test points with various geometry settings, shutting down the test article, reviewing the interstage aerodynamics, selecting a new series of test points using engineering judgement, and further diagnostic testing. This process is very time-consuming and expensive and rarely achieves a true optimum.

Compressor test facilities are often linked to large computers for online data feedback. Experience in compressor development and system simulation indicates that utilizing a software package through a logical series of iterations could guide decisions of the test engineer and, thus, reduce the number of data points required to achieve an optimum performance goal. Ultimately, a system could conceivably be used to control the search for optimum performance. This contract effort developed a computer program (Reference 1) in FORTRAN IV language capable of guiding the optimization of vane and bleed settings in multistage axial compressors.

The technical approach to the development of software for optimization of vane and bleed settings in multistage axial compressors involved definition of optimization goals, development of the performance-seeking logic, creation of a computer program to complement the logic, and demonstration of the function of the software.

In this report, a comparative evaluation of optimization methods is presented for relating data available from a compressor test to the decision to vary a selected vane or bleed in order to reach a predetermined goal. The methods studied were:

- Fletcher-Reeves
- Powell
- Brent
- Hooke-Jeeves
- Rosenbrock
- Broyden
- Aird
- Box-Wilson
- Feasible Direction — COPES/CONMIN

Using compressor simulations, the effectiveness of the various methods was measured by the number of tests required to achieve an optimum performance goal. The influence of measurement errors and finite vane travel were also prime considerations. Based on the results of the comparative evaluations, COPES/CONMIN approximate optimization technique was selected for the optimization of vane and bleed settings in multistage axial compressors.

SECTION II BACKGROUND OF THE PROBLEM

Optimization of compressor bleeds and variable vanes is an important part of compression system development. Three basic techniques are used to optimize performance of variable-vaned compressors — interstage characteristic (phi-psi) analysis, diagnostic testing, and statistical analysis. The statistical or diagnostic optimization methods provide for greater control since they are planned before the test commences rather than during the test, thus substantially reducing downtime. In the past, P&WA has conducted studies to determine which method should be used for efficiency and surge optimization.

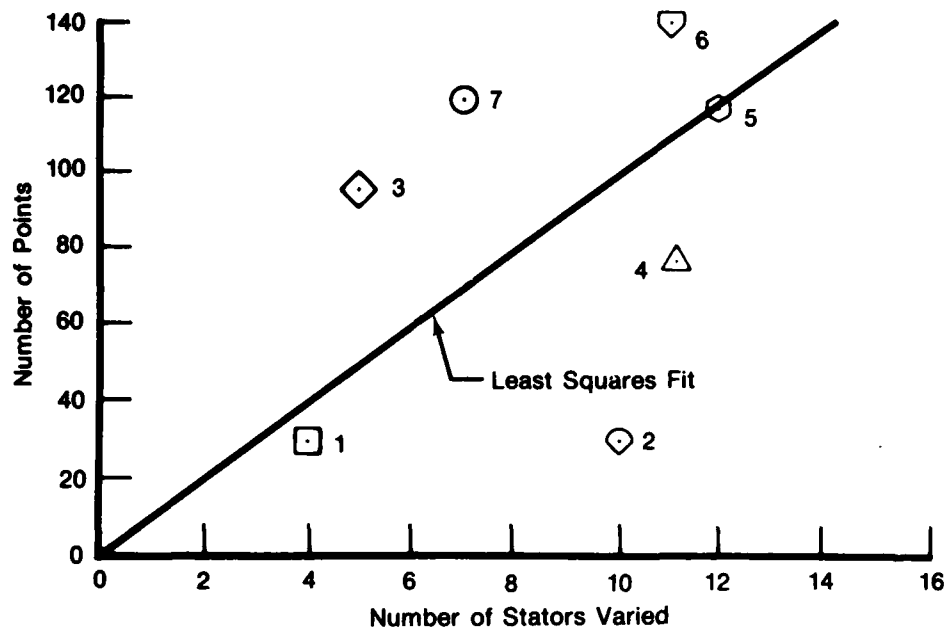
The following conclusions regarding efficiency optimization resulted:

- A statistical vane optimization matrix should be used for efficiency optimization.
- The matrix approach is significantly faster than the engineering judgement (phi-psi) approach, both in running time and downtime. (Points/hour rates for matrix acquisition are nearly three times faster than average test.)
- More information and vane changes are provided per unit time with the vane matrix.
- Follow-up points after completion of the matrix should be those recommended after statistical analysis of the matrix data.
- The optimum vane setting for efficiency from the vane matrix differs little from the optimum vane setting for surge line; the usual difference is an entire group of stages is opened or closed the same amount from the optimum efficiency schedule.

Conclusions regarding surge optimization were:

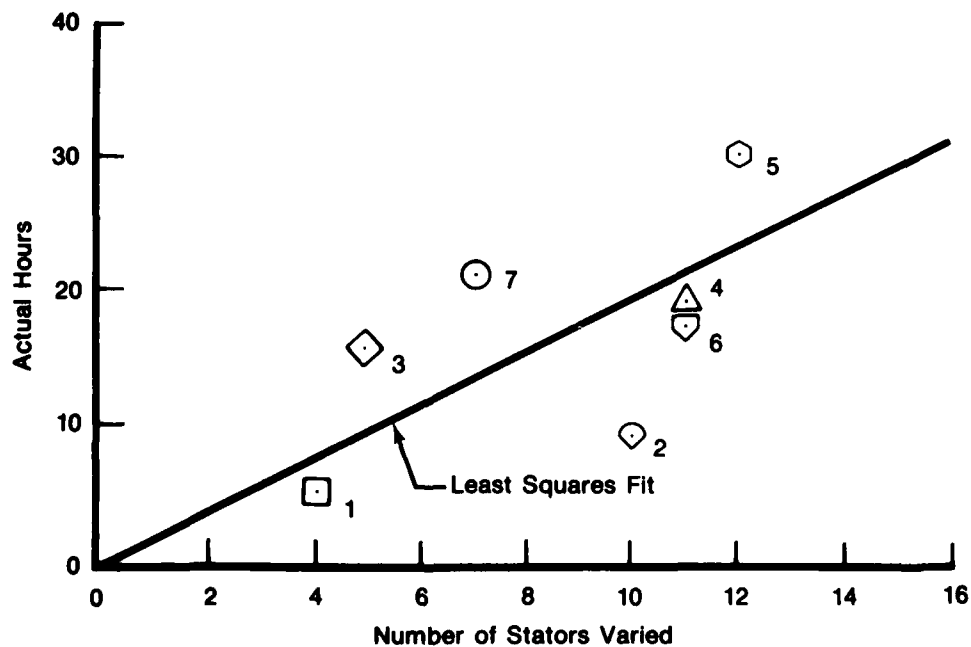
- Five-point speedlines to surge with individual vanes opened and closed, or groups of vanes if more than four stages, should be used at desired speeds.
- The individual vane (groups of vanes) approach is significantly faster than the engineering judgement approach, both in running time and downtime.
- Follow on points after completion of the surge optimization steps should be the natural result of statistical analysis, not engineering judgement (phi-psi analysis).
- Post-surge check points should be minimized unless these are a necessary part of meeting goals (e.g., effect of tip clearance on performance).
- Avoiding surge prior to efficiency optimization near the beginning of a test by running only partial speedlines is costly.

A typical test program would consist of running a matrix of data points with various geometry or bleed settings, shutting the test article down, reviewing the data, selecting a new series of test points and further testing. This process is time consuming and expensive. Figures 1 and 2 show the number of data points and run hours, respectively, required for the



FD 154179

Figure 1. Points Required for High-Speed Efficiency Optimization



FD 154180

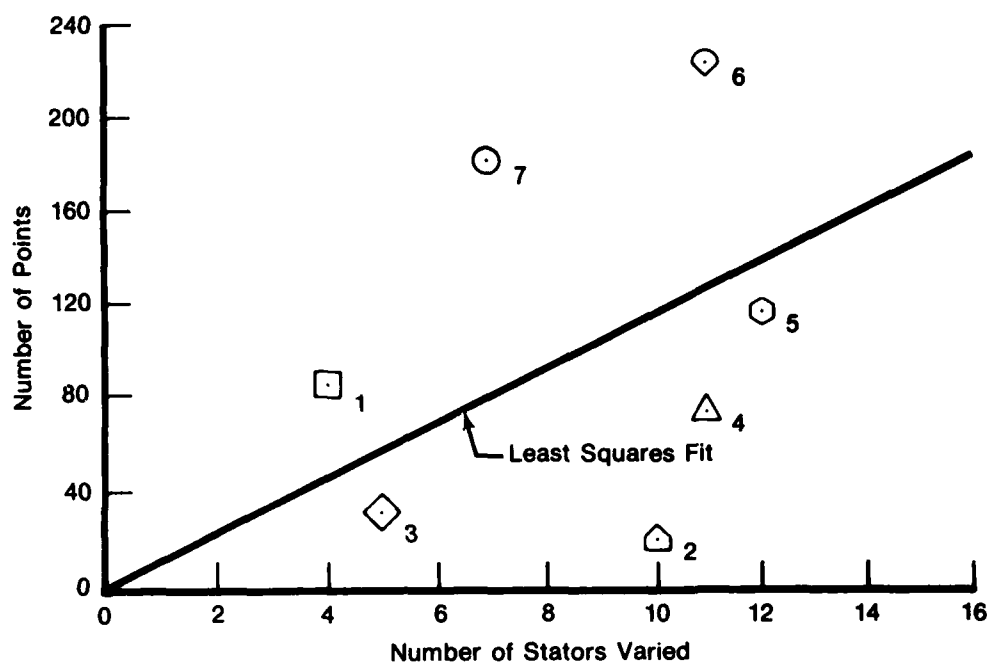
Figure 2. Time Required for High-Speed Efficiency Optimization in Actual Hours

high-speed efficiency optimization of seven compressors. As shown in figures 1 and 2, up to 140 data points and 30 hours of actual run time were required to perform the optimization when a large number of variable vane rows were present. Compressors 1 and 2 were near their goals at the start of testing and little optimization was required. Downtime for these compressors was not available but it must be kept to a minimum to reduce test costs. Experience has shown that the weekly test costs are constant whether the rig runs or not.

For surge line optimization the diagnostic approach of acquiring speed lines to surge with each vane or group of vanes opened and closed is generally used. The number of data points and run hours for typical high-speed surge line optimization are shown in figures 3 and 4. As for the efficiency optimization, a large number of data points and run hours are also required for this optimization.

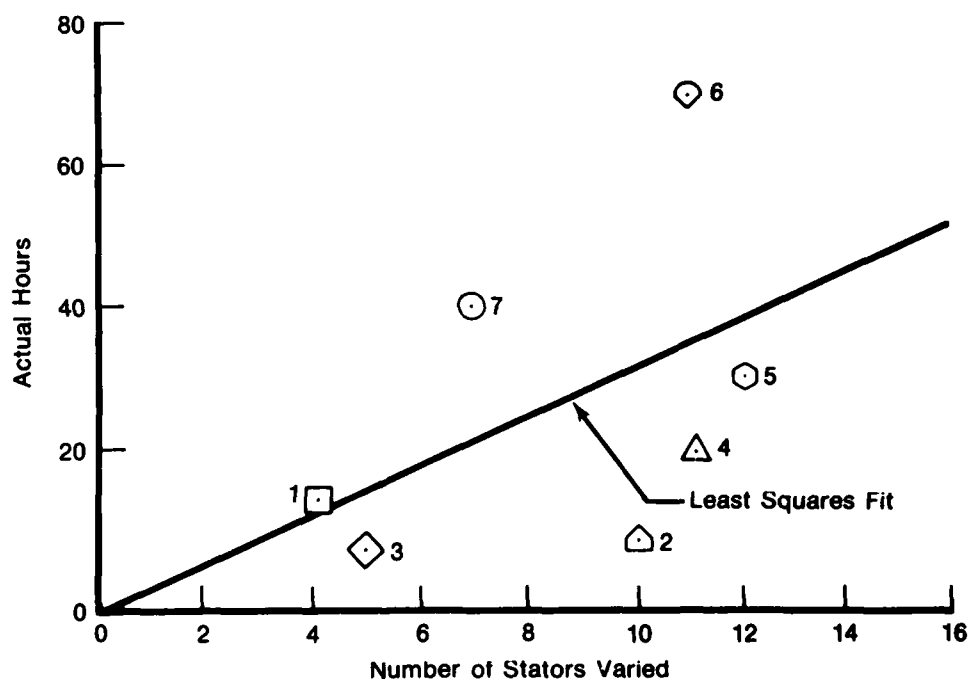
Experience in compressor development and system simulation indicates that test time and thus cost could be reduced by automating this task with a software program to guide the test engineer in searching and achieving an optimum performance goal. Initially, the test engineer would utilize the computer program in a manual mode with real time data reduction and operator-controlled adjustments. However, the long-range objective should be to achieve an optimization routine of sufficient credibility and effectiveness to allow direct computer control of the test in a feedback loop. Optimization could then proceed without operator interaction.

An automated approach using a computer search routine to perform the optimization process must address problems unique to variable-stage compressors. The optimization goal must include mechanical constraints introduced by compressor stall, stress limits, flutter, resonance and highly nonlinear operating regimes. Performance constraints of minimum surge margin and efficiency, and constant speed, pressure ratio, flow, vane angle and bleed conditions must also be defined in the optimization goal. In all cases, the optimization goal definition must rely on an approach which combines an analytical understanding of compressor design with realistic testing and experience.



FD 154181

Figure 3. Total Number of Points for High-Speed Surge Optimization



FD 154182

Figure 4. Actual Number of Hours for High-Speed Surge Optimization

SECTION III OPTIMIZATION GOALS

1. PERFORMANCE GOALS

Axial flow compressors are designed with variable vanes which influence the direction and speed of the gas flowing through the various stages of the compressor. These stators, in turn, affect the stage performance and, ultimately, the overall performance of the compressor. At important flight points, these vane settings should be optimized to provide operation at near-peak performance. The primary compressor performance goals to be considered include: maximum efficiency, maximum stall margin, maximum flow range, and maximum pressure ratio. Table 1 presents a matrix of optimization goals which may be achieved during a compressor test program. These goals are discussed in the following paragraphs.

a. Efficiency

Establishing the maximum efficiency point involves an optimization process performed by varying vane position while holding various parameters constant. The first case in the matrix of optimization goals maintains a constant speed and discharge valve setting. This is the simplest procedure because no adjustments other than vane settings are necessary. The second case maintains a constant speed and operating line, but requires readjustment of the pressure ratio to the operating line each time the vanes are reset. The third case maintains a constant flow and pressure ratio, but requires readjustment of flow and pressure ratio to a reference point for each vane setting. In addition, since speed is varied in this case, constraints on the maximum allowable speed change can be imposed.

Efficiency is calculated as a function of mass averaged temperature ratio and pressure ratio across the compressor:

$$\eta = \frac{PR^{\frac{\gamma-1}{\gamma}} - 1}{TR - 1}$$

Since the pressure ratio remains constant in the third case, efficiency may be maximized by minimizing the mass averaged temperature ratio.

A compromise vane schedule in terms of maximum efficiency and minimum acceptable stall margin may also be determined. Efficiency is determined as before. The compressor is then stalled by varying the pressure ratio while maintaining a constant speed. Transient measurements of temperature and/or pressure sense the stall initiation point. Vane angle settings may then be shifted to establish a compromise maximum efficiency with minimum acceptable stall margin.

For some optimizations where stall margin is used as a performance constraint, only a partial speedline may be needed to obtain the minimum acceptable stall margin. This control provides a less demanding program by reducing the number of stall points to be run. When the minimum stall margin has been obtained, the speed line is terminated and the discharge valve reset for the next vane angle settings.

b. Stall Margin

Establishing the maximum stall margin is similar to maximizing efficiency, except that a new stall point must be determined for each vane setting. Stall margin may also be maximized while maintaining a minimum acceptable efficiency.

Table 1. Matrix of Optimization Goals

Case No.	Goal	Optimization Condition				Aero Constraints		
		Corrected Speed	Corrected Flow	Pressure Ratio	Discharge Value	Operating Line	Stall Margin	Efficiency
1	Efficiency	Hold			Hold			
2	Efficiency	Hold				Hold		
3	Efficiency		Hold	Hold				
4	Efficiency	Hold			Hold		Input Min Value	
5	Efficiency	Hold				Hold	Input Min Value	
6	Efficiency		Hold	Hold			Input Min Value	
7	Stall Margin	Hold			Hold			
8	Stall Margin	Hold				Hold		
9	Stall Margin		Hold	Hold				
10	Stall Margin	Hold			Hold			Input Min Value
11	Stall Margin	Hold				Hold		Input Min Value
12	Stall Margin		Hold	Hold				Input Min Value
13	Stall Margin W/Bleed	Hold	Hold*					
14	Maximum Flow	Hold					Input Min Value	Input Min Value
15	Minimum Flow	Hold				Hold	Input Min Value	Input Min Value
16	Pressure Ratio	Hold	Hold				Input Min Value	Input Min Value
17	Pressure Ratio	Hold				Hold	Input Min Value	Input Min Value

*Exit corrected flow is held constant during optimizations examining bleed.

The influence of interstage bleed may also be considered in the stall margin optimization by using two or three discrete values of bleed flow for each vane setting. Optimizing the stall margin for bleed extraction, requires that the exit corrected airflow be held at the reference value without bleed. At constant speed and discrete vane angle and bleed settings, the pressure ratio is adjusted to the reference exit corrected airflow. The stall point is then established by varying the pressure ratio until the compressor stalls. The vane angles and bleed settings are then shifted until the stall margin is maximized.

Many definitions have been used for stall margin in the past. The definitions fall into two general categories: stall margin defined at constant airflow and stall margin defined at constant rotor speed. Stall margin defined at constant airflow has advantages for engine-inlet airflow matching and stability audits. Inlet distortion is a function of airflow. Engine distortion tolerance can also be expressed as a function of airflow. Consequently, the matched inlet-engine airflow passing through the interface plane can be used as the common denominator for both inlet distortion and engine distortion tolerance. If the stall line has not been defined at higher airflows than the speed line of interest by testing at higher rotor speeds, extrapolation of the stall line is required to define stall margins with non-vertical speed lines.

Stall margin defined at constant rotor speed has certain advantages for the engine manufacturer because compressor testing is carried out at constant rotor speed. Consequently, analysis of test results is easier. Also, extrapolation is not required to define surge margin at the limiting rotor speed.

Figure 5 illustrates two stall line extrapolations. In this figure, it is not intended to show that one extrapolation results in a higher stall line than the other. One stall line extrapolation uses a linear slope through the surge point. The slope may be the value obtained from the baseline test of the compressor and is input by the test engineer. The other extrapolation assumes a parabolic stall line, as shown below:

$$PR - 1 = kWc$$

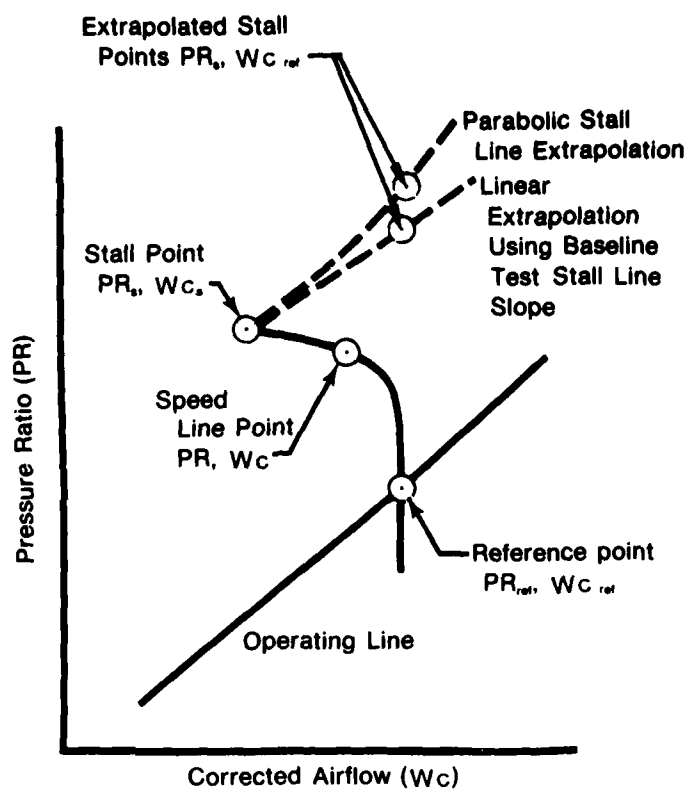
Note that this extrapolation does not require an input by the engineer. Using the nomenclature of figure 5, equations for calculation of stall margin resulting from constant speed and constant airflow definitions are given in table 2. The definitions can be applied to either inlet corrected flow or during optimizations with interstage bleed, exit corrected flow.

c. Flow Range

Varying vane angle while holding the operating line and constant speed establishes the maximum and minimum flow points to provide the maximum flow range. In addition to airflow measurements, performance constraints of minimum acceptable efficiency and stall margin also define the flow range; thus, their evaluations must be considered for each geometry setting. It should be noted that stress limits, discussed later in this report, also compromise the vane schedule in this optimization.

d. Pressure Ratio

Determination of maximum pressure ratio results from varying vane angle settings at constant speed and airflow and maintaining minimal acceptable values of efficiency and stall margin. Initially at each geometry setting, pressure ratio is adjusted to either the reference corrected flow or operating line and efficiency is calculated. The pressure ratio is then varied to achieve compressor stall and the stall margin is calculated.



FD 212384

Figure 5. Performance Map To Illustrate Stall Margin Definitions

Table 2. Stall Margin Definitions

Constant Airflow Definitions

$$SM = \frac{PR_s - PR_{ref}}{PR_{ref}} \times 100$$

$$SM = \frac{PR_s - PR_{ref}}{PR_s} \times 100$$

$$SM = \frac{PR_s - PR_{ref}}{PR_{ref} - 1} \times 100$$

Constant Speed Definitions

$$SM = \frac{(PR/Wc)_s - (PR/Wc)_{ref}}{(PR/Wc)_{ref}} \times 100$$

$$SM = \frac{(PR/Wc \sqrt{TR})_s - (PR/Wc \sqrt{TR})_{ref}}{(PR/Wc \sqrt{TR})_{ref}} \times 100$$

$$SM = \frac{(PR/Wc)_s - (PR/Wc)_{ref}}{(PR/Wc)_s} \times 100$$

$$SM = \frac{PR_s - PR_{ref}}{PR_{ref}} \times 100$$

$$SM = \frac{PR_s - PR_{ref}}{PR_s} \times 100$$

$$SM = \frac{PR_s - PR_{ref}}{PR_{ref} - 1} \times 100$$

2. AEROMECHANICAL CONSTRAINTS

While undergoing computer-guided vane and bleed schedule optimization, aeromechanical constraints must be maintained to ensure compressor integrity. Table 3 summarizes the instrumentation and data reduction that may be employed to evaluate the structural integrity of the compressor. The minimum evaluation required should consist of vibratory stresses measured from several strain-gage-instrumented airfoils located in each blade row.

Since stresses build up rapidly if flutter is encountered, a useful parameter to measure would be the logarithmic decrement of the strain gage output. This parameter which is determined from responses to random excitations senses the onset of flutter, as shown in figure 6.

Blade "mistuning" presents another area of concern because the integrity of all blades cannot be ensured with only a few airfoils in each blade row strain-gage monitored. Mistuning is the circumferential variation in mass and stiffness that results in large difference in blade-to-blade amplitude and phase response. Figure 7 illustrates the differences which could allow some blades without strain gages to operate beyond their endurance limits. Other techniques, such as photoelectric sensors or high-response pressure measurements described in table 3, would permit monitoring of the condition of all blades. Once calibrated with strain-gage data, these monitoring techniques would also provide long-term safety coverage.

In addition, maximum speed and exit temperature limits will always be necessary to ensure compressor rig safety from a steady-state loading standpoint.

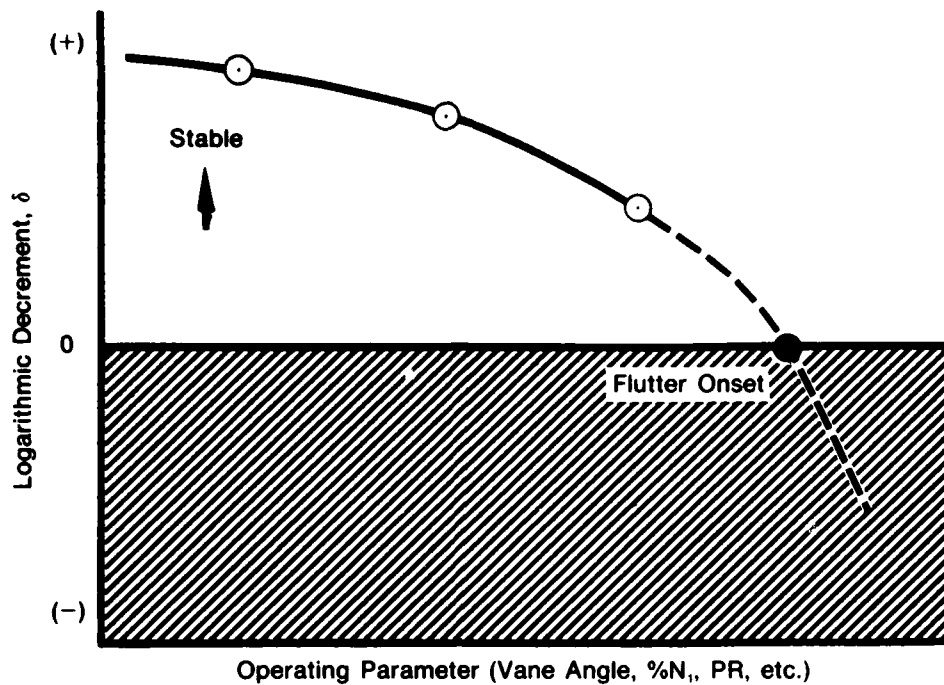
3. OVERALL DECISION LOGIC

An overall logic was formulated to allow the optimization of compressor vane and bleed settings. The function of this logic is to control the sequence of events necessary to successfully run a data point during the optimization and, in particular, defines the manner in which the constraints should be handled. The primary objective of the decision logic is to perform the optimization in the shortest possible time — the logic being developed with this in mind. A second objective identified was to minimize the complexity of the logic while still meeting all the program goals. The format selected, therefore, is a minimization algorithm operating within a simple framework of controller logic which coordinates all rig activities. This enables an optimum to be found with reduced test time and, hence, reduced cost.

Two key factors which influence the total rig test time are the number of data points taken and the time required to run each point. The selection of optimization algorithms will dictate the number of data points that must be run, while the test time for each point will depend on the mechanism designed to move the rig from point to point. Recognizing this, the recommendation is to have automatic regulation of any operating parameter, i.e., inlet corrected airflow, exit airflow, pressure ratio, operating line, and corrected rotor speed. Although the design of automatic controls is not within the scope of this program, it became evident as the decision logic developed that the logical structure depended on the availability of computer control. During normal operation, feedback control has little bearing on the decision logic, but when constraints are encountered, closed-loop control becomes mandatory to achieve a true optimum within a reasonable time.

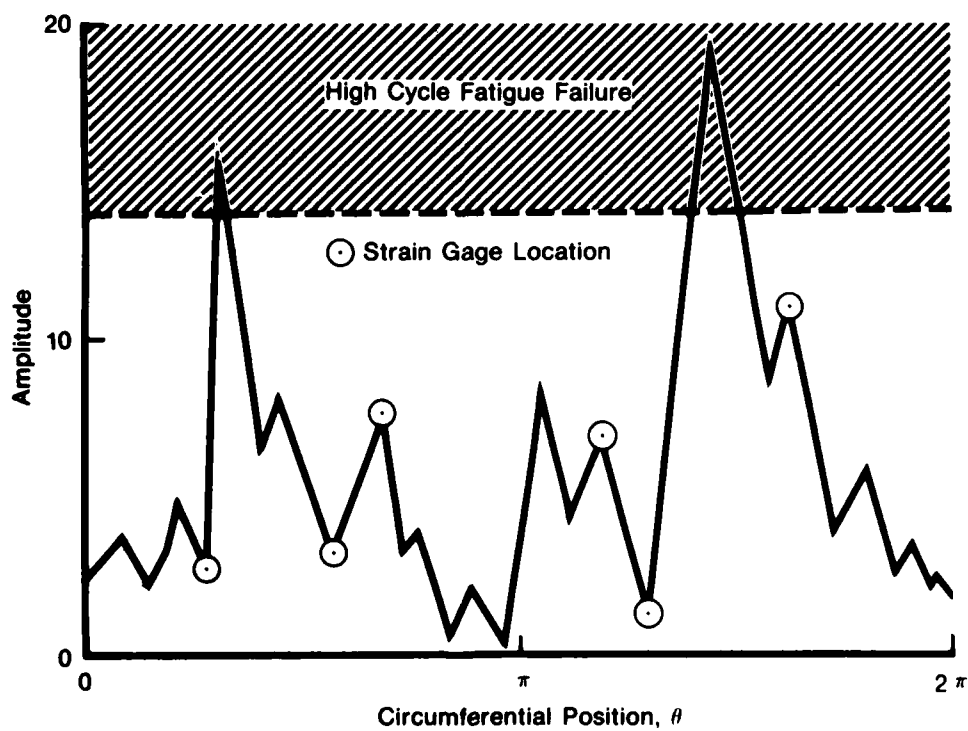
Table 3. Structural Integrity Instrumentation

Method	Flutter		Comment
	Measures	Characteristics	
Strain Gage (blade mounted)	● Vibratory Stress, $\pm \sigma$	● High Stress	● Essential
	● Frequency, Hz or nE	● Non-Integral Frequency	● Sets Operating Limit of $\pm \sigma$ as f(N,T)
	● Random Logarithmic Decrement (System damping)		● Not Durable
Photoelectric Sensors (PES) (case mounted at blade tip)			● Forewarns Flutter Onset
	● Deflection Amplitude, ϕ, h	● High ϕ, h	● Calibrated with S/G Data, Provides Durable Barometer
	● Frequency, Hz or nE (spatial)	● Non-Integral Frequency	● Monitors All Blades which protects against blade-to-blade variation (mistuning)
	● Random Logarithmic Decrement		● Forewarns Flutter Onset
	● Random Logarithmic Decrement		● Calibrated with S/G Data, Monitors Flutter, Wave Direction, Harmonic Content
Kulite Transducers 1. Case mounted at blade tip, 3 locations 2. Downstream flow field.	● Unsteady Pressure Amplitude and Frequency (spatial)	● Non-Integral Frequency	● Forewarns Flutter Onset



FD 212385

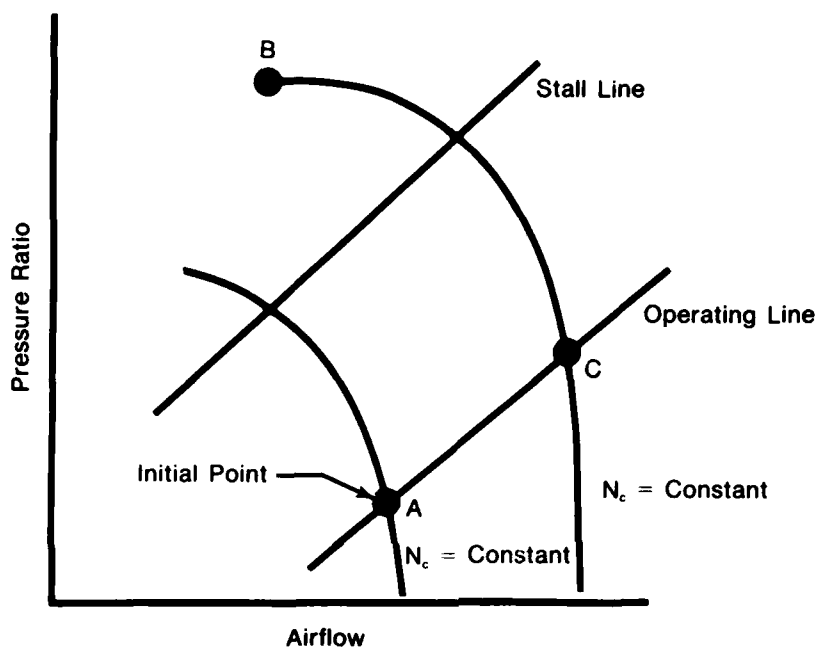
Figure 6. Random Logarithmic Decrement Warning



FD 212386

Figure 7. Mistuning Danger

To illustrate the necessity of closed-loop control, it is desired to maximize efficiency at constant speed while maintaining some prespecified operating line. Further assume that speed control is available while the operating line must be held by manually adjusting the discharge valve area. Figure 8 illustrates a compressor stall being induced as vane positions are adjusted from point A to point B. The new set of angles is rejected, while the angles chosen would have been acceptable (point C) if the compressor operating line had been held by opening the discharge valve.

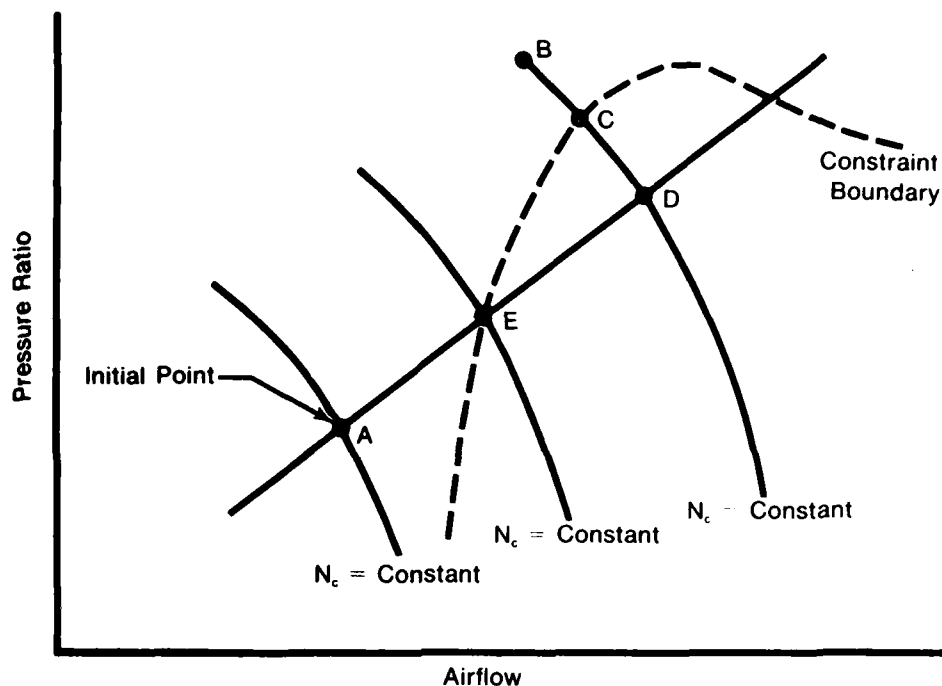


FD 212387

Figure 8. Example 1 Illustrating the Necessity of Closed Loop Control

A second example shown in figure 9 assumes for the same conditions that the requested vane angles move the match-point at constant speed from point A to point B, which is an acceptable point. As the discharge valve is opened, a constraint boundary is encountered at point C before the requested point D is reached. This point does not satisfy the specified conditions of the optimization, i.e., hold constant operating line. To reach a satisfactory point, a number of time-consuming iterations must be made, alternately adjusting the vane angles and discharge valve to get to point E on the operating line. Point E is required if boundary following and true optimization is to be realized.

The decision logic comprises four major sections, each described in turn under the headings: initialization, vane angle selection, constraint monitoring, and stall margin evaluation. Figure 10 shows the program flow in simplified form, while figure 11 shows a detailed version of the program.



FD 212388

Figure 9. Example 2 Illustrating the Necessity of Closed Loop Control

a. Initialization

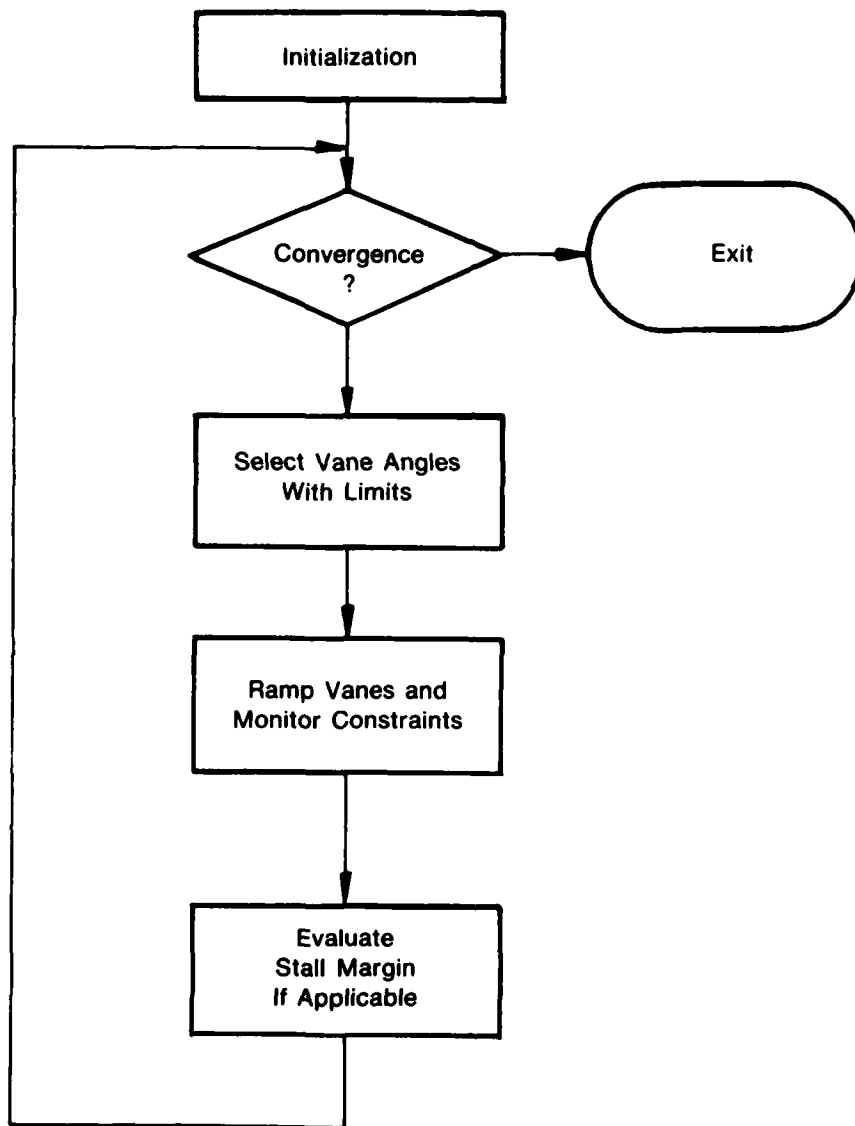
To begin the optimization, the computer prompts the operator for the following information:

- Identification number of the optimization goal
- Number of vanes to be varied
- Vane travel limits for each variable vane
- Stall margin definition
- Minimum stall margin, if applicable
- Minimum efficiency, if applicable
- Starting vane angles
- Values for operating condition, e.g., speed, pressure ratio.

The operator is then requested to select automatic control of the two operating parameters.

An appropriate performance index (PI) is defined based on the optimization goal selected. In some cases, this may be efficiency or stall margin alone, both of which are available from the facility. Other cases require an augmented PI. For example, during efficiency optimization with a minimum stall margin requirement, the PI may be $\eta + f(\text{SM})$.

The operator is now requested to run the starting point. The decision logic enters a wait loop at this stage and remains inactive until the base case has been run and the rig has reached steady state. This concludes the initialization sequence.



FD 212389

Figure 10. Simplified Decision Logic

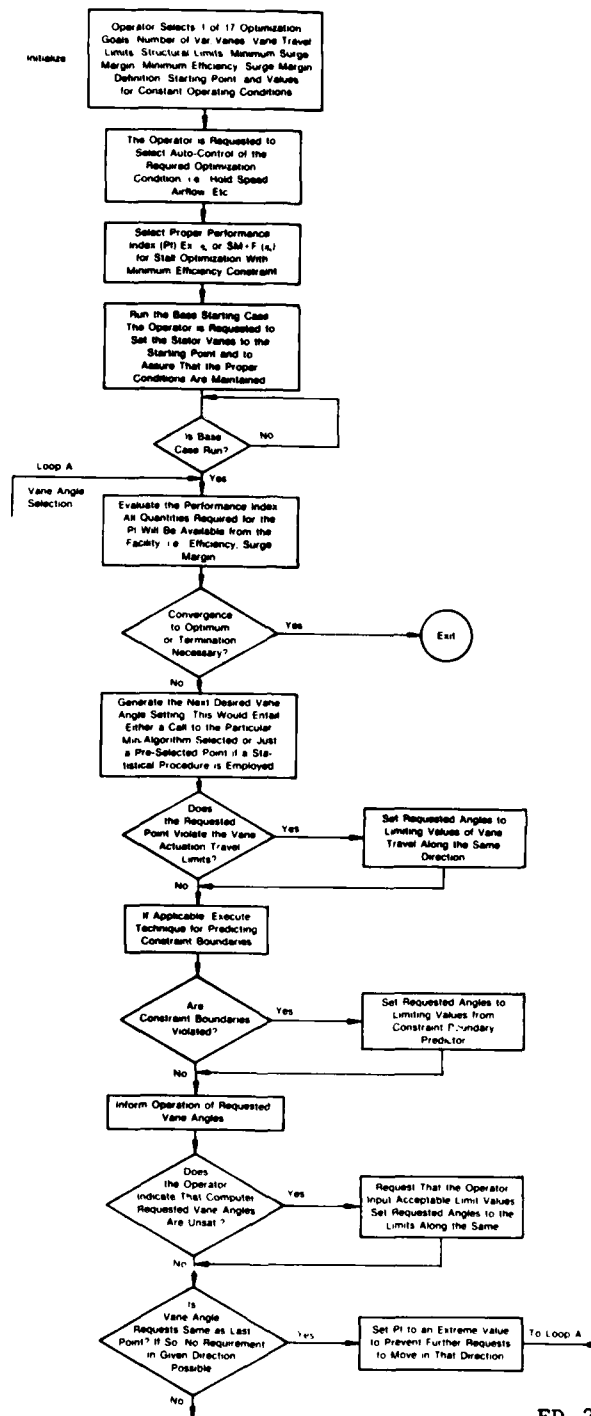
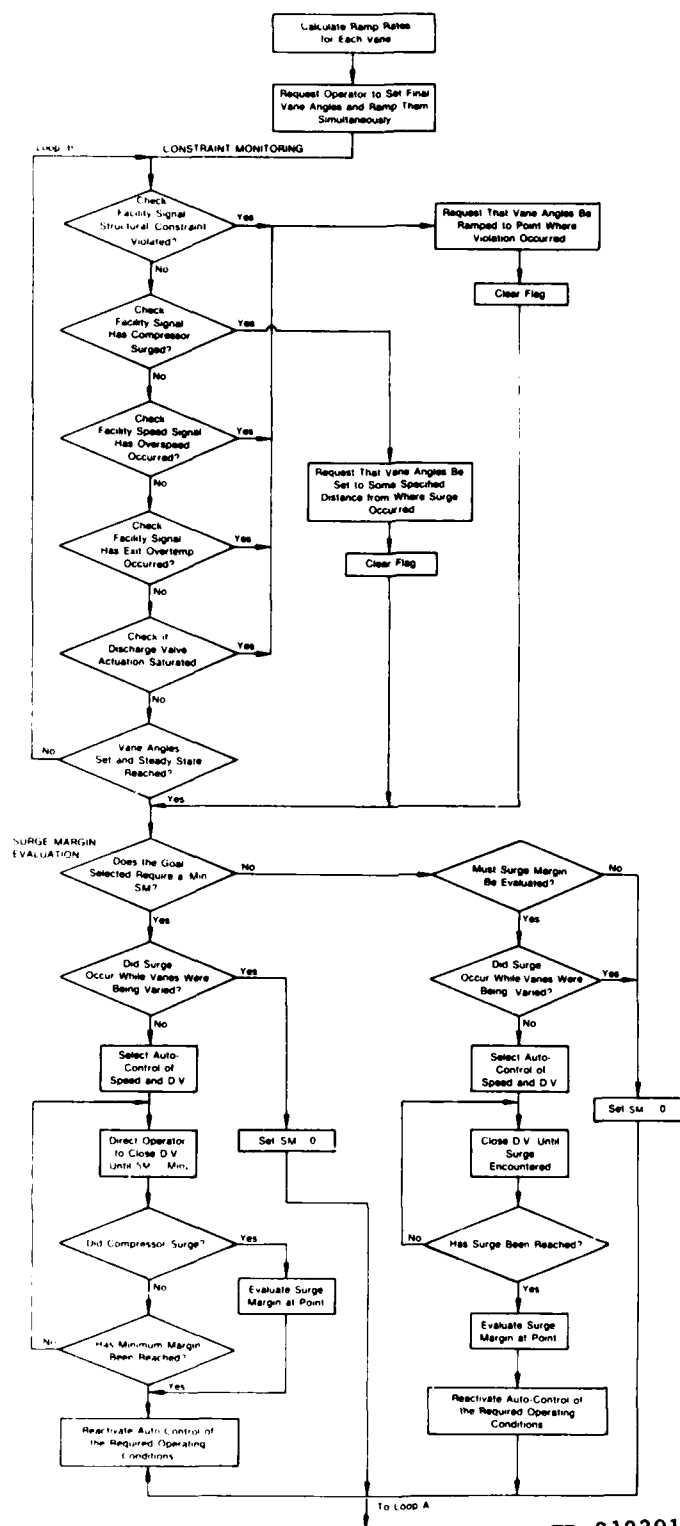


Figure 11a. Detailed Decision Logic (Part 1)



FD 212391

Figure 11b. Detailed Decision Logic (Part 2)

b. Vane Angle Selection

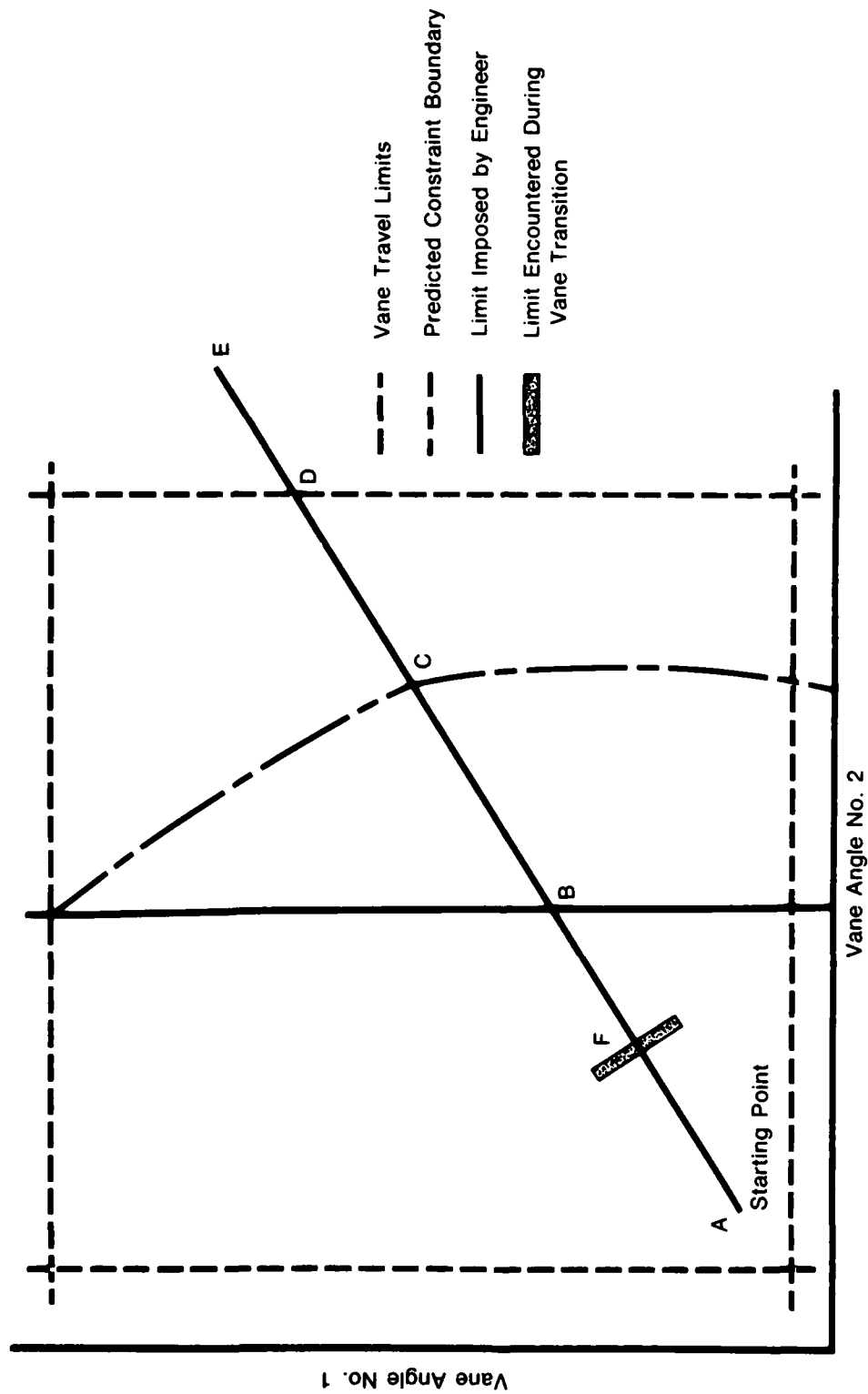
The performance index is now evaluated using the quantities available from the facility and the value is used to either generate the next set of vane settings or terminate the program, if it has converged to an optimum. If there is no reason to terminate, the optimization algorithm is called. The vane angles requested are compared with the known vane travel limits to assure that no violation occurs. An option can be invoked to further limit vane angle travel if some constraint boundaries should occur in the vane angle space. Final limitations on vane angle can be imposed interactively by the responsible engineer on the test stand. These limits are input when it is indicated that the vane settings requested are unacceptable. As an example, figure 12 shows the selection of new stator angles for the two-dimensional (two variable stators) case. The originally requested angles (E) violate the actuator travel limits so a compromise point (D) is necessary. Next, limitations are imposed by the constraint predictor (C) and then the test engineer (B). The fact that direction of travel is preserved in all cases is graphically illustrated in the picture. All constraints can be handled in this manner whether physical, structural, stall-related, or engineer-imposed. The constraint boundary can be parameterized as a function of the independent variables (vanes and bleeds) and the most stringent limit will prevail. For example, if during movement from A to B on figure 12, a structural constraint is violated at point F, this limit will be enforced. This example also supports the argument for automatic control of the operating conditions since figure 12 is plotted only for constant operating conditions. If constant conditions do not prevail, the constraint boundaries will shift.

A final function in the selection of vane angles checks if the limitations imposed will allow no movement in the search direction. When this happens, no data is taken and the PI is set to some extreme value to prevent further movement along that line. To evaluate a feasible point, the operator is requested to ramp the vanes to the specified positions. Ramp rates are calculated so that movement remains on the line in the search direction. Additionally, transition must be slow enough to allow the compressor to remain in a quasi-steady state condition, i.e., the operating conditions do not change appreciably. Ramp rate selection is based on the disturbance rejection properties (bandwidth) of the closed loop system.

c. Constraint Monitoring

During transition to a new data point, the logic continually checks signals coming from the facility to determine if any undesirable events have occurred that violate the established constraints and necessitate the pursuit of a different course of action. These signals are monitored while in Loop B, of figure 11, which is continually executed until the requested vane angles are reached and the rig settles into a steady-state condition. The facility signals are binary in nature and are specifically:

- A flag to indicate that any structural constraint has been violated. This flag is set by the facility for any aeromechanical limit reached which compromises structural integrity. Flutter, resonance, or vibratory stress limit violations encountered in any blade or row will cause this alarm signal to be set.
- A flag to indicate that the compressor has stalled, or that surge recovery has been initiated.
- A flag to indicate that an overspeed has occurred.
- A flag to indicate that compressor exit temperature limit has been violated.



FD 212392

Figure 12. Effect of Constraints on Vane Angle Selection

- A flag to indicate discharge valve actuator saturation. When this happens, the compressor rig may be in no danger, but it will not be possible to hold the operating conditions with further movement of the vanes.

When a flag is set, it is not the responsibility of the logic to initiate any type of recovery action. For instance, given that surge has occurred, the facility must respond by opening the discharge valve and stator vanes. The same rule applies for each constraint listed. At the time of violation it is essential that the current position of the stator vanes be known by monitoring feedback signals from the variable vane servomechanisms. The feasibility of determining the values of the vane angles when stall or flutter is encountered must be addressed. The quickness of response of the sensors may dictate the ramp rate during vane transition.

The action taken by the decision logic in case of a constraint violation is to request that the stator vanes be ramped to the values where the limit was hit with some margin to account for uncertainty. The appropriate flag is then cleared and execution continues in wait loop B until final values are achieved for all parameters. Exit from the loop occurs when a flip-flop is set indicating the transient phenomena has ceased.

d. Stall Margin Evaluation

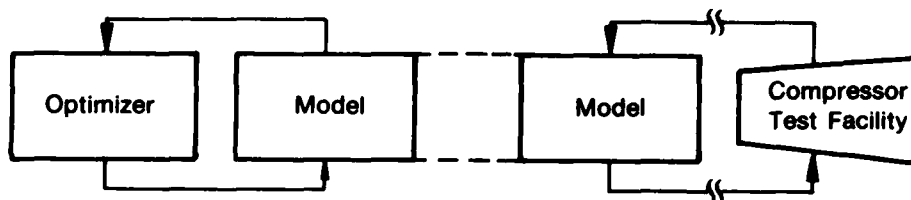
Before the current point can be completed, stall margin is evaluated, if applicable. For maximum stall margin, the discharge valve must be closed until the compressor stalls. For optimizations requiring a minimum stall margin, the discharge valve may need only be closed until minimum stall margin is verified. If the optimization goal is independent of stall margin or if stall was encountered during vane transition, this section of code is skipped. In the first case, no decision is made on stall margin and in the second, it is known that no margin is available. For the two cases where stall margin must be evaluated, the sequence of events is as follows. The operator is first requested to select control of corrected rotor speed and discharge valve area. The operator then closes the discharge valve moving the compressor toward stall. If stall margin is to be maximized, the valve should be closed until stall is actually encountered. This stall and subsequent recovery action proceeds in the normal manner for the rig. When a minimum stall margin constraint is in effect, the operator closes the valve until either minimum stall margin is verified or the rig stalls, indicating that the inequality constraint is violated. When conditions permit, the operator takes appropriate action to return to the previous point and auto-control of the operating conditions is reactivated. This concludes the evaluation of a single data point. For the next point, branch to loop A and perform an identical cycle.

The decision logic is valid for the seventeen optimization goals outlined in table 1. In addition, it is independent of the specific optimization algorithm selected to vary the vanes because it is inherently flexible in form. In the simplest case, a matrix of data points can be specified. Alternatively, any of the powerful search methods which interrogates the compressor itself can be substituted. For a more sophisticated approach, an adaptive model can be incorporated and prediction techniques utilized as analytical skills become more reliable. An advantage is thus gained since techniques can easily be substituted, if so desired.

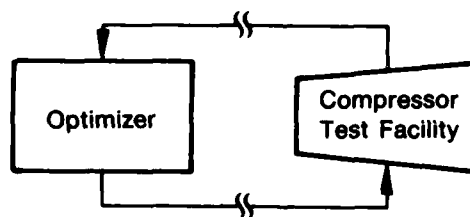
SECTION IV COMPRESSOR OPTIMIZATION METHODS

Two distinct approaches to the compressor optimization problem are possible. The first, hereafter referred to as the on-line interactive approach, is a numerical search routine varying each vane sequentially by a small amount to maximize a performance parameter. The second, referred to as the model adaptive approach, involves a method incorporating a mathematical model of compressor behavior which utilizes test data to update and fine-tune the model. A third possibility is to combine these two approaches so that the information gained during the search procedure would also be used to calibrate the compressor model.

The two primary approaches are illustrated in figure 13. In the model adaptive approach, the optimum vane and bleed setting calculator and the compressor test rig do not interact directly and the model serves as the intervening agent. In the on-line interactive approach, the optimizer communicates directly with the test rig so that an eventual improvement in the performance objective is achieved. The technical requirements for the two approaches are significantly different in that, for the former, the critical factor is the fidelity of the model and the procedures employed to calibrate this model with test data. The development of the goal-seeking logic is a secondary concern. For the interactive method, the emphasis is on the optimizing algorithm and its ability to isolate the peak-setting parameter value in spite of random variations in the measurements.



A. Model Adaptive Approach



B. On-Line Interactive

FD 158416A

Figure 13. Optimization Approaches

The two general approaches are compared in table 4. The most obvious advantage of the model adaptive approach is that a more efficient analytical optimization algorithm can be applied to the model and that the overall procedure is more test time efficient. However, the latter assertion is questionable since it is difficult to estimate how much time is involved in fine tuning the model to ensure its fidelity. In fact, it is very likely that many more test points are required to fine tune the model than are required to complete the on-line optimum search, since the interactive approach only requires an extensive sampling of the compressor performance in the vicinity of an optimum vane and bleed setting, while the modelling approach depends on a global characterization of the compressor.

Table 4. Comparison of Optimization Approaches

On-Line Interactive	Model Adaptive
<i>Advantages</i>	
<ul style="list-style-type: none"> ● Logical step towards closed loop optimization ● More adaptable to any test rig ● Can be expanded to include adaptive modeling 	<ul style="list-style-type: none"> ● Enables more efficient optimization algorithm ● Involves less test time ● Model would apply to other design activities
<i>Disadvantages</i>	
<ul style="list-style-type: none"> ● Requires more test time ● Requires noise immune search 	<ul style="list-style-type: none"> ● Requires global characterization ● Model dependent solution ● More rig specific

The obvious advantage of the on-line interactive approach is the fact that it is more suited to the closed-loop control application. This method is also more flexible in that little or no modification of the technique is required to adapt the procedure to a different rig. Alternatively, the model adaptive approach might require an extensive reworking of the compressor model to account for differences in the design of the two rigs, i.e., number of stages, bleeds, etc. The principal disadvantage of the interactive approach is that it requires a less efficient optimization algorithm that is insensitive to nonlinear phenomena and measurement uncertainties.

Based on an assessment of the problem and related experience, the most viable alternative for the optimization of vane and bleed settings of a multistage compressor is the on-line interactive approach. This approach is more flexible in that it can accommodate a variety of compressor configurations without a significant change in the procedure. Further, the method is straightforward and requires less specific knowledge of the compressor behavior than the model adaptive approach.

SECTION V

LOCAL UNCONSTRAINED OPTIMIZATION TECHNIQUES

The problem of finding extreme values of functions has received great attention, and methods of finding minima and maxima of analytically known functions are abundant. The simplest problem involves a univariate function with no restrictions placed on the domain of the optimization variable. More complicated cases arise for multivariate functions with constraints placed on the optimization vector $\mathbf{x} = [x_1, x_2, \dots, x_n]$. The general nonlinear constrained static optimization problem is defined as:

Find $\mathbf{x} = \mathbf{x}^*$ to maximize the objective function $f(\mathbf{x})$
Subject to the constraints $g(\mathbf{x}) \geq 0, g(\mathbf{x}) = 0$

Multivariate numerical optimization methods usually involve several iterations consisting of three basic steps identified in figure 14. In the first step, a search vector is identified. This search vector is defined by linear combination of optimization parameters, i.e., vane and bleed setting, and is normally selected to coincide with the direction of maximum increase in the objective function or to coincide with one of the principal axes of the function. In the second step, a one-dimensional search is accomplished to identify the maximum of the function along the search vector. Finally, the iterative process is examined to determine whether a maximum point has been identified.

Additionally, to accommodate the physical limitations of the process, it is necessary to evaluate each test point to determine whether a constraint will be violated and adjust the search procedure as required. Thus, the selection of a specific method to implement the goal-seeking logic involves three aspects: a multivariate search procedure, a one-dimensional search procedure, and a constraint avoidance procedure. Each of these aspects is discussed further in the following paragraphs.

1. MULTIVARIATE SEARCH ALGORITHMS

One important class of multivariate search algorithms are those which generate mutually conjugate search vectors at each successive iteration. Conjugate vectors are similar to orthogonal vectors in that the condition excludes linear dependence and that N mutually conjugate vectors form a basis for the N -dimensional parameter space.

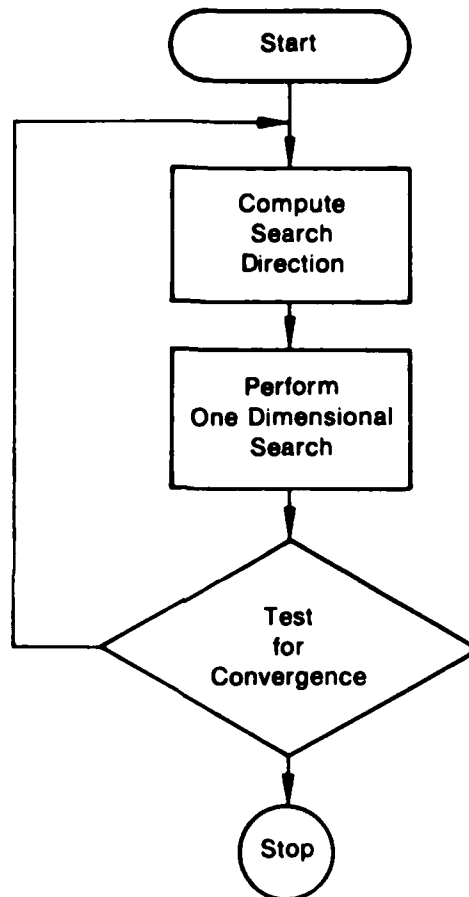
These conjugate gradient methods are attractive because convergence is guaranteed. The same guarantee generally applies to an arbitrary function since, in the vicinity of a maximum, the function can be approximated by a quadratic. Three conjugate gradient methods are considered appropriate to the compressor optimization problem. These are the:

Fletcher and Reeves Algorithm (Reference 2) — This popular method starts with the gradient vector as the search direction and at each subsequent iteration. The algorithm selects search directions which are conjugate to each previous search vector. The method requires numerical differentiation to identify these conjugate vectors.

Powell's Algorithm (Reference 3) — This method is similar to the Fletcher-Reeves Algorithm except that it does not require numerical differentiation to generate the conjugate vectors. Instead, the vectors are generated by exploiting a geometric property of quadratic functions. This property states that a line joining the extreme points along two parallel vectors is mutually

conjugate to these two vectors (see figure 15). Thus, only two simple one-dimensional searches are required to generate a new conjugate direction. Numerical differentiation is not required.

Brent's Algorithm (Reference 4) — This method is a refinement of Powell's Algorithm in that it eliminates the possibility that each successive conjugate search vector is not unique. This additional feature is gained at the expense of greater numerical complexity.



10-158418

Figure 14. The Optimization Process

The direct search methods are another class of numerical optimization techniques. These heuristic methods are essentially intelligent refinements of a brute force hill climbing technique. The decision to proceed in a given direction is based on an absolute indication that either an improvement or no improvement in the objective function is realized. Two direct search methods are considered appropriate to the compressor optimization problem. These are the:

Hooke and Jeeves Algorithm (Reference 5) — In this method, a sequence of exploratory moves are made in each of the independent variables. If an improvement is realized, the point is considered successful and the search

Rosenbrock's Algorithm (Reference 6) — This method is similar to Hooke and Jeeves Algorithm in that it also involves a sequence of exploratory moves. However, after the exploratory sequence, a set of orthogonal search directions is generated from the previously successful search vectors. The exploratory sequence is then repeated.

The final selection of an appropriate algorithm essentially involves a systematic comparison of the capabilities and limitations of a given method, since no one method is ideal for all problems, with the requirements and peculiarities of the compressor optimization problem.

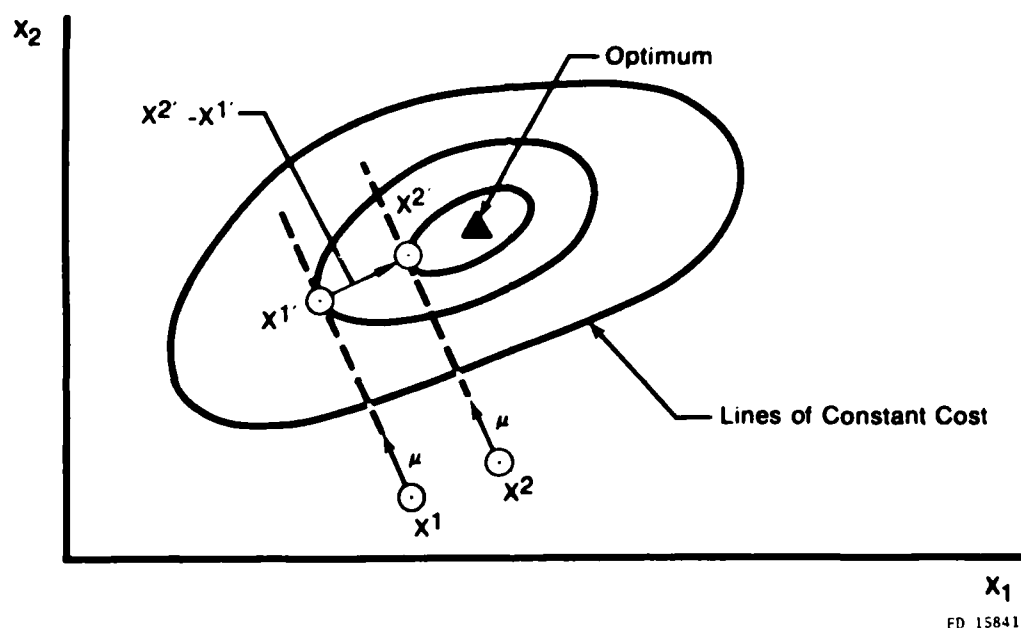


Figure 15. Generation of Conjugate Directions in Powell's Algorithm.

2. MULTIVARIATE SEARCH SPECIFICS

a. The Fletcher and Reeves Algorithm

The conjugate gradient algorithm of Fletcher and Reeves is one form of the general classification of steepest descent or gradient procedures. Initially, the search is accomplished in the direction of the gradient. Subsequent search directions are then chosen to be mutually conjugate to the gradient vector.

The principal advantage of the conjugate gradient method is that, for quadratic objective functions, the method is guaranteed to converge in n iterations, where n is the number of independent variables. The basic Fletcher-Reeves algorithm is as follows:

An initial value of the vector \mathbf{x} is chosen and $f(\mathbf{x})$ is evaluated. The value $\mathbf{f}'(\mathbf{x})$ is then evaluated (either analytically or numerically by finite differences after n evaluations of the function). The initial search is in the direction of the gradient

$$\mathbf{u}(\mathbf{x}) = \frac{\mathbf{f}'(\mathbf{x})}{\|\mathbf{f}'(\mathbf{x})\|}$$

where $\|\mathbf{f}'(\mathbf{x})\|$ denotes the magnitude or Euclidean norm of the vector. A one-dimensional search is then performed to find a new \mathbf{x} according to

$$\mathbf{x}^{\text{new}} = \mathbf{x} - \lambda \mathbf{u}(\mathbf{x})$$

where the scalar λ is picked to minimize

$$g(\lambda) = f(\mathbf{x} - \lambda \mathbf{u}(\mathbf{x}))$$

This concludes the first iteration. To begin the second iteration $f(\mathbf{x}^{\text{new}})$ and $\mathbf{f}'(\mathbf{x}^{\text{new}})$ are evaluated. The method of Fletcher-Reeves is applied to generate a conjugate direction. This involves computing

$$\beta = \frac{\mathbf{f}'(\mathbf{x}^{\text{new}}) \cdot \mathbf{f}'(\mathbf{x}^{\text{new}})}{\mathbf{f}'(\mathbf{x}) \cdot \mathbf{f}'(\mathbf{x})}$$

and using this scalar to compute the estimated conjugate gradient

$$\mathbf{G}(\mathbf{x}^{\text{new}}) = \mathbf{f}'(\mathbf{x}^{\text{new}}) + \beta \mathbf{u}(\mathbf{x})$$

At this point in the sequence, the notation \mathbf{x}^{new} is replaced by simply \mathbf{x} . The search direction at \mathbf{x} is $\mathbf{u}(\mathbf{x}) = \mathbf{G}(\mathbf{x}) / \|\mathbf{G}(\mathbf{x})\|$. A one dimensional search is then accomplished to find a scalar λ minimizing

$$g(\lambda) = f(\mathbf{x} - \lambda \mathbf{u}(\mathbf{x}))$$

and again the new \mathbf{x} is defined by

$$\mathbf{x}^{\text{new}} = \mathbf{x} - \lambda \mathbf{u}(\mathbf{x})$$

This concludes the second iteration.

The third iteration is identical to the second; the process is repeated through a cycle of $n+1$ iterations. If a sufficiently accurate estimate of the minimum has not been found at this point, a new cycle can be started by setting β for the first iteration in the new cycle.

b. Powell's Algorithm

Another conjugate direction algorithm which is of interest is the method of Powell, which, unlike Fletcher-Reeves, does not require the calculation of derivatives or their estimation by finite differences. The algorithm makes use of the fact that, for quadratic functions, if minimum values \mathbf{x}^1 and \mathbf{x}^2 in some direction \mathbf{u} are chosen by a one-dimensional search technique but from different starting points, the vector $\mathbf{x}^2 - \mathbf{x}^1$ will be mutually conjugate to \mathbf{u} .

Thus, we have a simple way of generating conjugate directions with fewer function evaluations and without the uncertainty involved with small differences of potentially noisy signals. Powell's method is as follows.

Let u' be a set of n linearly independent vectors (usually the coordinate axes) and x'' be some starting point. For each u' perform a one-dimensional search to find λ_i to minimize

$$g(\lambda) = f(x'' + \lambda u')$$

After each minimization is performed, set $x' = x'' + \lambda_i u'$. Now, for each $i = 1, 2, \dots, n-1$, replace u' by u'' . Then replace u'' by $x'' - x'$. Thus, we have eliminated one direction and replaced it with a new search direction. A one-dimensional search is now performed in that direction, i.e., find λ that minimizes

$$g(\lambda) = f(x'' + \lambda (x'' - x'))$$

The process is now repeated with a one-dimensional search in each direction to evaluate a new conjugate search vector. The oldest search vector is then discarded in favor of the newly calculated conjugate direction. The process continues until the stopping rule is satisfied. For a quadratic function, the method will converge to an optimum in n such iterations.

c. Brent's Modification of Powell's Algorithm

A problem which has been observed in the conjugate gradient method of Powell is that if any λ_i in the one-dimensional search becomes zero, the directions are no longer mutually conjugate but become linearly dependent. In fact, the directions often do become linearly dependent. The modification of Brent is to reset the search directions u' to a set of mutually conjugate principal vectors after each N iterations. This is similar to resetting $\beta=0$ after each cycle of the Fletcher-Reeves conjugate gradient algorithm except that we retain the characteristic of mutually conjugate directions. The penalty for this improvement is the extra computation involved in finding the set of principle axes — but the cost appears justifiable in many cases. Brent has exercised the algorithm on certain standard test functions and convergence properties are excellent. The calculation of the principal axes will not be demonstrated here.

d. The Hooke-Jeeves Algorithm

In the algorithm developed by Hooke and Jeeves, function evaluations alone are performed (no derivatives are required) and the method progresses only to points which offer improvement. A typical search scheme proceeds as follows:

A base point x'' is selected and the function evaluated at that point. A new point x' is chosen and, if an improvement is realized at

$$f(x') > f(x'')$$

the new point, x' becomes the new base point. If no improvement is realized, the point is rejected and an alternative x' is selected. The process of choosing a test point, evaluating the function, and comparison continues until some stopping criterion is satisfied. It should be emphasized that the comparison is not a quantitative one; the comparison will only indicate success or failure. The argument for this type of method is more intuitive than analytical: when making function evaluations any improvement found at some test point is retained by making that point the new base point. The justification for neglecting information concerning the numerical difference in function values between two points is that the local derivative

information is of dubious value, particularly when uncertainties exist in the function determinations. Clearly, the success of any direct search method depends upon the manner by which new test points are chosen. The choice of test points in the Hooke-Jeeves algorithm is logically sound. The first points chosen, termed exploratory moves, are designed to acquire local information concerning the function's behavior. When knowledge of the function is obtained a pattern move is then made.

To begin the algorithm, an initial point x'' and a set of mutually orthogonal unit vectors u^1, u^2, \dots, u^n are selected. The vectors are usually chosen parallel to the coordinate axes. A step size h is also selected. The first exploratory move is

$$x^1 = x'' + hu^1$$

if the condition

$$f(x^1) > f(x'')$$

is satisfied the point is a success and x^1 replaces x'' . Otherwise, the point is termed a failure and

$$x^1 = x'' - hu^1$$

The comparison is repeated, and if successful, x^1 replaces x'' . If both the positive and negative perturbations yield failures, the base point remains at x^1 . The exploratory move is repeated for each of the n unit vectors.

The pattern move begins by determining which exploratory moves were successful. If the exploratory move for the i^{th} direction demonstrated success in either the positive or negative sense, the pattern move will be in that direction. In the case of improvement in neither sense for some direction, the pattern move remains fixed for that direction. Thus, the pattern moves consist of the vector sum of each successful exploratory move, i.e.,

$$x^p = x'' + (x^n - x'')$$

where x^n is the final position after all exploration is completed.

If the pattern move is itself successful, the procedure begins with exploratory moves from the new base point x^p . If, however, the pattern move is found to fail and $x^n \neq x''$ exploration is begun from x'' . In the case where $x^n = x''$, the step size is reduced ($h = h/k$, k constant > 1) and exploration is repeated. The algorithm terminates when h is less than some predetermined value.

e. Rosenbrock's Algorithm

Rosenbrock's algorithm is a variation on the technique of univariate probing. The procedure is as follows:

Let u^1, u^2, \dots, u^n be a set of unit vectors parallel to the coordinate axes and choose k^1, k^2, \dots, k^n to be a set of step sizes for each direction. From the initial point x'' move the new point

$$x^1 = x'' + k^1 u^1$$

for each of the directions in turn and evaluate the function. The comparison

$$f(x^1) > f(x'')$$

is made, if true, k' is doubled and x' replaces x^* . If the comparison turns out false, x' is rejected and $k' \leftarrow -\frac{1}{2}k'$. The method proceeds for each of the n directions, returning to the first direction and continues until one successful step has been followed by one unsuccessful step in each direction. Then, a new set of directions u' is calculated by

$$u' = \sum_{i=1}^n k' u' / \left| \sum_{i=1}^n k' u' \right|$$

The remaining $n-1$ vectors are then generated using the Gram-Schmidt orthonormalization algorithm. The resulting set thus forms an orthogonal basis.

3. EVALUATION OF MULTIVARIATE SEARCH ALGORITHMS

To evaluate the capabilities and limitations of the goal-seeking algorithms a stage-by-stage compressor model with two variable stages was developed. It is a generic model in the sense that it does not simulate any particular compressor, but represents an abstraction of the fundamental steady-state characteristics of axial compressors. Each stage (rotor plus stator) in the model is represented by the normalized pressure rise and temperature rise functions, Ψ and λ , as a function of the normalized airflow and vane angle, ϕ and α . The pressure, temperature, and airflow at the inlet of each stage, as well as the corrected speed and vane angle, must be known before the calculations can proceed. Each stage calculation is identical in form and the calculations are simply cascaded to represent a compressor with multiple variable-geometry stages (figure 16).

To illustrate the operation of the compressor model, a series of points were run by varying discharge area at several different values of corrected speed. Figure 17 shows a performance map of the model characteristics.

For the purpose of this evaluation, the optimization goal selected involved maximizing efficiency at constant speed while holding the discharge valve area constant (Case 1 in the matrix of optimization goals). The optimization problem can be formulated as:

$$\begin{aligned} &\max \eta(\alpha_1, \alpha_2, N, \text{AREA}) \\ &\alpha_1, \alpha_2, N, \text{AREA} \end{aligned}$$

Subject to:

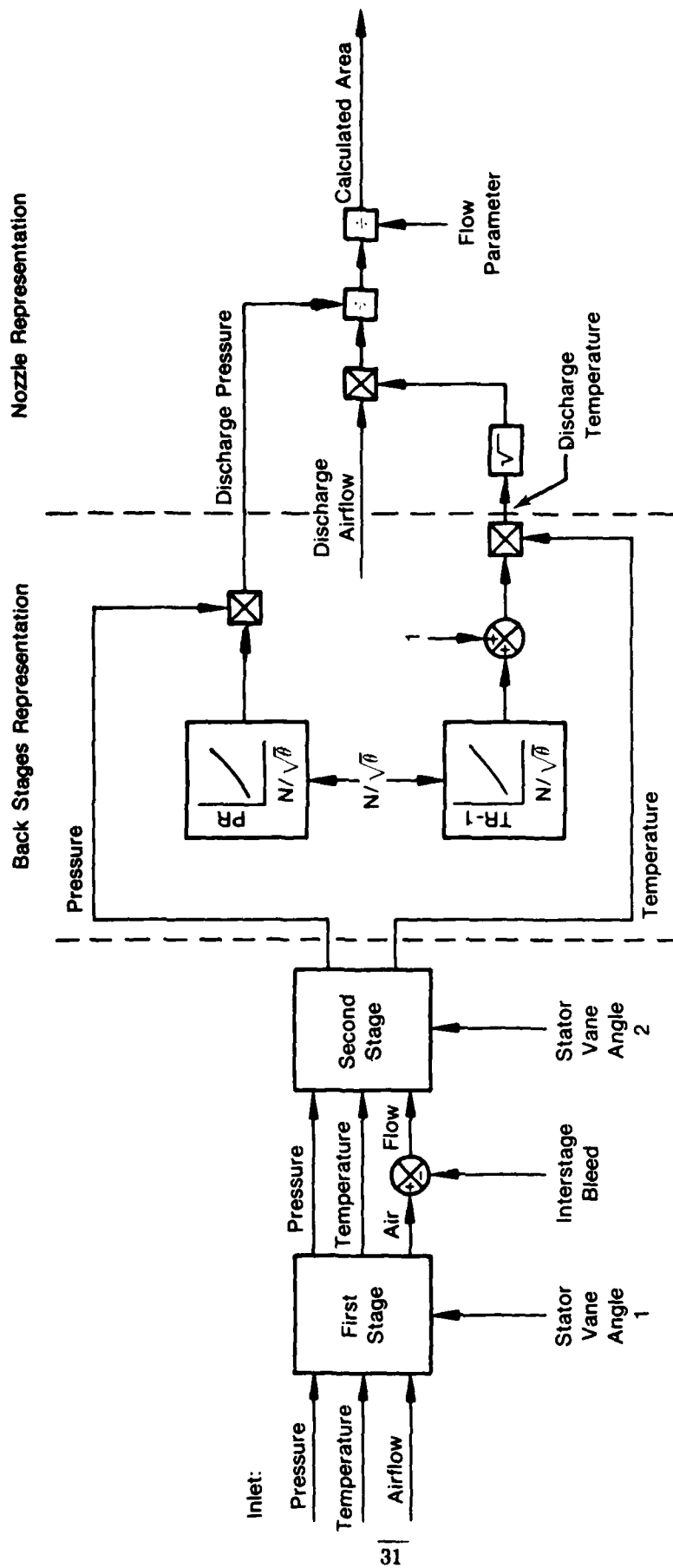
- (a) $\alpha_{1_{\min}} \leq \alpha_1 \leq \alpha_{1_{\max}}, \alpha_{2_{\min}} \leq \alpha_2 \leq \alpha_{2_{\max}}$
- (b) $\text{AREA} = \text{AREA}_0$
- (c) $N = N_0$

Constraints (b) and (c) indicate that the performance index can be written as:

$$\begin{aligned} &\max \eta(\alpha_1, \alpha_2, N, \text{AREA}) \\ &\alpha_1, \alpha_2 \end{aligned}$$

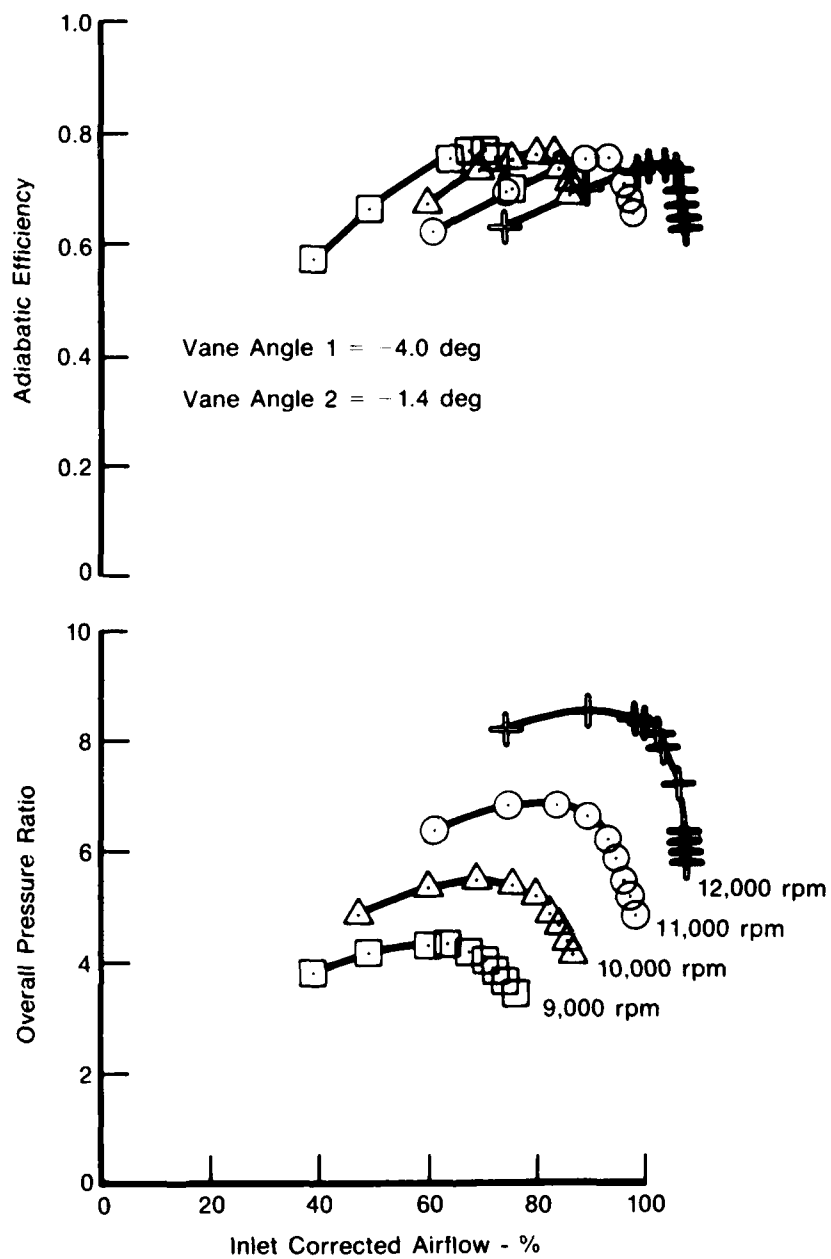
Since most optimization schemes minimize, rather than maximize, a performance index, the negative of the function is selected for the performance index in the manner shown below.

$$\begin{aligned} &\min K(1 - \eta)^2 \\ &\alpha_1, \alpha_2 \end{aligned}$$



FD 212393

Figure 16. Multistage Compressor Calculation



FD 212384

Figure 17. Performance Map of Model Characteristics

Selection of a quadratic performance index is preferable because a large class of optimization algorithms converge to the local minimum for such an index. Note also the constraint (c) is not really a constraint since speed N is an input to the model and can be held constant. In effect, the optimization problem becomes: minimize performance index subject to the inequality constraint (a) and the equality constraint (b).

Four of the five local goal-seeking algorithms were programmed in FORTRAN into an IBM 3033, in conjunction with the two-stage analytical compressor model. Programming included the following four algorithms:

- Hooke-Jeeves
- Rosenbrock
- Powell's derivative free approach
- Brent's modification to the Powell algorithm

All of these algorithms compute the minimum without resorting to derivative evaluation. This is an attractive feature of these schemes, especially since an explicit evaluation of the derivatives is not feasible. For this reason, the Fletcher-Reeves conjugate gradient scheme was not explicitly studied in the course of this investigation. This method, however, is used in the COPES/CONMIN program (discussed in Section VIII) to solve unconstrained optimization problems. A comparative evaluation of the local algorithms against a criterion to determine efficacy of the various routines was performed. This criterion is commonly considered to be one of a number of function evaluations required to achieve a minimum for each of the minimization schemes. The number of function evaluations, to a large extent, determines computer time required to narrow to a minimum and quantifies the effort required using a particular scheme. In order that evaluation not be biased in favor of any particular scheme, the same performance index, starting points for α , and desired area (51.121) at the desired speed of 12,000 rpm were selected. Selection of the starting values ($\alpha_1 = -3$ deg and $\alpha_2 = -0.5$ deg) was such that it was hoped the minimization routine would converge to the maximum efficiency point with vane settings at ($\alpha_1 = -4$ deg and $\alpha_2 = -1.4$ deg).

Table 5 lists the results of the problem investigation for the various algorithms studied, using single precision arithmetic on the IBM 3033 with a stopping criterion such that between two successive iterations, the performance index did not change more than 1×10^{-6} .

Table 5. Evaluation of Multivariate Search Techniques (Starting Values: $\alpha_1 = -3$ deg, $\alpha_2 = -0.5$ deg)

Algorithm	Number of Function Evaluations	Optimum Efficiency (%)	Vane Angle		Airflow W_{2c} (lb/sec)	Area (in. ²)
			α_1 (deg)	α_2 (deg)		
Hooke-Jeeves	34	73.82	-4.0	-1.30	99.78	51.06
Rosenbrock	500	73.89	-4.0	-1.56	100.11	51.16
Powell	41	73.92	-4.0	-1.42	99.98	51.04
Brent	41	73.92	-4.0	-1.42	99.97	51.04
Optimum Point		73.91	-4.0	-1.40	99.97	51.12

This table indicates that the Hooke-Jeeves algorithm converged near the optimum design point in the fewest number of function evaluations. Results from Brent's modification of the Powell algorithm indicate little or no difference between the original and modified algorithms. Since the Brent algorithm makes an eigenvector evaluation every second iteration for the same number of function evaluations, it uses more computer time than the Powell algorithm. It is known that the Brent algorithm produces superior results only when the number of independent variables is large (>10). For the small number of variables anticipated to be used in this program, the Brent algorithm derives no benefit over the Powell algorithm. Examination of

table 5 further indicates that the Rosenbrock algorithm takes too many function evaluations to compute the minimum performance index. These conclusions were borne out also at starting values close to the operating point. For example, table 6 summarizes the same results using a starting value of 0 deg for α_1 and α_2 .

Detailed results for the Hooke-Jeeves algorithm with start vane settings of $\alpha_1 = -3$ deg and $\alpha_2 = -0.5$ deg are presented in figure 18. Note the rapid convergence obtained in the first few iterations (search and seek). Figure 19 shows the results obtained using different starting values of $\alpha_1 = 0$ deg and $\alpha_2 = 0$ deg. In both cases, the values eventually converge near the design point.

Results from application of the Rosenbrock algorithm to the vane optimization problem are detailed in figure 20. Due to the large number of function evaluations compared to other algorithms, the scheme was investigated for only a few cases. Figure 20 shows results for perhaps the best performance (i.e., least number of function evaluations). Rather extensive experimentation with this scheme had to be carried out because of the large number of algorithm parameters required to be set in the program. Therefore, this scheme is not recommended.

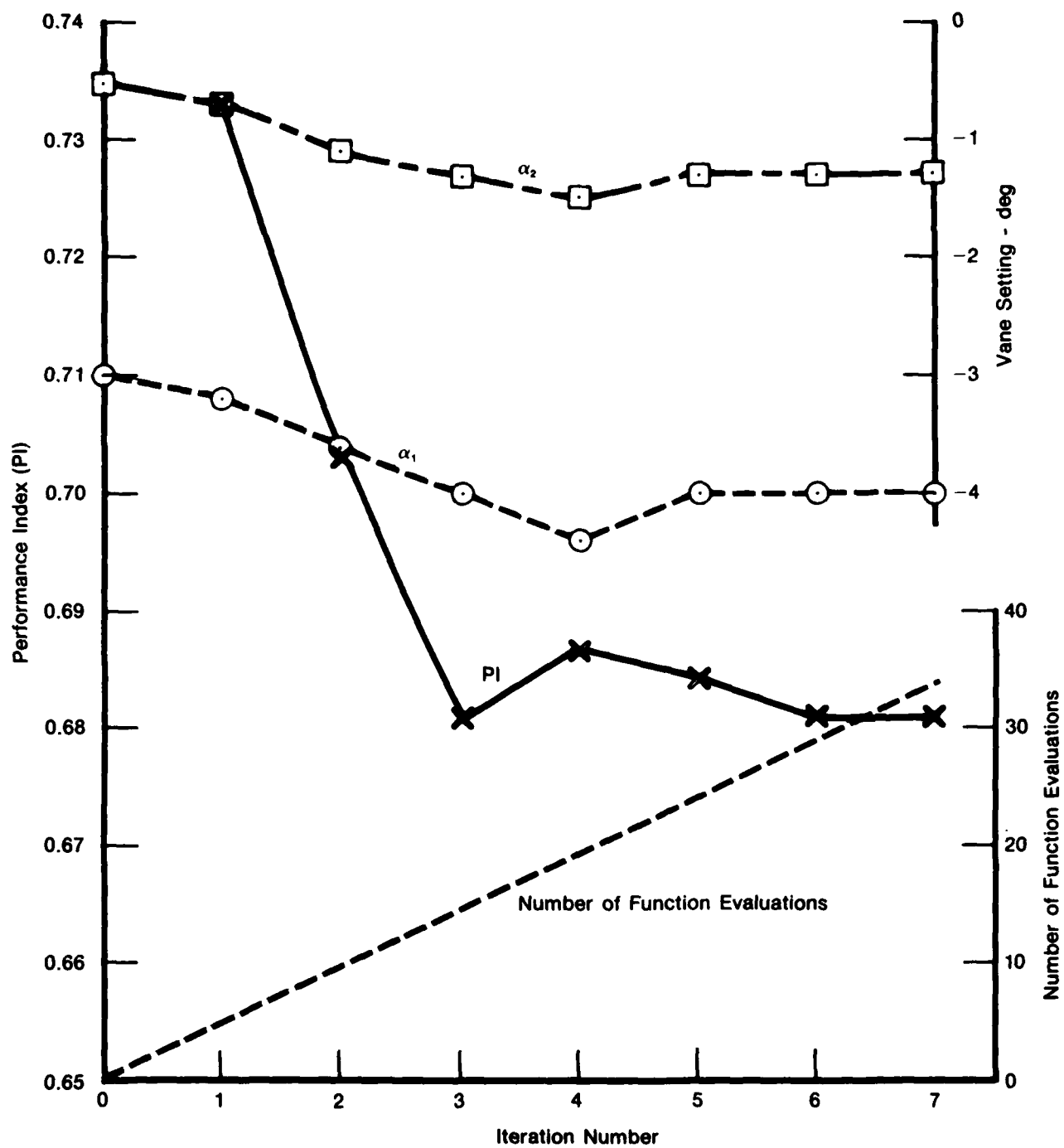
Figure 21 presents the results from the Powell algorithm. Note the rapid convergence of the algorithm vis-a-vis the Hooke-Jeeves results in figure 19. These results reflect a starting point of 0 deg for both α terms. As can be seen in table 6 with this initial starting point, the Powell algorithm converged to a different local minimum than the Hooke-Jeeves (figure 19) or Rosenbrock (figure 20) algorithms. However, for any given starting point, the rapid convergence of this scheme makes it extremely attractive.

The following conclusions may be drawn from this evaluation:

- The Brent algorithm offers no substantial improvement over the Powell algorithm for the small number of independent variables in this study.
- The Rosenbrock algorithm is rather slow in achieving the minimum of the performance index for this problem.
- This leaves a choice between the Hooke-Jeeves and the Powell algorithms. Even though the Powell algorithm at times takes more function evaluations (as indicated in table 5), it is preferable because of its convergent properties for a quadratic performance index.

4. PRACTICAL IMPLEMENTATION

To be useful in the compressor optimization process, the algorithm must be capable of handling the effects of finite incremental vane angle variations and measurement uncertainties. Experience has shown that minimum incremental vane angles of 0.5 deg and efficiency tolerances of $\pm 0.2\%$ are practical limits to be considered.



FD 212365

Figure 18. Behavior of Hooke-Jeeves Algorithm with Starting Values of $\alpha_1 = -3.0$ Deg and $\alpha_2 = -0.5$ Deg

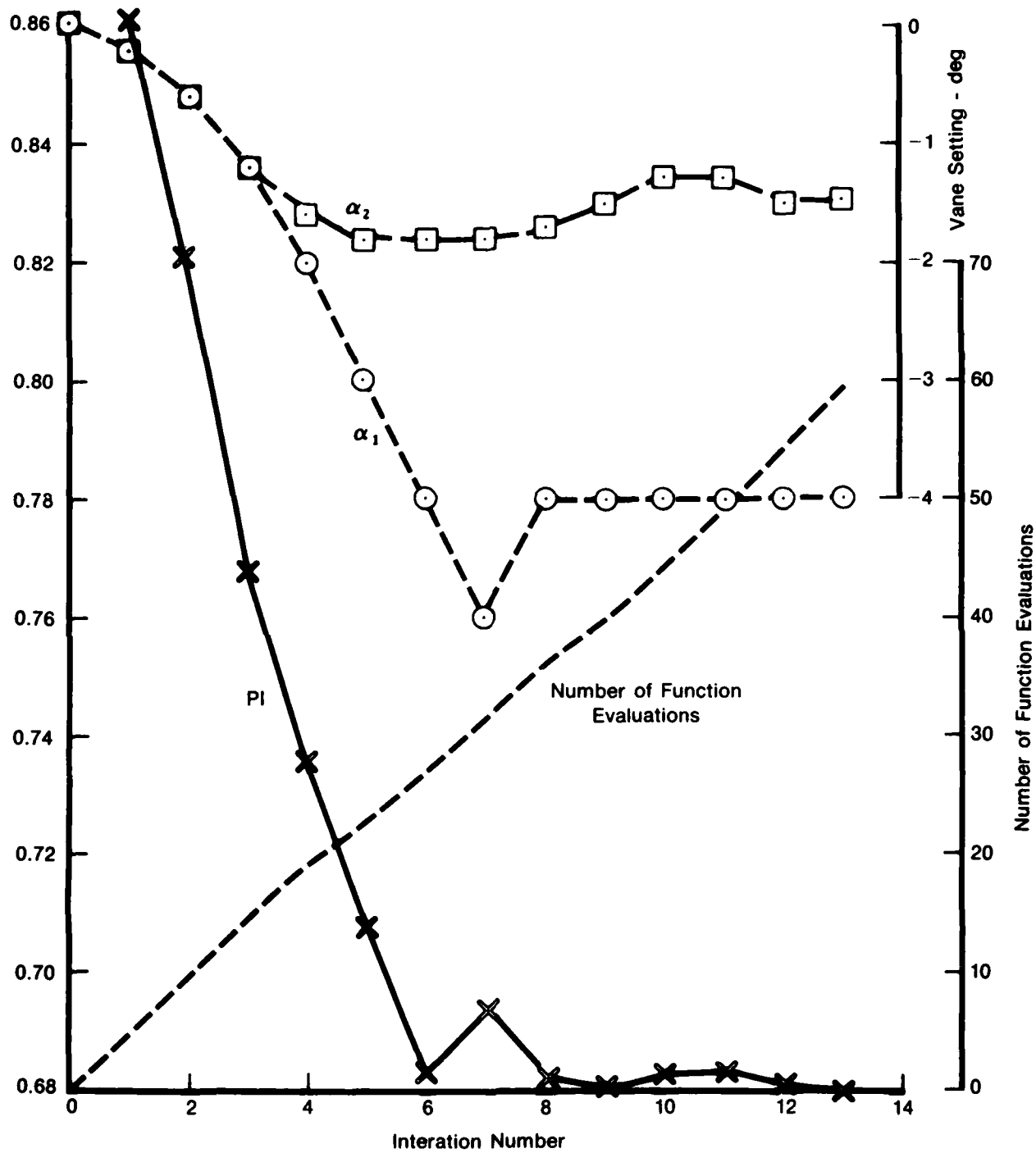


Figure 19. Behavior of Hooke-Jeeves Algorithm with Starting Values of $\alpha_1 = 0$ Deg and $\alpha_2 = 0$ Deg

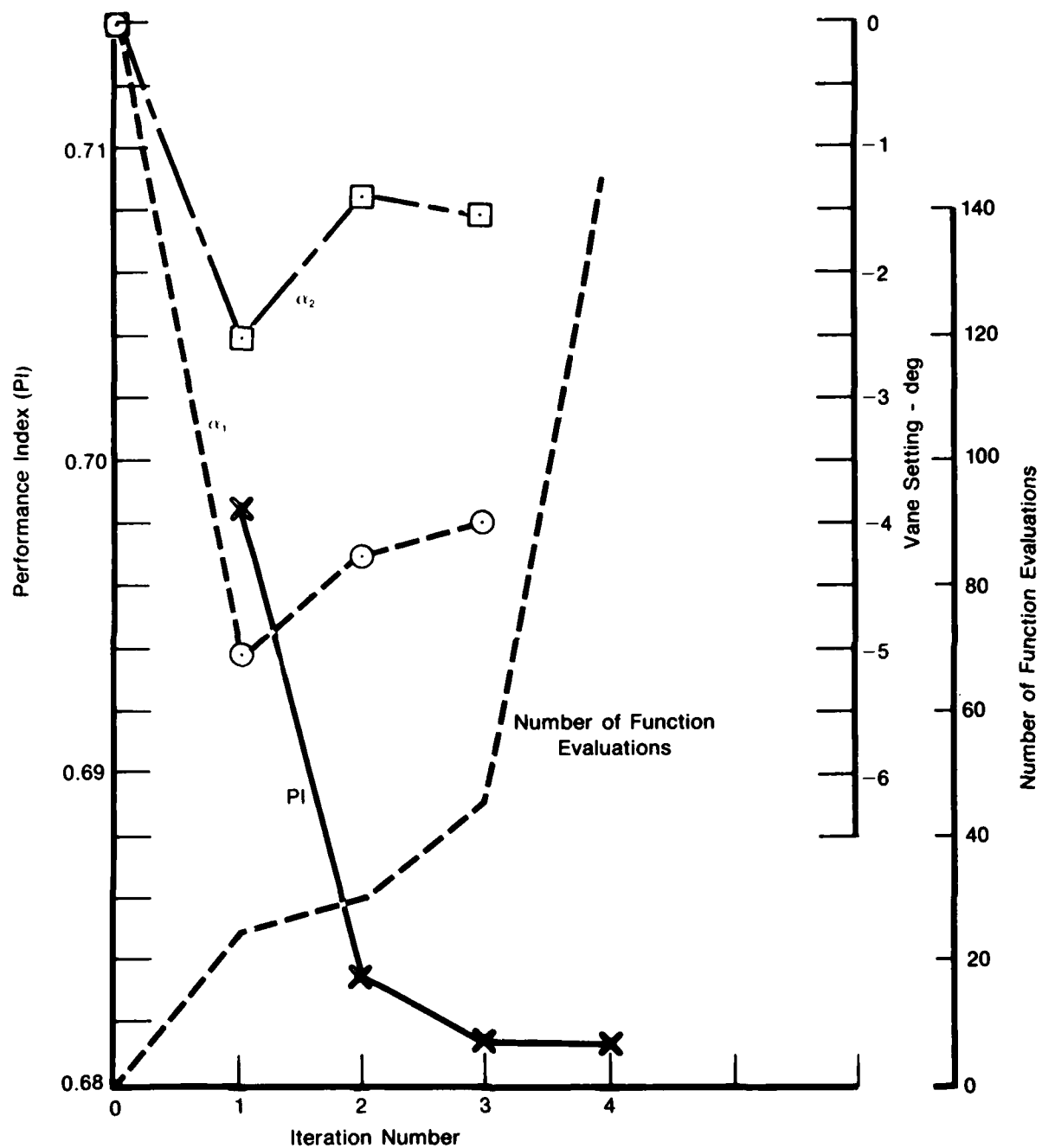


Figure 20. Behavior of Rosenbrock Algorithm with Starting Values of $\alpha_1 = 0$ Deg and $\alpha_2 = 0$ Deg

FD 212397

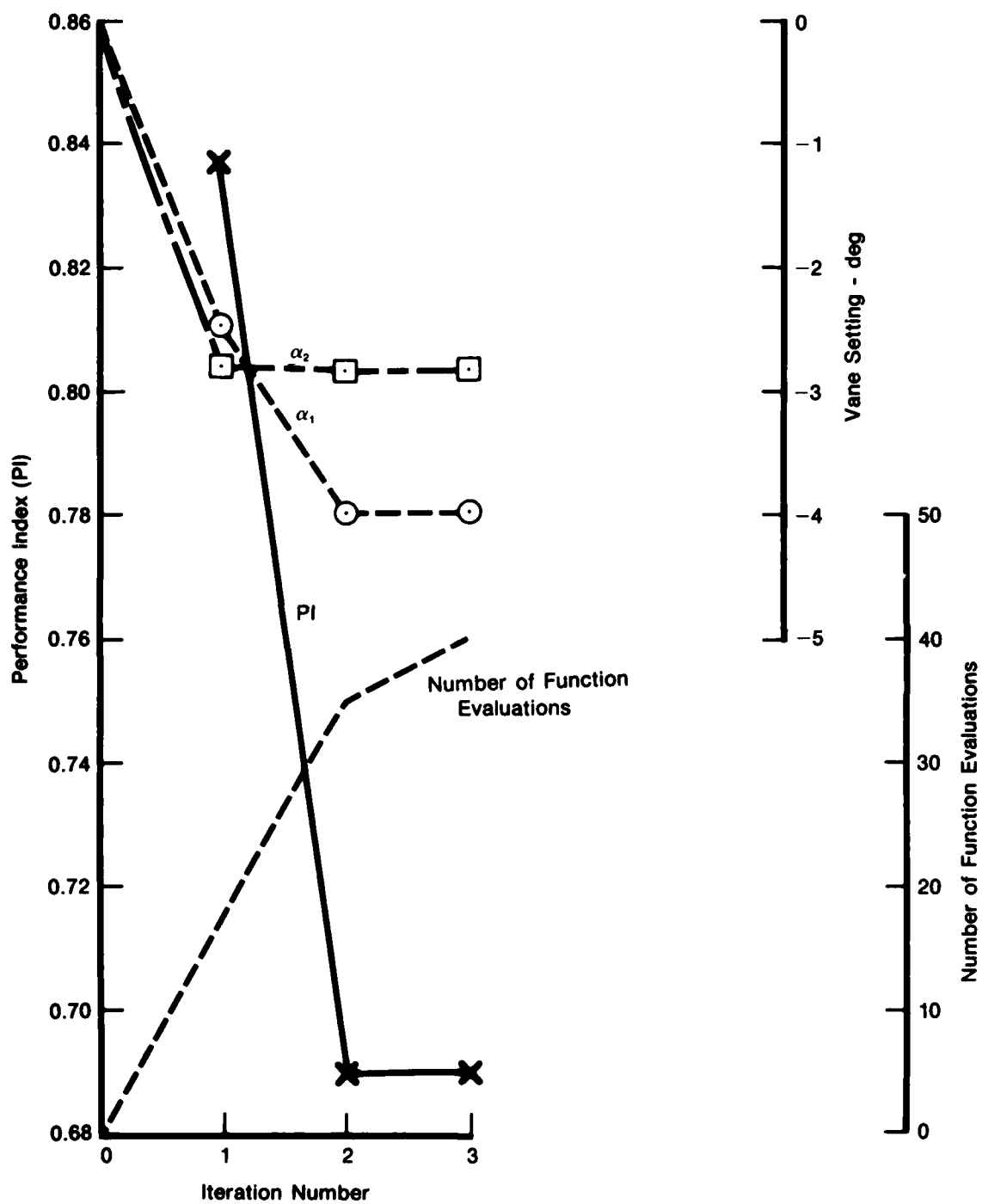


Figure 21. Behavior of Powell Algorithm with Starting Values of $\alpha_1 = 0$ Deg and $\alpha_2 = 0$ Deg

Table 6. Evaluation of Multivariate Search Techniques (Starting Values: $\alpha_1 = 0$ deg, $\alpha_2 = 0$ deg)

Algorithm	Number of Function Evaluations	Optimum Efficiency (%)	Vane Angle		Airflow W_K (lb/sec)	Area (in. ²)
			α_1 (deg)	α_2 (deg)		
Hooke-Jeeves	60	73.84	-4.0	-1.5	99.87	50.99
Rosenbrock	145	73.89	-4.0	-1.6	100.04	51.12
Powell	40	73.74	-4.0	-2.8	100.46	51.10
Brent	40	73.74	-4.0	-2.9	100.53	51.08
Optimum Point		73.91	-4.0	-1.4	99.97	51.12

a. Finite Vane Travel

When 1.0 degree incremental vane angle was introduced into the Powell algorithm, the minimization routine was unable to converge to a local optimum and, in fact, wandered off in the wrong direction. Close examination of the stage-by-stage model revealed the probable cause to be a large plateau in efficiency around the optimum. To obviate this problem, a quadratic characterization of the efficiency contour around an optimum was adopted to test the optimization routines. With constraints placed on vane angle resolution on the order of 1.0 deg, neither the Powell algorithm, nor any other direct search method, such as Hooke-Jeeves, was able to converge to the correct local optimum. The problem of finite resolution and the inability of the proposed algorithms to handle it caused a reexamination of optimization schemes proposed.

A scheme similar to the Powell method, but requiring gradients, was adopted. This scheme, called the Broyden scheme, (Reference 7) contains essentially the same convergence properties as the Powell method. The algorithm proceeds as

$$X_{N+1} = X_N - (H_N)^{-1} J_N$$

This is the conventional Newton-Raphson iteration, with H_N being the Hessian (matrix of 2nd partials) and J_N being the Jacobian. The Hessian is not explicitly evaluated, but rather updated using the following scheme.

$$\text{With: } \delta = X_N - X_{N-1}$$

$$\gamma = J_N - J_{N-1}$$

$$H_N = H_{N-1} + \frac{(\delta - H_{N-1} \gamma)(\delta - H_{N-1} \gamma)'}{\gamma(\delta - H_{N-1} \gamma)'}$$

$$H_0 = I, \text{ the identity matrix}$$

This method is very efficient. It converges to the correct optimum in $n+1$ iterations for quadratic performance indices, and the number of function evaluations is comparatively low.

In addition to the base point, the Jacobian about the base point needs to be computed. For a four variable-stage compressor, four additional test points are required if a simple differencing scheme for evaluating the Jacobian is used. Each element of the Jacobian can be evaluated as

$$\frac{\partial \eta}{\partial \alpha} \approx \frac{\eta(\alpha + \delta \alpha) - \eta(\alpha)}{\delta \alpha}$$

Thus, each iteration requires five test points ($n+1$). If a quadratic surface for efficiency is used with infinite resolution, the method should converge in $n+1$ iterations. The total number of test points for a four variable-stage compressor model becomes 26. However, as will be seen with finite vane travel, the method converges in less than the $n+1$ iterations, such that in practice even fewer test points will be required.

The efficiency representation used to study the behavior of Broyden method is a quadratic function of vane angle settings, as shown below:

$$\eta = 1 - \frac{\alpha_1^2 + \alpha_2^2 + \alpha_3^2 + \alpha_4^2}{1000}$$

The quadratic objective function minimized was

$$\min_{\alpha_1, \alpha_2, \alpha_3, \alpha_4} (1 - \eta) 1000$$

Results of the optimization study using different limits on vane angle travel, such as 1.0, 0.5, 0.25, and 0.10 deg are detailed below for initial α 's of 4, 5, 6, and 7 deg, and a stopping criteria, such that the process terminated if the objective function changed less than 10^{-4} between successive iterations.

Vane Angle Resolution = 1.0 deg.

<i>Iteration</i>	<i>Vane Angle (deg)</i>				<i>Objective Function</i>	<i>Cumulative No. of Test Points</i>
	α_1	α_2	α_3	α_4		
0	4	5	6	7	126	5
1	-5	-6	-7	-8	174	10
2	-0.5	-0.5	-0.5	-0.5	1	15
3	-0.5	-0.5	-0.5	-0.5	1	16

Total test points required for four variables equals 16.

Vane Angle Resolution = 0.5 deg

<i>Iteration</i>	<i>Vane Angle (deg)</i>				<i>Objective Function</i>	<i>Cumulative No. of Test Points</i>
	α_1	α_2	α_3	α_4		
0	4	5	6	7	126	5
1	-4.5	-5.5	-6.5	-7.5	149	10
2	-0.25	-0.25	-0.25	-0.25	0.25	15
3	-0.25	-0.25	-0.25	-0.25	0.25	16

Total test points required for four variables equals 16.

Vane Angle Resolution = 0.25 deg

<i>Iteration</i>	<i>Vane Angle (deg)</i>				<i>Objective Function</i>	<i>Cumulative No. of Test Points</i>
	α_1	α_2	α_3	α_4		
0	4	5	6	7	126	5
1	-4.25	-5.25	-6.25	-7.25	137.25	10
2	-0.125	-0.125	-0.125	-0.125	0.0625	15
3	-0.125	-0.125	-0.125	-0.125	0.0625	16

Total test points required for four variables equals 16.

Vane Angle Resolution = 0.10 deg

<u>Iteration</u>	<u>Vane Angle (deg)</u>				<u>Objective Function</u>	<u>Cumulative No. of Test Points</u>
	<u>α_1</u>	<u>α_2</u>	<u>α_3</u>	<u>α_4</u>		
0	4	5	6	7	126	5
1	-4.1	-5.1	-6.1	-7.1	130.44	10
2	-0.05	-0.05	-0.05	-0.05	0.01	15
3	-0.05	-0.05	-0.05	-0.05	0.01	16

Total test points required for four variables equals 16.

Analysis of the results indicates that the Broyden method provides a relatively efficient routine capable of accommodating large vane angle travel. It converges rapidly for quadratic surfaces with infinite resolutions in $n + 1$ iterations. With finite resolutions, it converges in less than $n + 1$ iterations, generally on the third iteration, requiring only $3(n + 1) + (n - 3)$ test points, rather than $(n + 1) + 1$ test points. The accuracy of the converged solution is one-half of the incremental vane angle. For 0.5 deg incremental vane angle, the resolution of 0.25 deg provides sufficiently accurate information for the compressor optimization problem.

b. Measurement Errors

Here the influence of measurement error on convergent ability of the Broyden modified Powell method is evaluated. The test case function is the quadratic surface efficiency representation:

$$\eta = 1 - \frac{\alpha_1^2 + \alpha_2^2 + \alpha_3^2 + \alpha_4^2}{1000}$$

with the optimization goal

$$\min_{\alpha_1, \alpha_2, \alpha_3, \alpha_4} 1000 (1 - \eta)$$

To simulate an efficiency measurement error ($\pm 0.2\%$), a random noise signal within the band of ± 2.0 was added to the evaluated objective function. The range in convergence ability was found to be extreme. Recall that runs with no error converged in four iterations (16 test points). The introduction of an error signal of less than ± 2 prevented convergence after 30 iterations (150 test points). Even a factor of ten reduction in the noise level to ± 0.2 , required 13 iterations (65 test points) for convergence.

The noise sensitivity problem is observed with the Broyden scheme because it makes use of a gradient evaluation at each new iteration. Noise affects each step (of the gradient evaluation) since there is no process to filter out the immediate impact of the erroneous value on the next iteration value.

The conclusion was drawn that the Broyden modification is not suitable for the compressor vane optimization problem because it is too sensitive to measurement error.

SECTION VI LOCAL CONSTRAINED OPTIMIZATION TECHNIQUES

None of the numerical procedures previously identified provide for the consideration of constraints on independent variables in the optimization problem. The constrained optimization problems were studied using the Method of Feasible Directions (Reference 8) as programmed in the computer program CONMIN (Reference 9). The basic analytic technique used by CONMIN is to minimize the performance index until one or more constraints become active. The minimization process then continues by following the constraint boundaries in a direction such that the value of the performance index continues to decrease. When a point is reached such that no further decrease in the performance index can be obtained, the process is terminated.

An indirect approach for dealing with constraints was also studied by attaching a penalty or barrier function to the performance index. Here, the constrained optimization problem was converted to an unconstrained problem and then the resulting system was solved using Powell's method. These results are reported alongside those obtained from CONMIN.

Considering the two-variable-stage analytical compressor model, the optimization problem evaluated was to maximize efficiency with stall margin constrained to be above a given level (Optimization Goal 4). This can be set up for CONMIN as

$$\min_{\alpha_1, \alpha_2} 10 (1 - \eta)^2 \text{ subject to } SM \geq 53.5\%$$

The problem can also be converted to an unconstrained optimization by augmenting the above performance index with inequality constraint. Thus,

$$\min_{\alpha_1, \alpha_2} 10 (1 - \eta)^2 + K(SM - 53.5)^2 H(SM - 53.5)$$

where H is the Heaviside step function:

$$\begin{aligned} H(SM - 53.5) &= 1 & SM < 53.5 \\ H(SM - 53.5) &= 0 & SM \geq 53.5 \end{aligned}$$

Results using both these schemes are reported below for the same starting set of vane angles:

With	$\alpha_1(0) = -3 \text{ deg}$	$\alpha_2(0) = -0.5 \text{ deg}$		
CONMIN:	$\alpha_1^{\text{OPT}} = -6 \text{ deg}$	$\alpha_2^{\text{OPT}} = -4 \text{ deg}$	$\eta^{\text{OPT}} = 0.731$	$SM^{\text{OPT}} = 54.7\%$
Indirect:	$\alpha_1^{\text{OPT}} = -5.2 \text{ deg}$	$\alpha_2^{\text{OPT}} = -3.8 \text{ deg}$	$\eta^{\text{OPT}} = 0.73$	$SM^{\text{OPT}} = 53.5\%$

Behavior of the two schemes is demonstrated in figures 22 and 23. As shown, CONMIN required the fewer number of iterations. Note that even though the indirect procedure uses the Powell procedure within its core, convergence in $n + 1$ iterations is no longer guaranteed as the performance index is not quadratic, but is rather a quadratic augmented by a Heaviside step function.

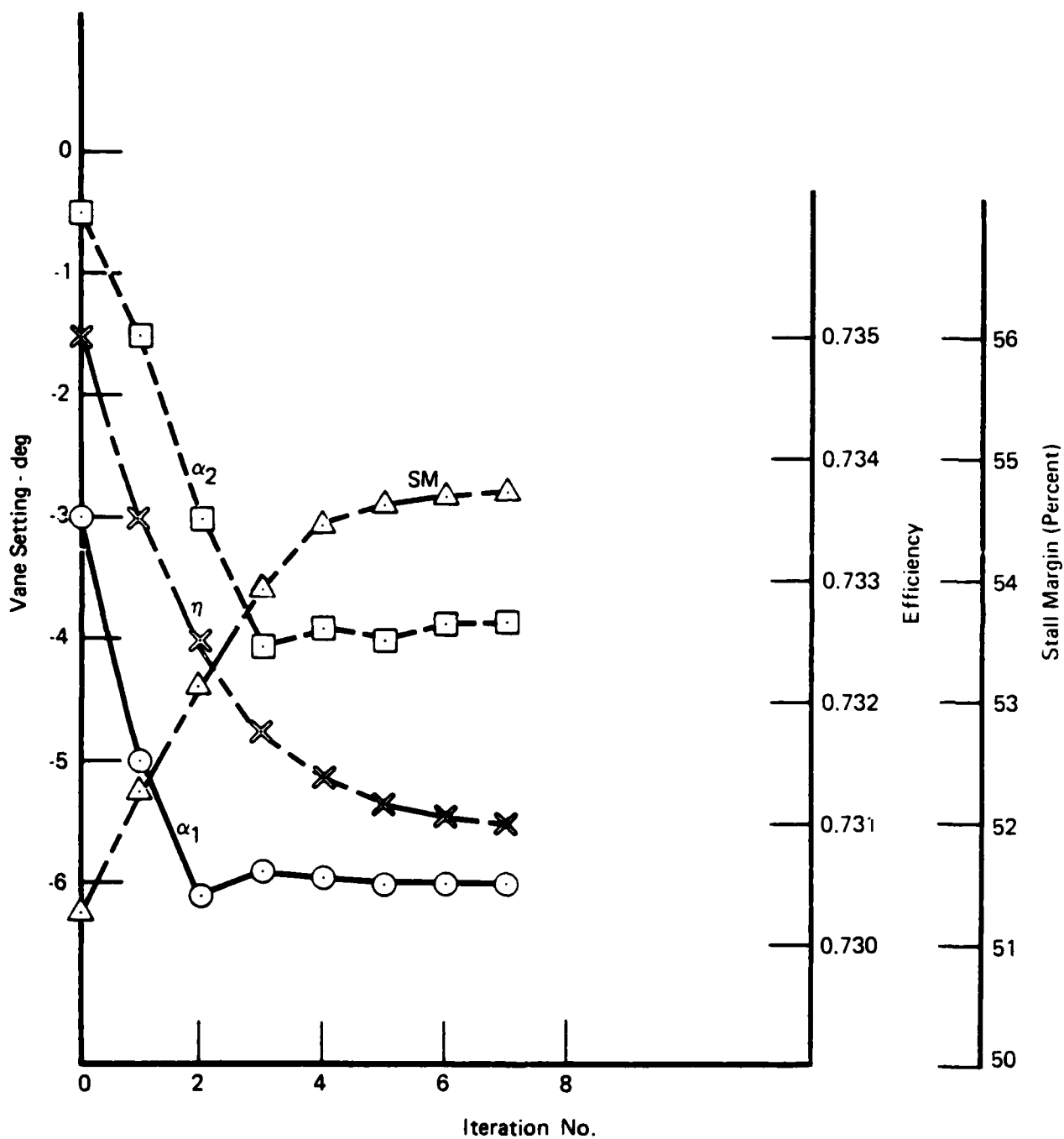
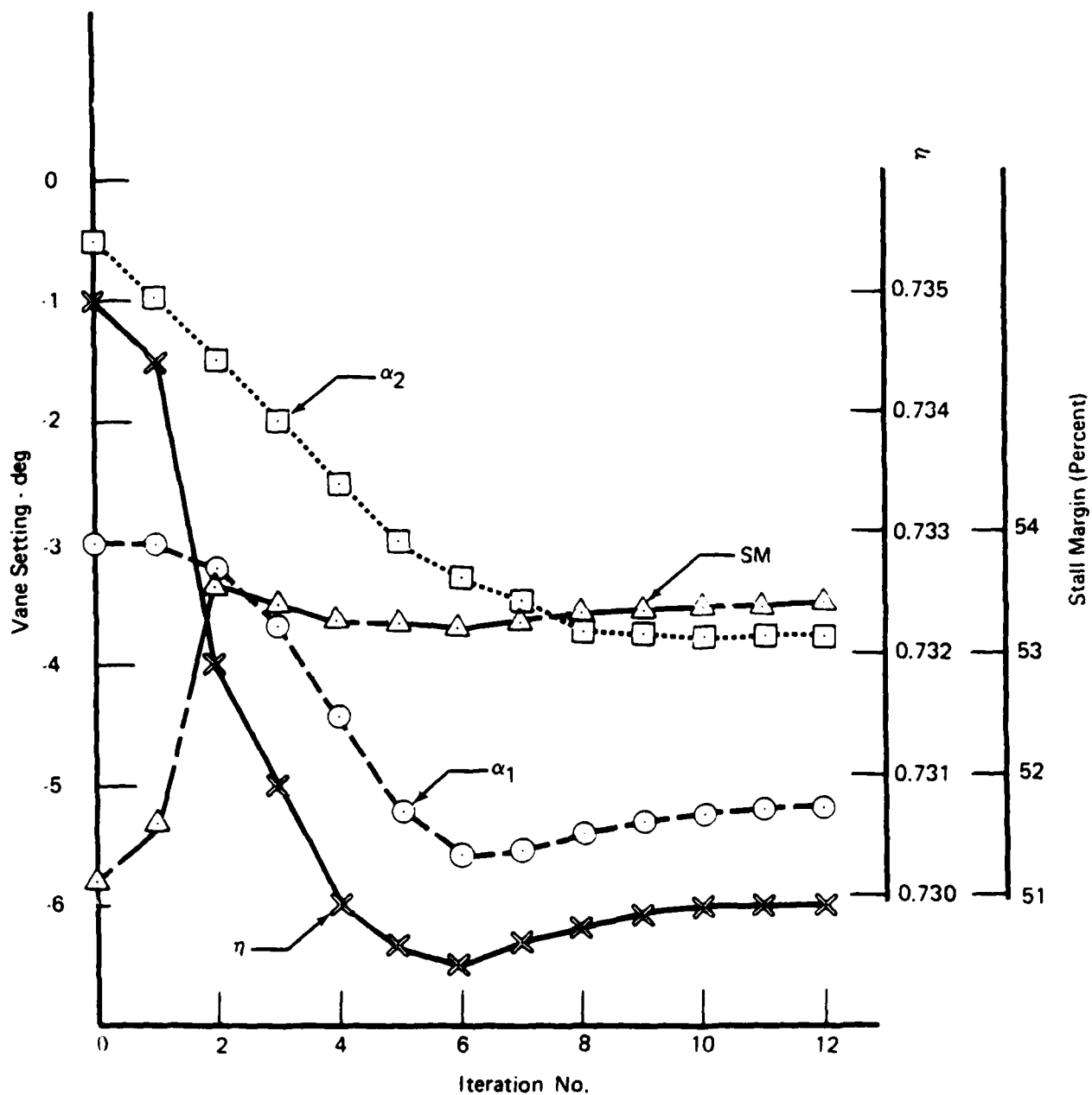


Figure 22. Performance of CONMIN on Constrained Optimization Goal 4



FD 1979084

Figure 23. Performance of Constrained Optimization Goal 4 Using an Indirect Approach

In the CONMIN results, two additional iterations are required after the aerodynamic constraint has been met. This is due to the convergence criteria that the difference between two successive evaluations of the performance index has to be less than a specified number for three iterations. Even with this convergence criteria, CONMIN requires fewer iterations than the indirect approach.

A summary of CONMIN performance on the stage-by-stage compressor model for Optimization Goal 4 is presented below:

<u>Number of Variable Vanes</u>	<u>Stopping Criteria</u>	<u>Number of Iterations</u>	<u>Number of Test Points</u>
2	3	7	34
2	1	5	26

The stopping criteria represents the number of consecutive iterations that the performance index changes by less than one-tenth of one percent (0.10%). Therefore, by relaxing the stopping criteria, fewer iterations are required, reducing the number of tests and cost to optimize the compressor.

SECTION VII

GLOBAL OPTIMIZATION METHODS

The goal-seeking algorithms previously described are suitable for computing only local minima or maxima. An assumption was that compressor design technology has progressed to the point where a starting set of vane angles can be chosen so that the final result is the global maximum. In any event, two procedures for computing the global maximum were also evaluated. An efficient systematic search routine for generating starting points for the local optimization routine is the method of Aird (Reference 10). Statistical methods like the Box-Wilson random scheme (Reference 11) were also investigated.

1. AIRD METHOD

The Aird algorithm was used in conjunction with the Powell search scheme, as illustrated in figure 24, to generate the global minimum from a set of local minima using the same optimization criterion as before (maximize efficiency). The vane angle space of the two variable vane stage-by-stage model searched for the global minimum was defined as:

$$\begin{aligned} -12.8 \text{ deg} < \alpha_1 < 48.8 \text{ deg} \\ -7.2 \text{ deg} < \alpha_2 < 33.7 \text{ deg} \end{aligned}$$

Fifty start points were generated in this vane angle interval to compute local minima. As suspected, quite a few local minima were located other than the design point. Some of these are tabulated in table 7 for a constant discharge area of 51.12 in.² Results are rounded off to the first decimal place for convenience. To adequately cover the search region, a large number of starting guesses was required, which is unacceptable in terms of the number of test points required to converge at the global optimum. Narrowing the search regions and increasing the incremental vane travel (0.1 deg was used for this study) would considerably reduce the number of start points.

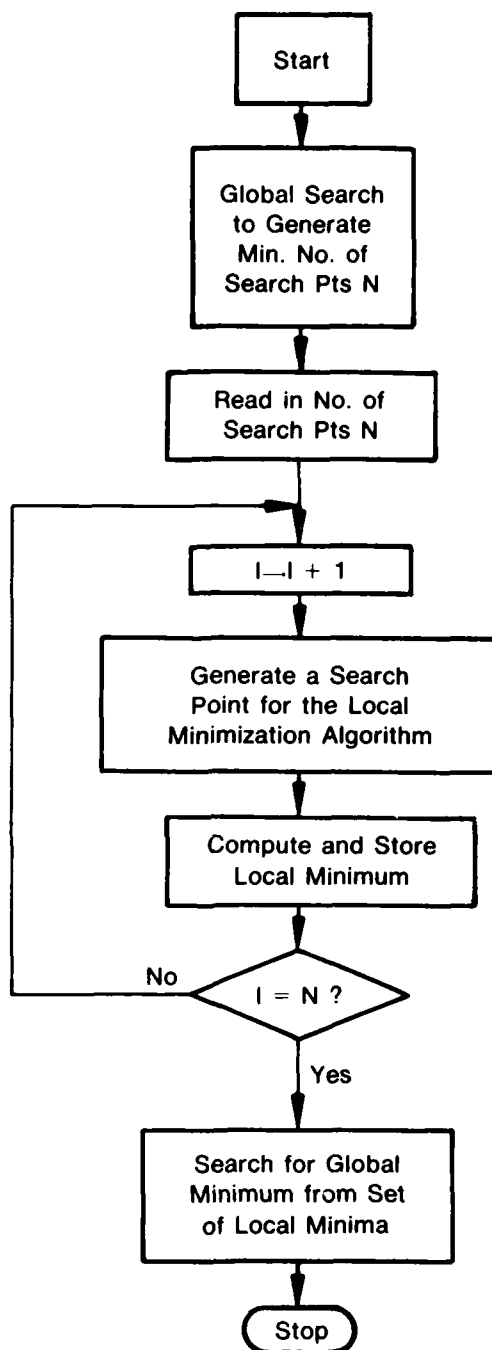
The point, corresponding to $\alpha_1 = -4$ deg and $\alpha_2 = 1.4$ deg is the global minimum. This global polyalgorithm was rather fast and the global minimum was located in the defined rectangle in 13 seconds of computer time on the IBM 3033 using single precision arithmetic.

2. BOX-WILSON METHOD

The Box-Wilson technique represents a procedure for reducing the number of experiments (test points) required to characterize the global optimum when a large number of factors (independent variables — vane angles and interstage bleed) are involved. The procedure calls for testing at three levels of each factor, fitting a quadratic curve (response surface) through the data obtained, and computing the optimum of the response surface. There are many variants of the Box-Wilson procedure, such as fractional factor experiments, and an extensive discussion of these is given by Myers (Reference 12). Here, a simple example of the applicability of Box-Wilson techniques was considered.

The problem at hand is Optimization Goal 1 in the matrix of optimization goals, viz., maximize efficiency. A Box-Wilson full factorial experiment at three levels involving nine ($3^2 = 9$ experiments — 3 levels, 2 factors: α_1, α_2) test points was carried out using the compressor simulation in the test region:

$$\begin{aligned} -5 \text{ deg} \leq \alpha_1 \leq +5 \text{ deg} \\ -5 \text{ deg} \leq \alpha_2 \leq +5 \text{ deg} \end{aligned}$$



FD 212399
811702
BT1 553

Figure 24. Global Polyalgorithm Consists of a Local Optimization Scheme and a Global Search Method

Table 7. Results of Global Search Method

Vane Angle		Efficiency	Airflow
α_1 (deg)	α_2 (deg)	η (%)	W_{H^*} (lb/sec)
-4.0	-4.4	73.6	101.0
-4.0	-1.4	73.9	100.0 (optimum point)
-3.9	-1.1	73.7	102.3
+35.0	-1.4	65.4	72.0
-3.7	-2.0	73.8	100.0
+0.9	-14.6	72.0	97.4
+0.2	-13.4	72.5	98.4
-3.9	-22.0	73.7	102.3

The three levels of α_1 and α_2 were:

$$\alpha_1 = -5, 0, +5 \text{ deg}$$

$$\alpha_2 = -5, 0, +5 \text{ deg}$$

Efficiency was computed at nine different levels of α_1, α_2 tabulated in table 8 and a response surface fitted through the η data.

Table 8. Results of a Box-Wilson Full Factorial Experiment

Vane Angle (deg)		Efficiency
α_1	α_2	η
-5	-5	0.734
-5	5	0.685
5	-5	0.680
5	5	0.625
0	0	0.703
-5	0	0.725
5	0	0.661
0	-5	0.720
0	5	0.660

Curve fitting a quadratic through this data (after scaling α_1 and α_2 by 5) resulted in

$$\begin{aligned} \eta(\alpha_1, \alpha_2) = & 0.7024 - 0.297 \times 10^{-1} \left(\frac{\alpha_1}{5} \right) - 0.273 \times 10^{-1} \left(\frac{\alpha_2}{5} \right) - 0.937 \times 10^{-2} \left(\frac{\alpha_1^2}{25} \right) \\ & - 0.1205 \times 10^{-1} \left(\frac{\alpha_2^2}{25} \right) - 0.1651 \times 10^{-2} \left(\frac{\alpha_1 \alpha_2}{25} \right) \end{aligned}$$

This yields for the optimum in the region $-5 \text{ deg} \leq \alpha_1, \alpha_2 \leq +5 \text{ deg}$

$$\alpha_1^{\text{opt}} = -5 \text{ deg} \quad \alpha_2^{\text{opt}} = -5 \text{ deg} \quad \eta^{\text{opt}} = 0.734$$

However, from previous results a global minimum exists at:

$$\alpha_1^{\text{opt}} = -4 \text{ deg} \quad \alpha_2^{\text{opt}} = -1.4 \text{ deg} \quad \eta^{\text{opt}} = 0.739$$

Thus, it was concluded that even through the Box-Wilson procedure results in many fewer test points than a global search technique, coarseness of the grid search may result in incorrect characterization of optima. For larger search regions, Box-Wilson techniques may result in grossly inaccurate results. Thus, efforts should concentrate on characterizing local minima using search techniques.

SECTION VIII

COPES/CONMIN APPROXIMATE OPTIMIZATION

As discussed in Section VI, CONMIN represents a general-purpose optimization program primarily designed for the optimization of constrained functions. The optimization algorithm used in CONMIN employs a direct search technique based on the Method of Feasible Directions. The algorithm has been modified to improve efficiency and numerical stability and to solve optimization problems in which one or more constraints are initially violated (Reference 13). While the program is intended primarily for efficient solution of constrained problems, unconstrained function optimization problems may also be solved, and the conjugate direction method of Fletcher and Reeves is used for this purpose. In a subroutine form, CONMIN can be called by a user-supplied main program. The user should supply a main program containing the analysis, constraints, equations, and objective function. Therefore, if an existing analysis program is used, the analysis portion may need some reorganization, and constraint equations must be prepared in accordance with CONMIN requirements.

In order to eliminate this inconvenience, a control program known as COPES (a FORTRAN Control Program for Engineering Synthesis) which is described in Reference 14 was developed by the same author as CONMIN. COPES combined with CONMIN enables the use of CONMIN as a "black box" for optimization in automated design synthesis. The user need only provide a FORTRAN analysis program for the particular problem being considered. COPES simply calls the user-supplied program written according to a simple set of guidelines. The capabilities of COPES/CONMIN include:

- Simple analysis
- Optimization
- Sensitivity analysis
- Two-variable function space generation
- Optimum sensitivity analysis
- Approximate optimization.

Particularly, the approximate optimization technique is suitable for the compressor vane optimization problem where the number of test points needed to perform the optimization is a limiting factor. Another advantage of this technique is the capability to handle measurement errors. The basic idea of approximate optimization technique involves sequentially optimizing an approximate design function surface that is generated from available information. In this program, the design surface represents a function of efficiency and stall margin. At the end of the optimization, the design surface is updated with information from a precise analysis, or test, at a new set of design variables. This new approximate problem is then optimized, following by a new precise analysis. This process repeats until the solution has converged.

COPES/CONMIN possesses the capability to do up to a second-order approximation. If excessive data are available, the extra data are applied to a weighted least-square fit, rather than in obtaining higher order approximations. If the problem at hand can be approximated by a quadratic function, the second-order approximation would be precise. The technique will work well on problems involving experimental measurements and finite step sizes of the independent variables.

An outline of the sequential approximation approach (Reference 15) is given below. The second-order approximate form derives from the Taylor series expansion of any function, as noted below.

$$\Delta f \approx \bar{\nabla} f \cdot \Delta \bar{x} + \frac{1}{2} \Delta \bar{x}^T [H] \Delta \bar{x}$$

where:

$$\Delta \bar{x} = \bar{x} - \bar{x}^0$$

$$\Delta f = f - f^0$$

$$\bar{\nabla} f = \left[\frac{\partial f}{\partial x_1} \quad \frac{\partial f}{\partial x_2} \quad \dots \quad \frac{\partial f}{\partial x_n} \right]^T$$

$$[H] = \begin{bmatrix} \frac{\partial^2 f}{\partial x_1^2} & \frac{\partial^2 f}{\partial x_1 \partial x_2} & \dots & \frac{\partial^2 f}{\partial x_1 \partial x_n} \\ & \frac{\partial^2 f}{\partial x_2^2} & & \\ & & \ddots & \\ & & & \frac{\partial^2 f}{\partial x_n^2} \end{bmatrix}$$

Symmetric

$$n = \text{number of design parameters}$$

$$\bar{x}^0 = \text{nominal design analyzed to yield } f^0.$$

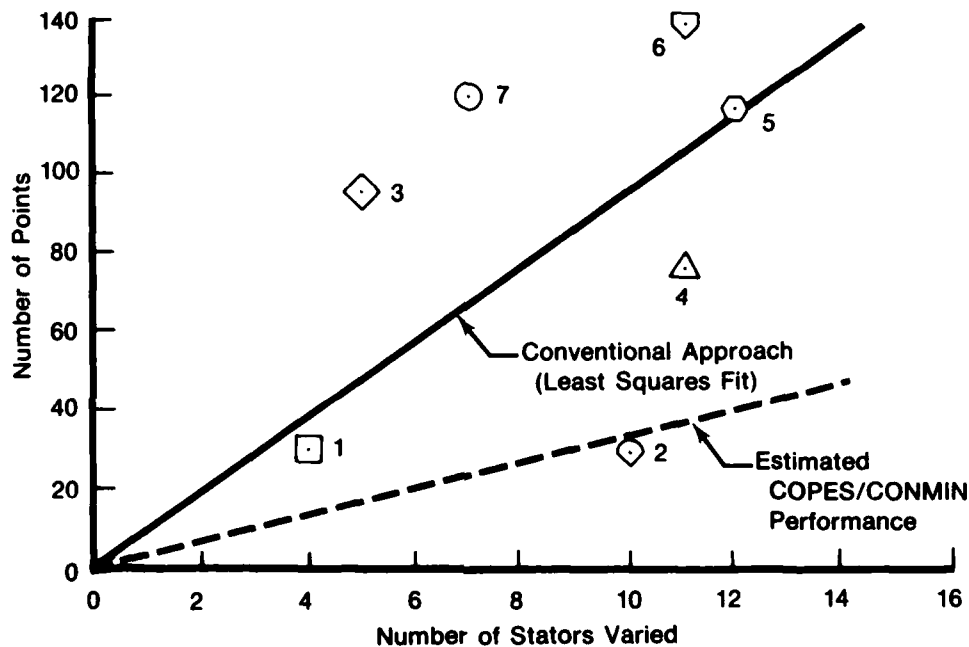
The Taylor series expansion holds for both objective and constraints. The unknowns are:

$$\frac{\partial f}{\partial x_1} \dots \frac{\partial f}{\partial x_n} \text{ and } \frac{\partial^2 f}{\partial x_1^2} \dots \frac{\partial^2 f}{\partial x_n^2}$$

for a total of $\ell = n + n(n+1)/2$. Since one analysis is required for the nominal design, a total of $\ell+1$ test points are required to determine the unknowns, $\bar{\nabla} f$ and $[H]$. If more than $\ell+1$ tests are available, a weighted least-square fit is used.

Since previous test data show that efficiency and stall margin can be closely approximated locally in quadratic form in terms of the vane angle, quadratic approximation in the compressor vane optimization is considered quite reasonable. The fact that analysis data obtained in one optimization are used to improve the design surface for subsequent optimization enables the test engineer to choose a new test point; i.e., the result obtained in one optimization becomes the recommended test point and the test result obtained at this point is added to the new approximate optimization problem.

Numerical experience shows that a full quadratic approximation is not necessarily required even when the design function surface is quadratic. An approximation that includes up to the diagonal terms of the Hessian matrix in the Taylor series expansion is quite accurate for a quadratic surface. This approximation requires a minimum of $2n+1$ test points (n tests for linear terms, n tests for diagonal terms of the Hessian matrix, and one test for the initial design point). If more than $2n+1$ designs are available, they are used in a weighted least-square fit. The COPES/CONMIN program provides the user with the option to use the approximate design surface constructed using only up to the Hessian diagonal terms in the approximate optimization. Figure 25 compares the estimated number of tests required for convergence with the efficiency optimization experience. Because this technique can significantly reduce the number of expensive test points without losing the quality of the solution, it was selected for implementation in a computer program for the optimization of vane and bleed settings in multistage axial compressors. In the following sections, the numerical results for example problems are presented.



FD 154179A

Figure 25. Comparison of Points Required for High-Speed Efficiency Optimization

1. NUMERICAL RESULTS — QUADRATIC SURFACE

a. Constrained Problem

The example considered here is defined as:

Find $\alpha_1, \alpha_2, \alpha_3, \alpha_4$ to maximize the efficiency η , while meeting a minimum stall margin requirement $SM \geq SM^0$, where,

$$\eta = 1 - \frac{(\alpha_1^2 + \alpha_2^2 + \alpha_3^2 + \alpha_4^2)}{1000}$$

$$SM = 22.5 + \frac{(\alpha_1^2 + \alpha_2^2 + \alpha_3^2 + \alpha_4^2)}{1000}$$

SM^0 = given value.

The functions for η and SM are not rigorously accurate expressions for real compressors, but are devised quadratic surfaces to study the approximate optimization technique. The initial five test points shown as Schedule A in table 9 were used in the first examples. Because of experimental conditions, at least one of the four vane angles was forced to change not less than one degree in each iteration. Additionally, to reduce experimental errors, vanes are not reset between tests with this sequence.

Table 9. Initial Test Points — Schedule A

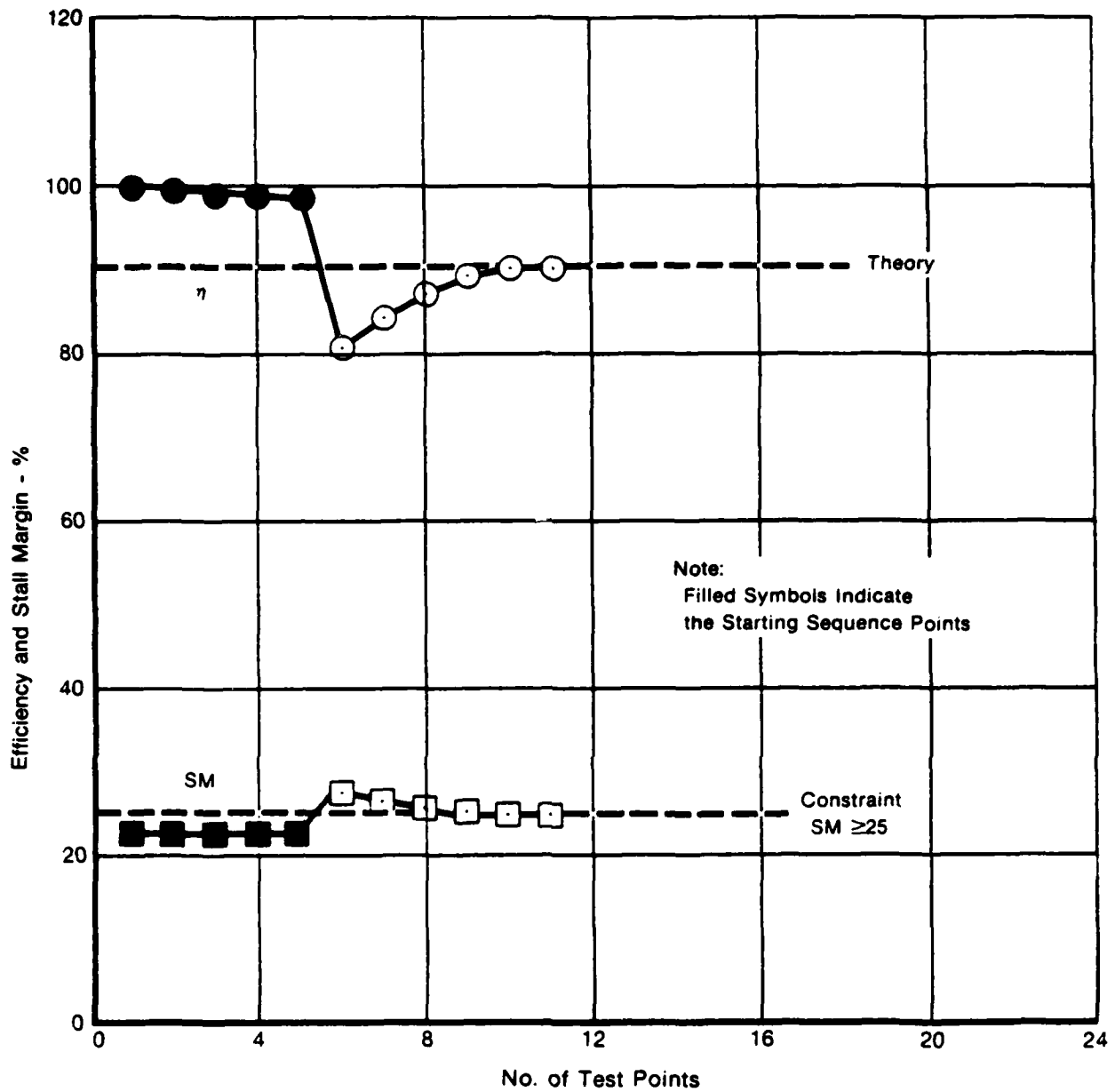
Test Point Number	Vane Angle (deg)			
	α_1	α_2	α_3	α_4
1	1	1	1	1
2	2	1	1	1
3	2	2	1	1
4	2	2	2	1
5	2	2	2	2

The stopping criteria used in this sequence are that (1) the number of test points are not less than 10 and (2) the change of each vane angle is less than 0.25.

Case 1. Maximize η subject to $SM \geq 25$

It was assumed that the exact values of η and SM were available; i.e., no experimental error or noise. As shown in figure 26, the result converged to the theoretical η in less than 12 test points. The values of η and SM corresponding to the initial points are depicted as the solid symbols in all the figures in this section.

Case 2. Maximize η subject to $SM \geq 25$



FD 181288A

Figure 26. Performance of COPES/CONMIN for Constrained Optimization Using Starting Schedule A

In order to take into account any measurement errors, the random errors shown in table 10 were added to the exact values obtained from the efficiency and stall margin equations. As shown in figure 27, a converged solution was obtained after 13 test points. The additional data points show that the system does not go unstable after the optimum is found.

Table 10. Measurement Error

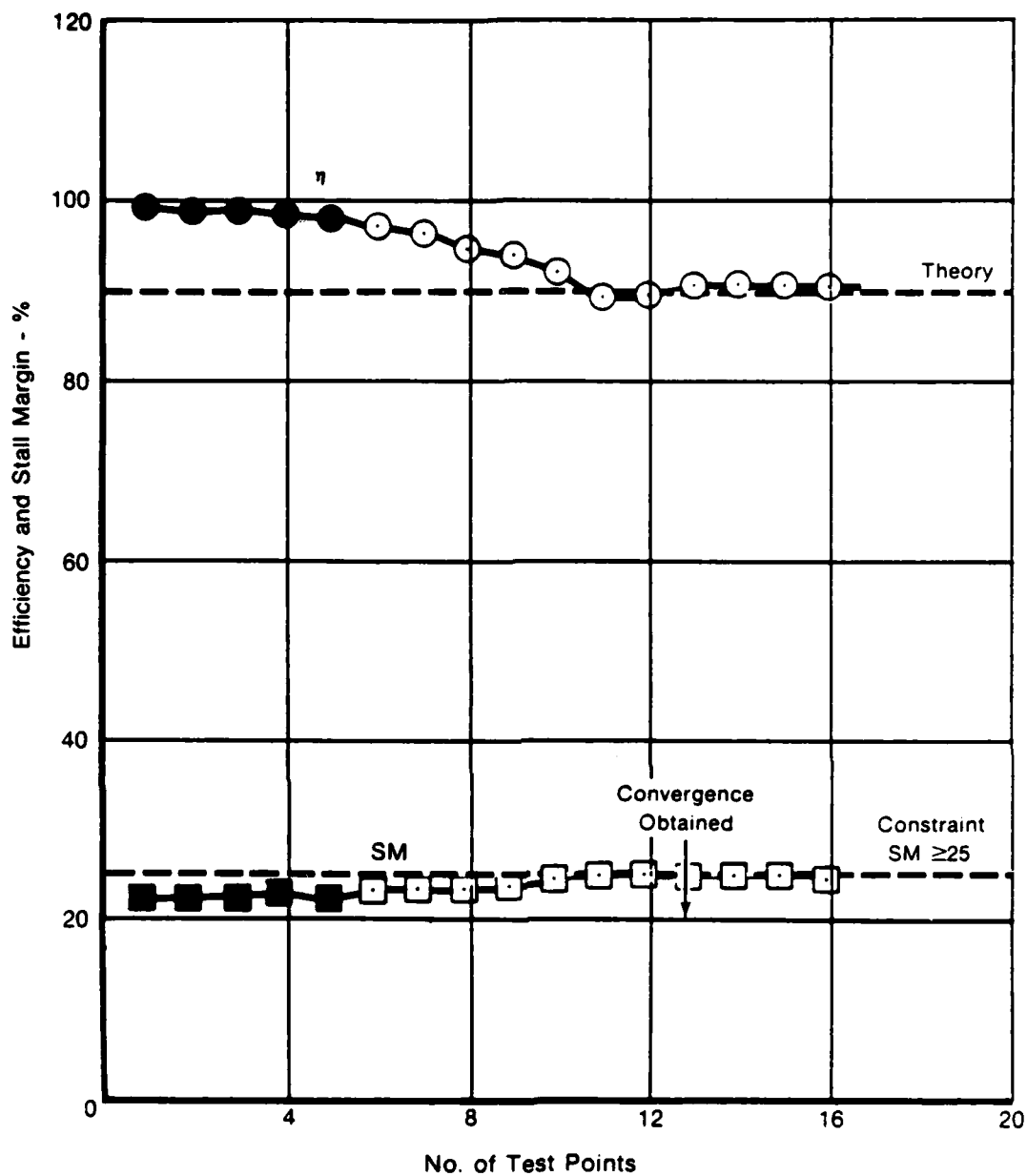
Test Point Number	Efficiency Error (%)	Stall Margin Error (%)	Test Point Number	Efficiency Error (%)	Stall Margin Error (%)
1	-0.10	0.10	9	0.20	-0.20
2	-0.15	0.15	10	-0.15	0.15
3	0.10	-0.10	11	0.10	-0.10
4	-0.20	0.20	12	-0.10	0.10
5	0.15	-0.15	13	-0.12	0.12
6	-0.15	0.15	14	0.08	-0.08
7	-0.12	0.12	15	0.00	0.00
8	0.13	-0.13	16		

As shown in figure 27, a slightly larger efficiency was obtained compared to the case without measurement error. Assuming that the errors are comparable to those in table 10, acceptable results can be obtained.

Case 3.

The same problem as Case 1 is considered, except that the initial starting sequence is modified. This example is designed to show the effect of randomly chosen initial starting points. Two sets of initial points were tested, as shown in tables 11 and 12.

Results based on starting Schedules B and C appear in figures 28 and 29, respectively. Converged solutions were obtained with 11 test points, the same as with Schedule A. The efficiency and stall margin converged to virtually the same values of $\eta=90\%$ and $SM=25\%$ for all three starting schedules. Thus, the analysis is relatively insensitive to the incremental vane angle used in starting sequence.



FD 181287A

Figure 27. Influence of Measurement Error on the Performance of COPES/CONMIN for Constrained Optimization Using Starting Schedule A

Table 11. Initial Test Points — Schedule B

Test Point Number	Vane Angle (deg)			
	α_1	α_2	α_3	α_4
1	1	1	1	1
2	3	1	1	1
3	3	3	1	1
4	3	3	3	1
5	3	3	3	3

Table 12. Initial Test Points — Schedule C

Test Point Number	Vane Angle (deg)			
	α_1	α_2	α_3	α_4
1	1	1	1	1
2	4	1	1	1
3	4	4	1	1
4	4	4	4	1
5	4	4	4	4

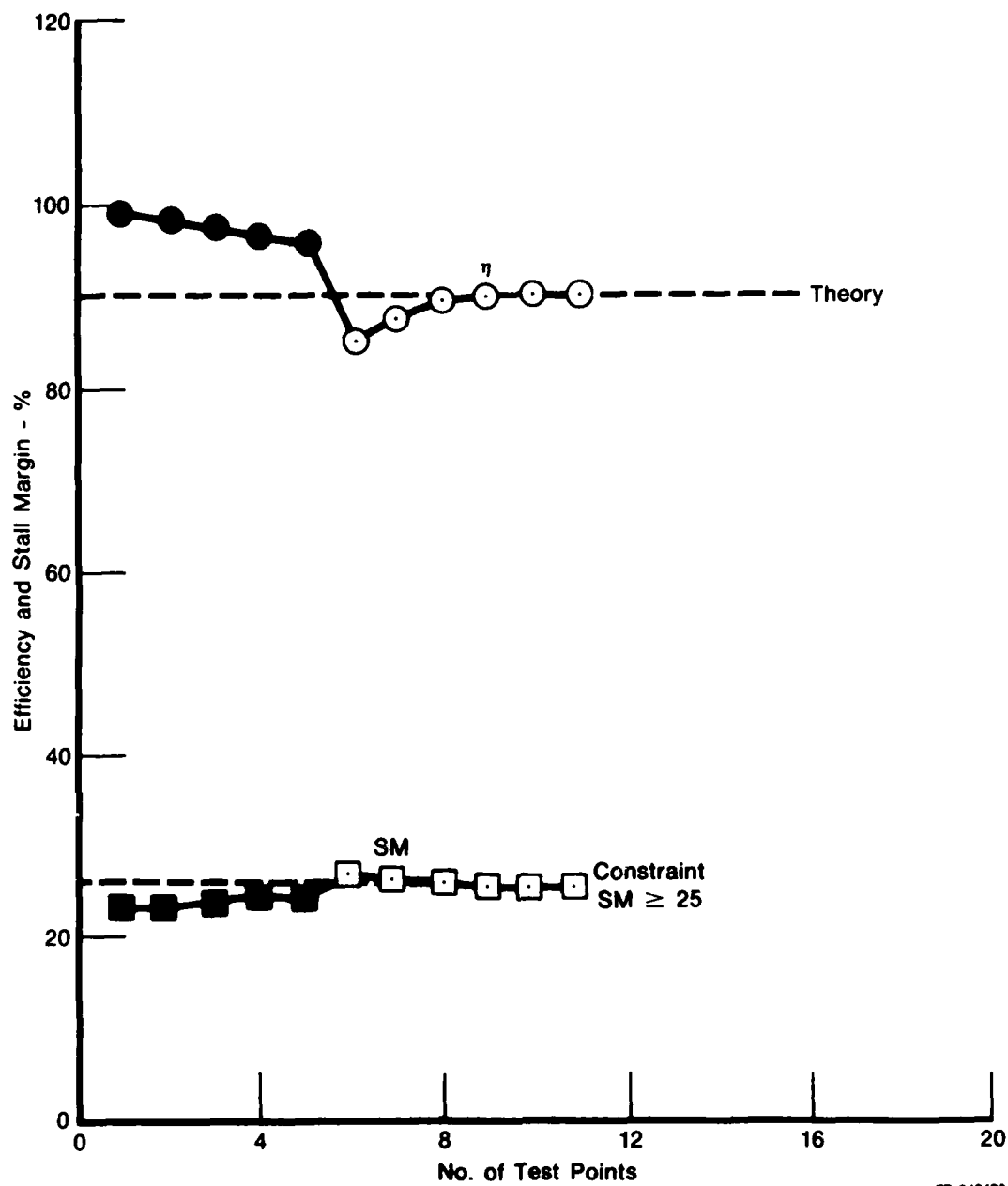
b. Unconstrained Problem

The objective of this example was to test a problem which is physically unconstrained, but mathematically constrained. Test engineers, therefore, can use the constrained optimization option by relaxing the constraint limits without switching to the unconstrained optimization option. The problem was defined as

Maximize η subject to $SM \geq 0$

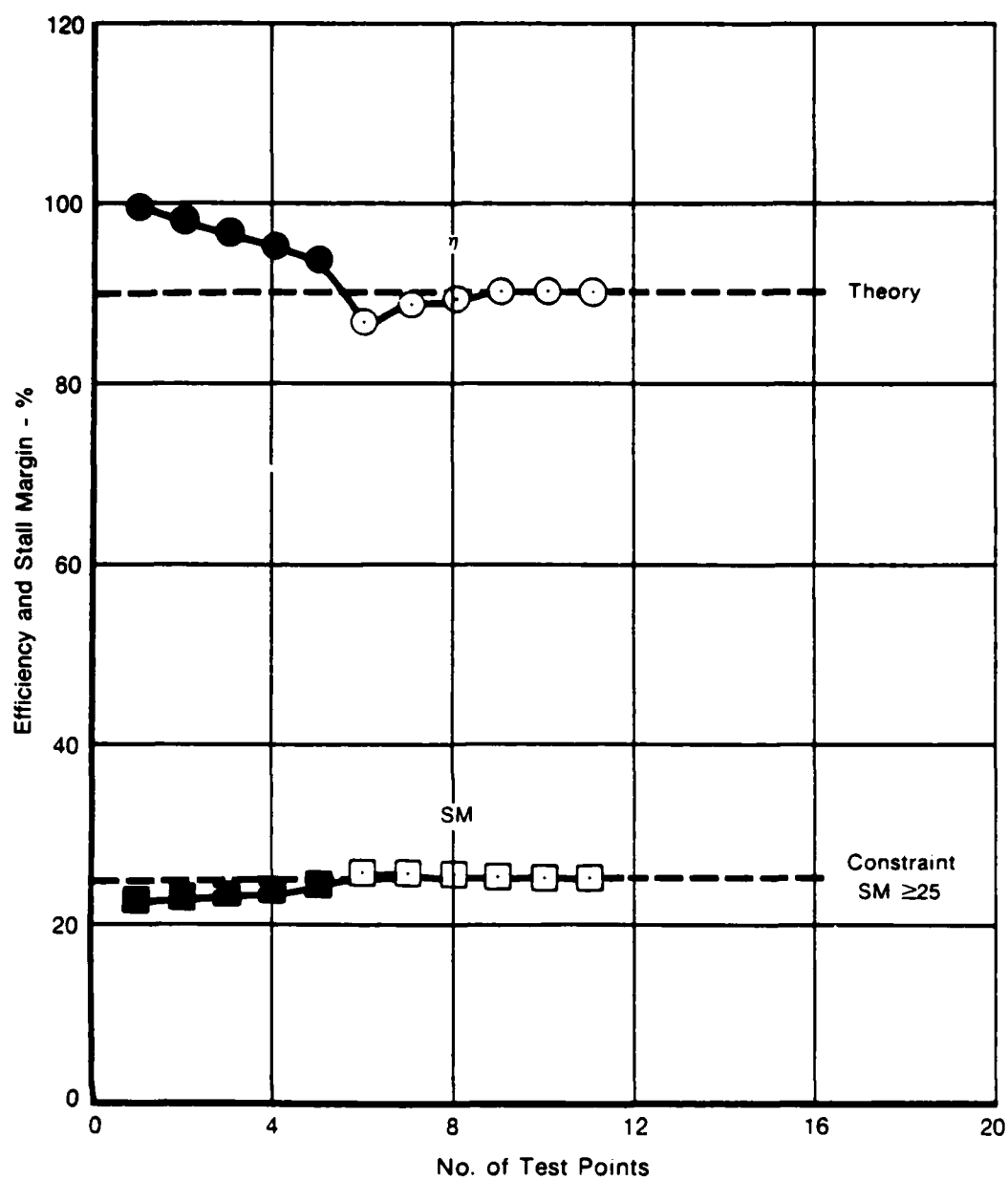
Since the stall margin is always greater than 22.5%, this problem is actually unconstrained even though it contains a constraint. A numerical experiment was carried out for the same cases of the constrained problem by simply setting $SM \geq 0$, instead of $SM \geq 25$. Results appear in figures 30 through 33. The optimizations converged to virtually the same solution, which was theoretically known. Vane angles at the converged solution for each case are tabulated in table 13. Theoretically, the known solution is:

$$\alpha_1 = \alpha_2 = \alpha_3 = \alpha_4 = 0 \text{ and } \eta = 100.$$



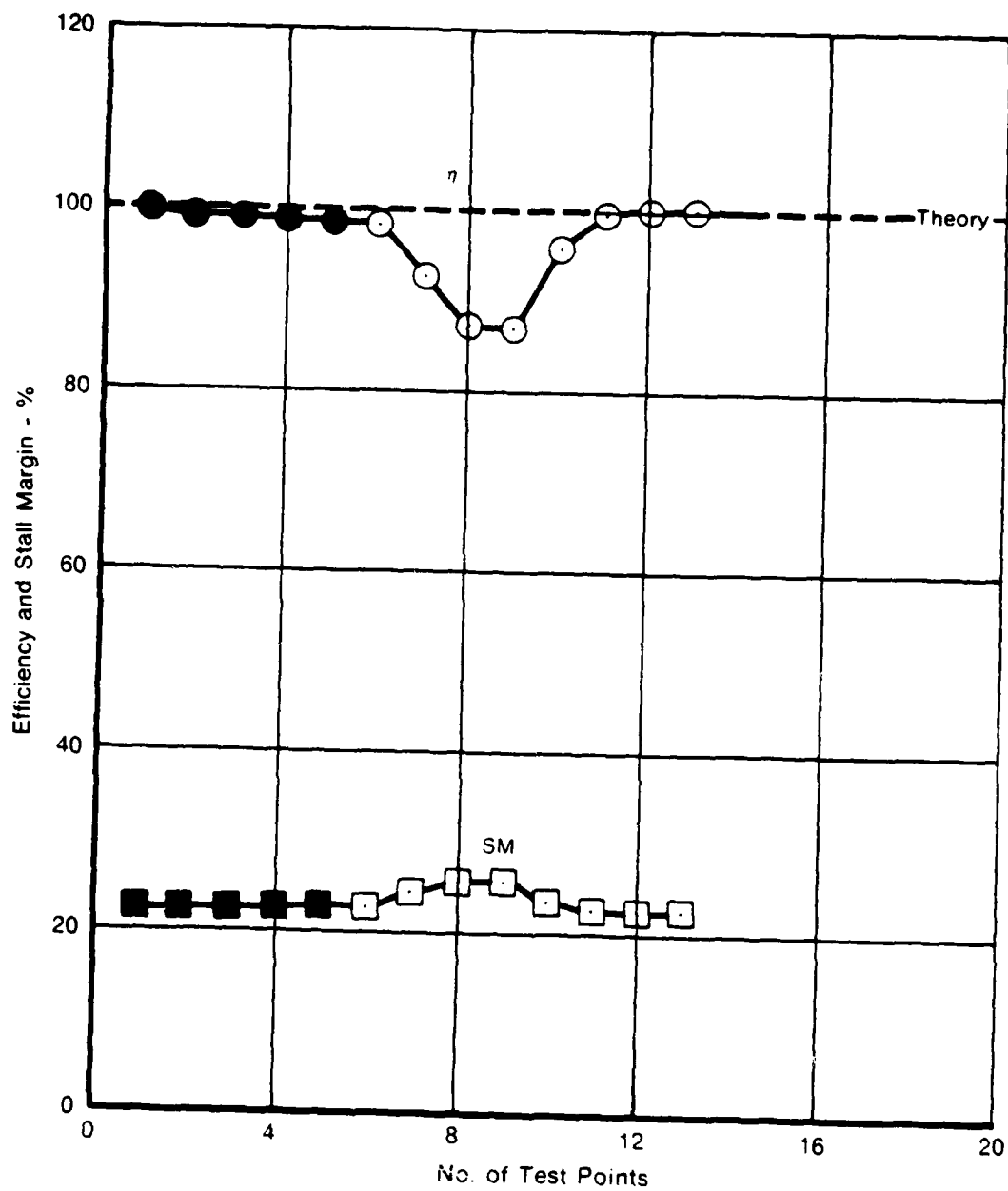
FD 212400

Figure 28. Performance of COPES/CONMIN for Constrained Optimization Using Starting Schedule B



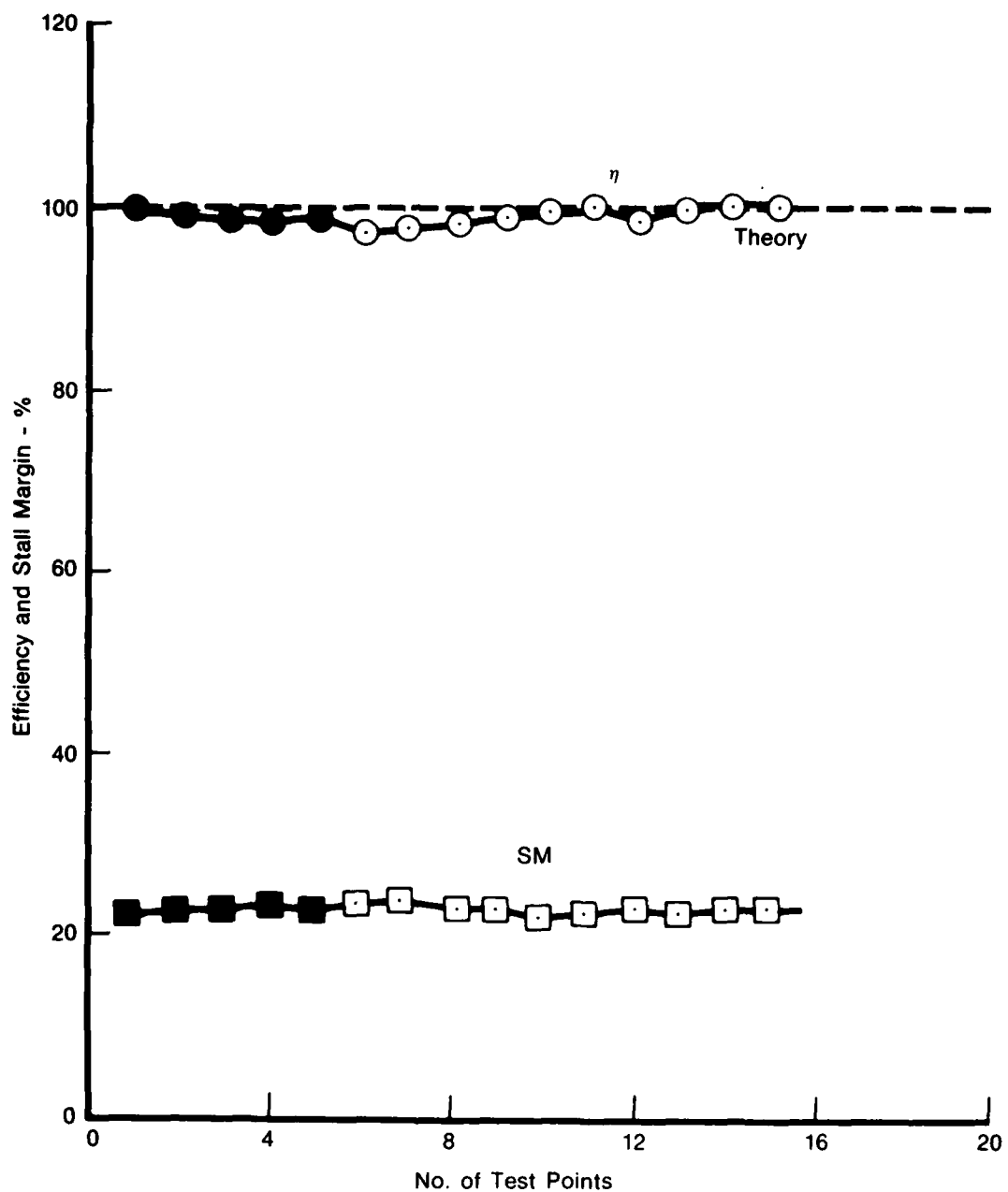
FD 181289A

Figure 29. Performance of COPES/CONMIN for Constrained Optimization Using Starting Schedule C



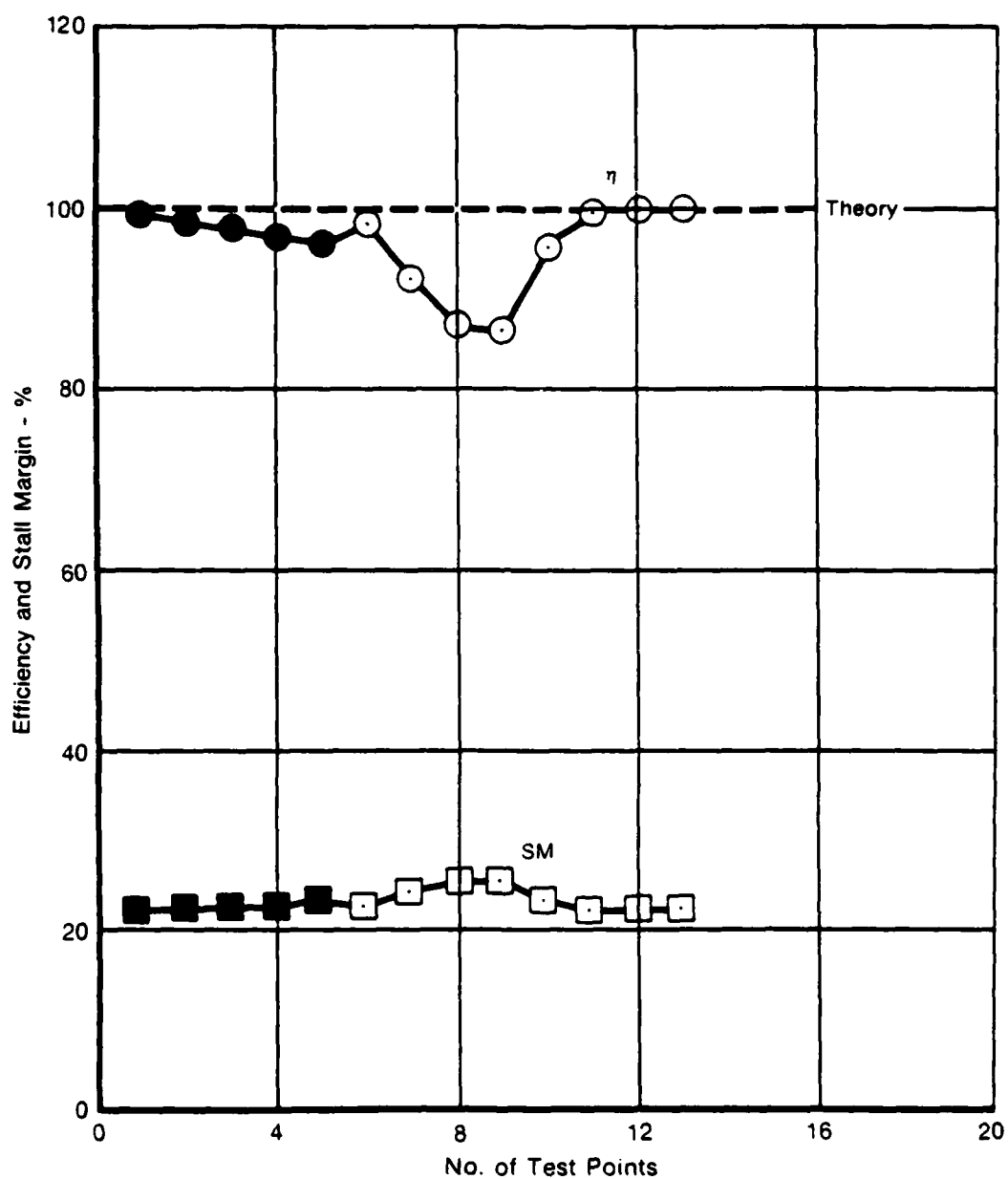
FD 181290A

Figure 30. Performance of COPES/CONMIN for Unconstrained Optimization Using Starting Schedule A



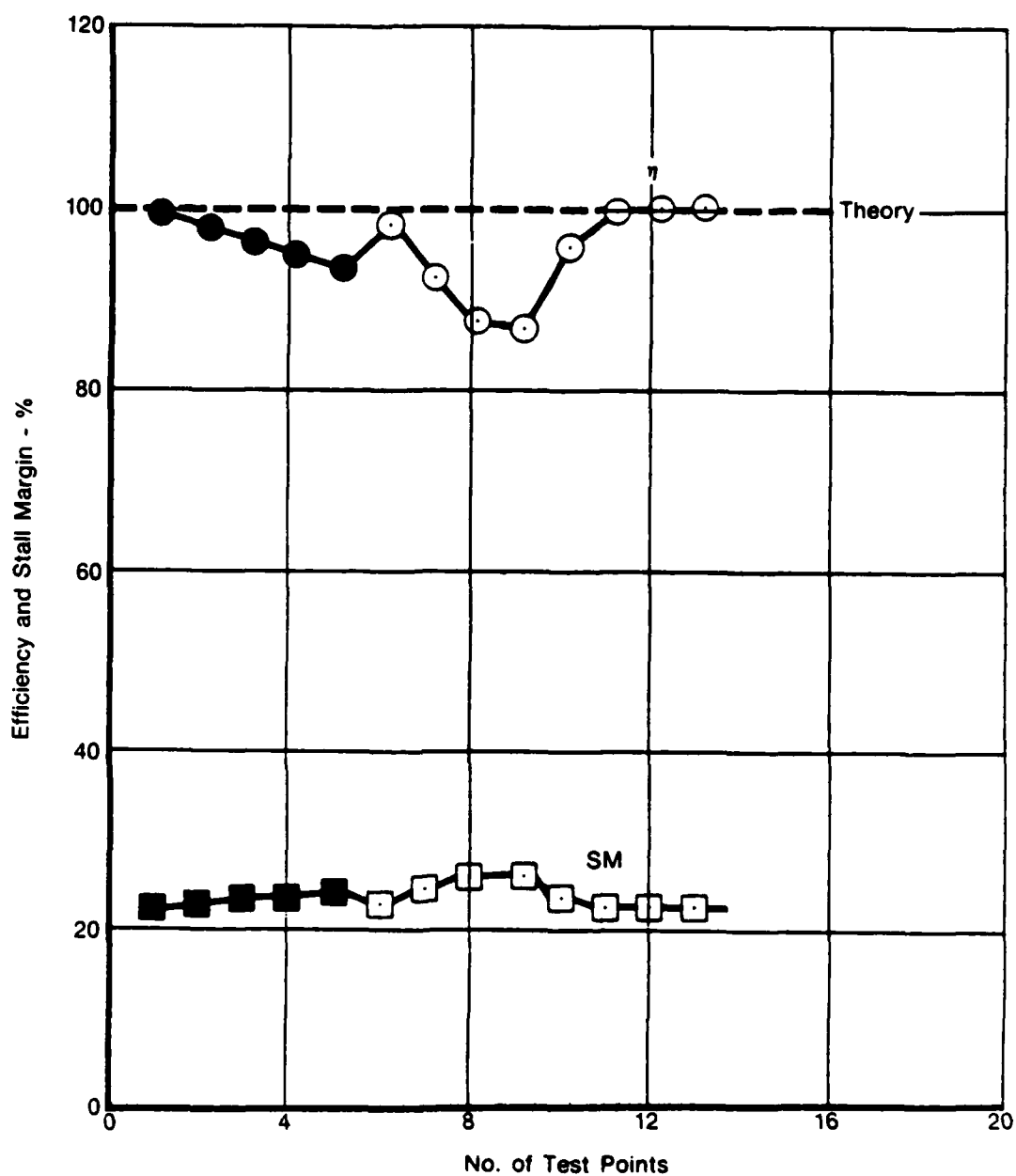
FD 212251

Figure 31. Influence of Measurement Error on the Performance of COPES/CONMIN for Unconstrained Optimization Using Starting Schedule A



FD 181292A

Figure 32. Performance of COPES/CONMIN for Unconstrained Optimization Using Starting Schedule B



FD 181293A

Figure 33. Performance of COPES/CONMIN for Unconstrained Optimization Using Starting Schedule C

Table 13. Optimum Vane Angles When $SM \geq 0$

Case Number	Vane Angle (deg)			
	α_1	α_2	α_3	α_4
1	-0.1109×10^{-4}	-0.3950×10^{-4}	0.5450×10^{-4}	0.1535×10^{-4}
2	-0.1109	0.2300	0.0353	0.0966
3B	0.1634×10^{-4}	-0.4675×10^{-4}	0.2186×10^{-4}	0.3511×10^{-4}
3C	0.2254×10^{-4}	0.2200×10^{-4}	0.1751×10^{-4}	0.9187×10^{-5}

2. NUMERICAL RESULTS — COMPRESSOR SIMULATION

Further evaluation of the COPES/CONMIN approximate optimization technique was performed using a stage-by-stage compressor simulation representative of an 11-stage, four-variable-vane compressor. The stall line used to provide the compressor performance appears in figure 34. The illustrations shown in figures 35 through 38 depict the efficiency and stall margin variations with vane angle computed at two degree increments, while holding speed and discharge area constant.

It should be noted that efficiency and stall margin calculations in the compressor simulation have an accuracy of $\pm 0.05\%$, which may be attributed to the following factors:

1. Stage characteristic modeling
2. Interpolations between stage characteristics
3. Flow balance iterations.

Thus, the performance calculations from this model can be considered to have an inherent $\pm 0.05\%$ measurement error.

The following paragraphs detail the results for various optimization goals using the optimization program on the stage-by-stage compressor simulation. A summary of the problems solved and the resulting solutions is presented in table 14. A complete documentation of the optimization path for each example is contained in Reference 1.

a. Unconstrained Optimization

Example 1:

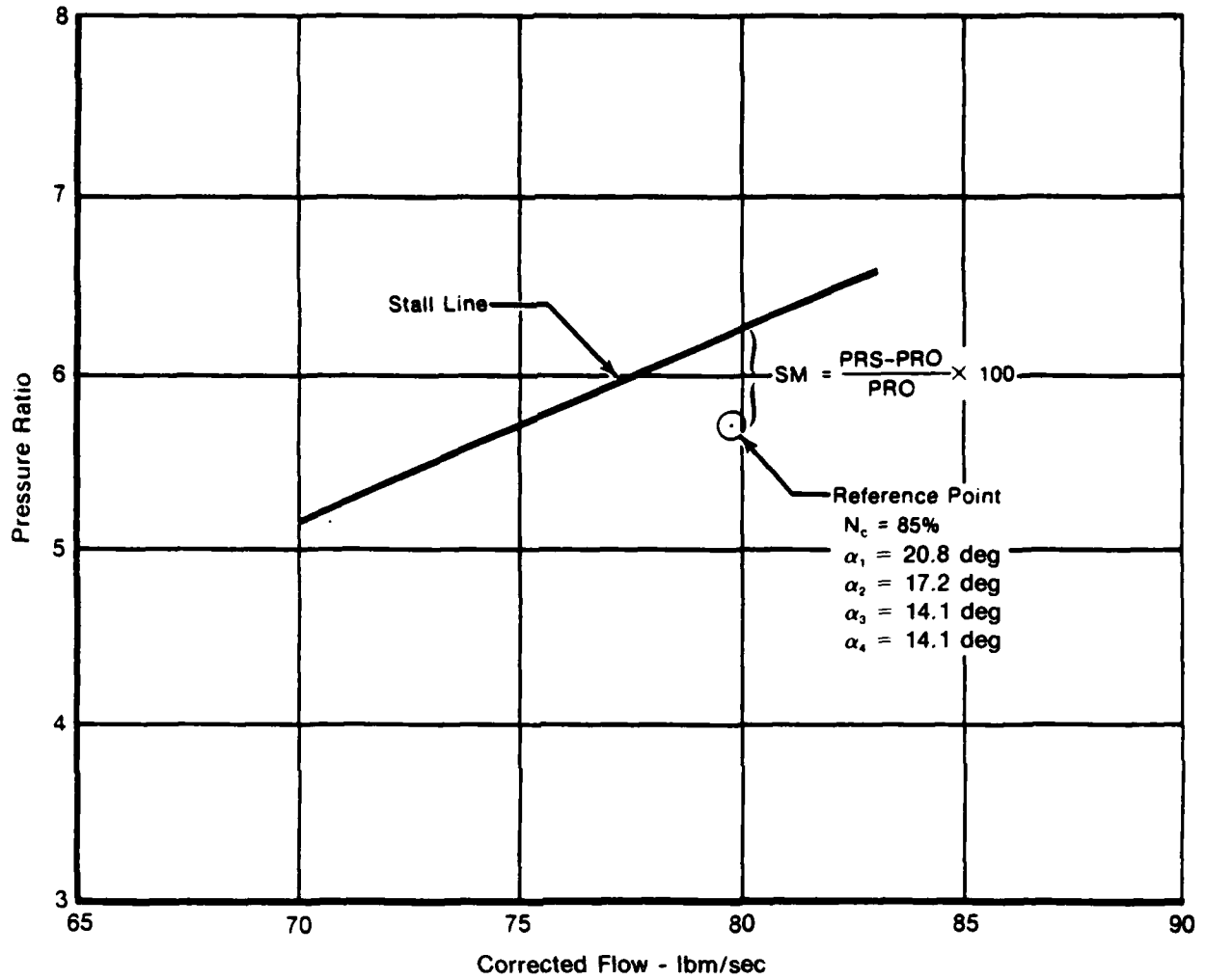
The objective of this problem involves the optimization of four variable vanes for maximum efficiency, while holding speed and discharge area constant (Optimization Goal 1). The optimization problem can be formulated as

$$\begin{aligned} \max \quad & \eta(\alpha_1, \alpha_2, \alpha_3, \alpha_4, N, \text{AREA}) \\ & \alpha_1, \alpha_2, \alpha_3, \alpha_4, N, \text{AREA} \end{aligned}$$

subject to

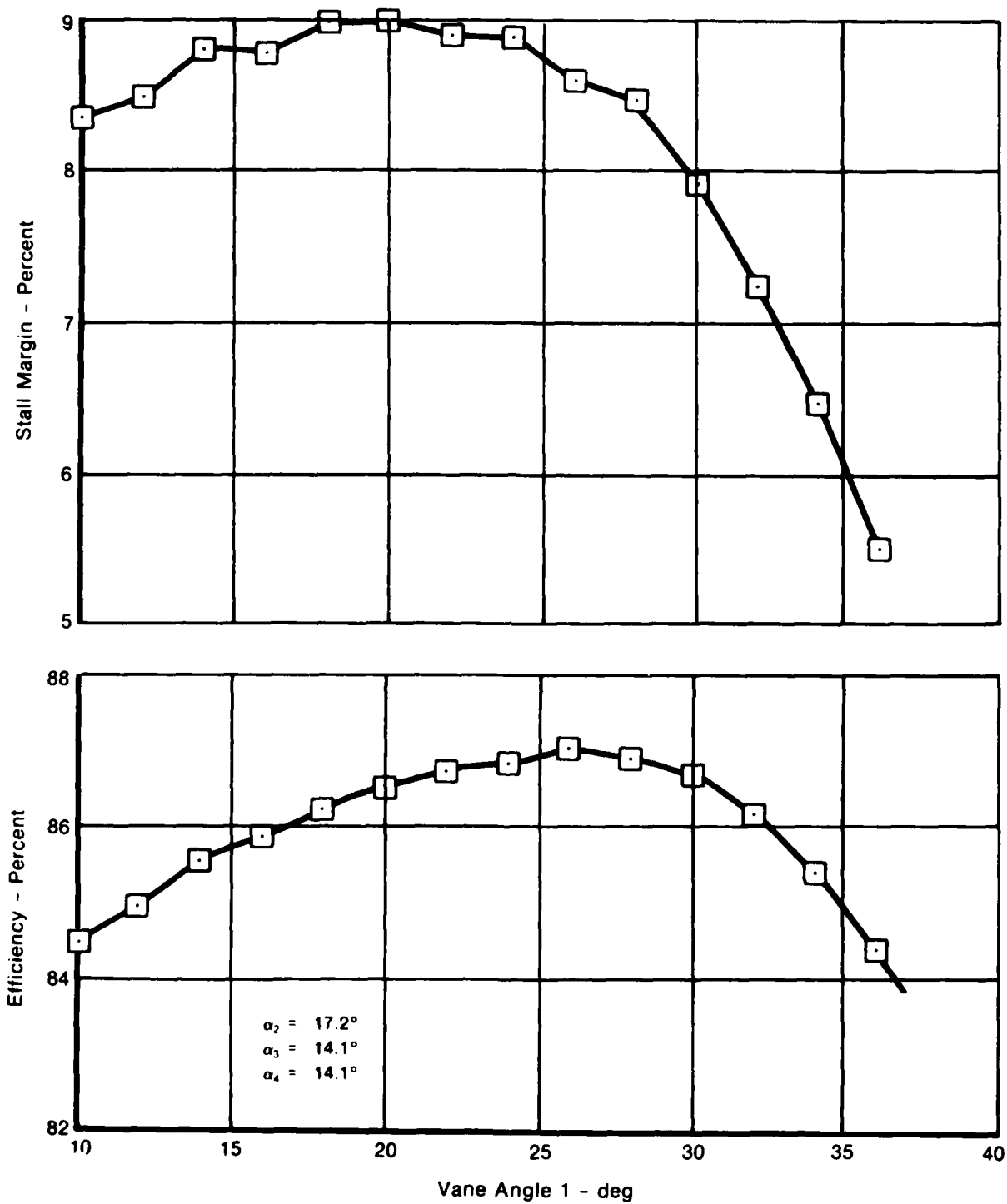
- $\alpha_{1_{\min}} \leq \alpha_1 \leq \alpha_{1_{\max}} \qquad \alpha_{2_{\min}} \leq \alpha_2 \leq \alpha_{2_{\max}}$
 $\alpha_{3_{\min}} \leq \alpha_3 \leq \alpha_{3_{\max}} \qquad \alpha_{4_{\min}} \leq \alpha_4 \leq \alpha_{4_{\max}}$
- $\text{AREA} = \text{AREA}_0 = 76.779$
- $N = N_0 = 5567.5 \text{ rpm } (\% \text{ } N_c = 85)$

The upper and lower bounds imposed on vane travel appear in table 15.



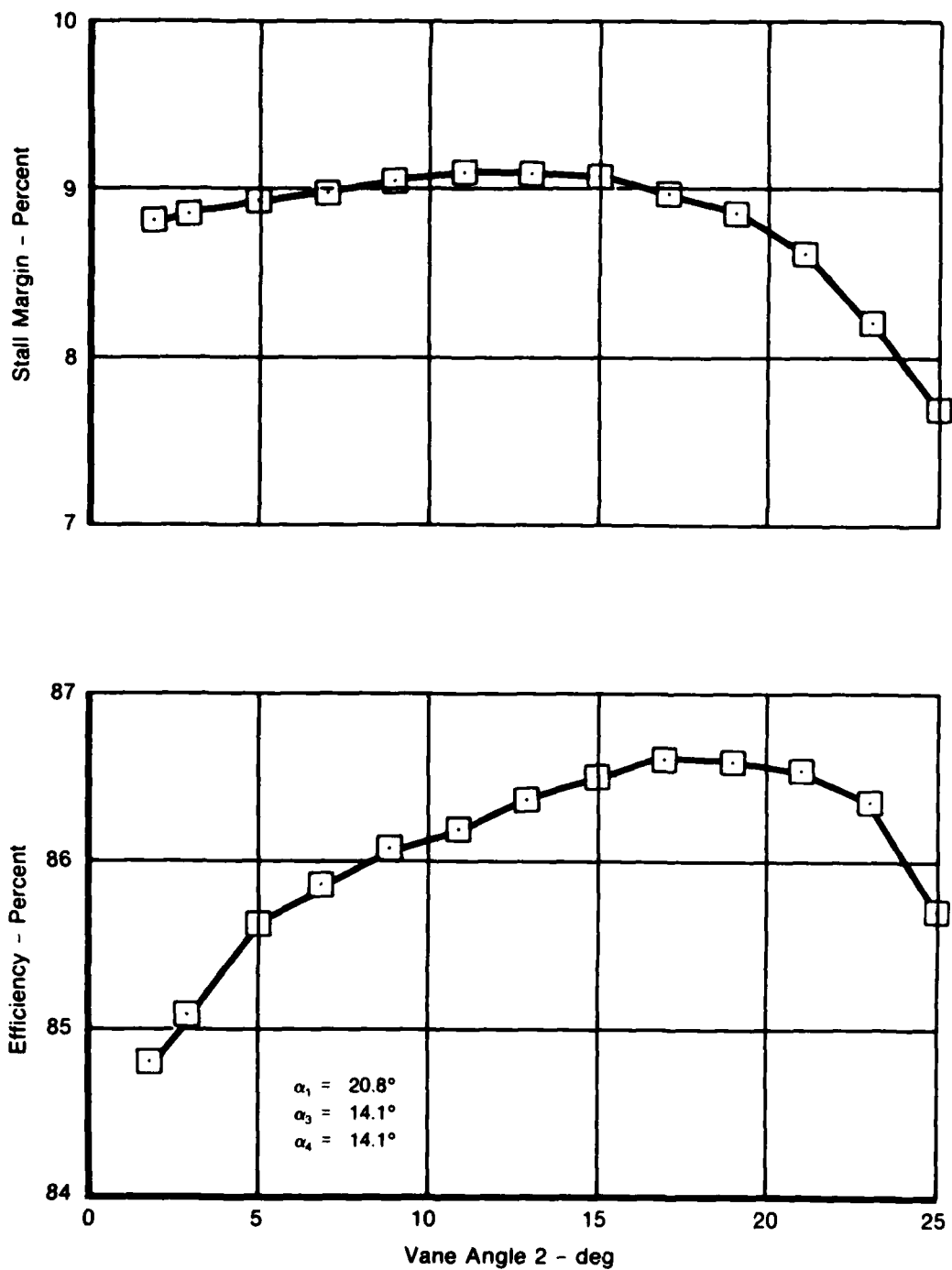
FD 181294A

Figure 34. Compressor Model Performance Map



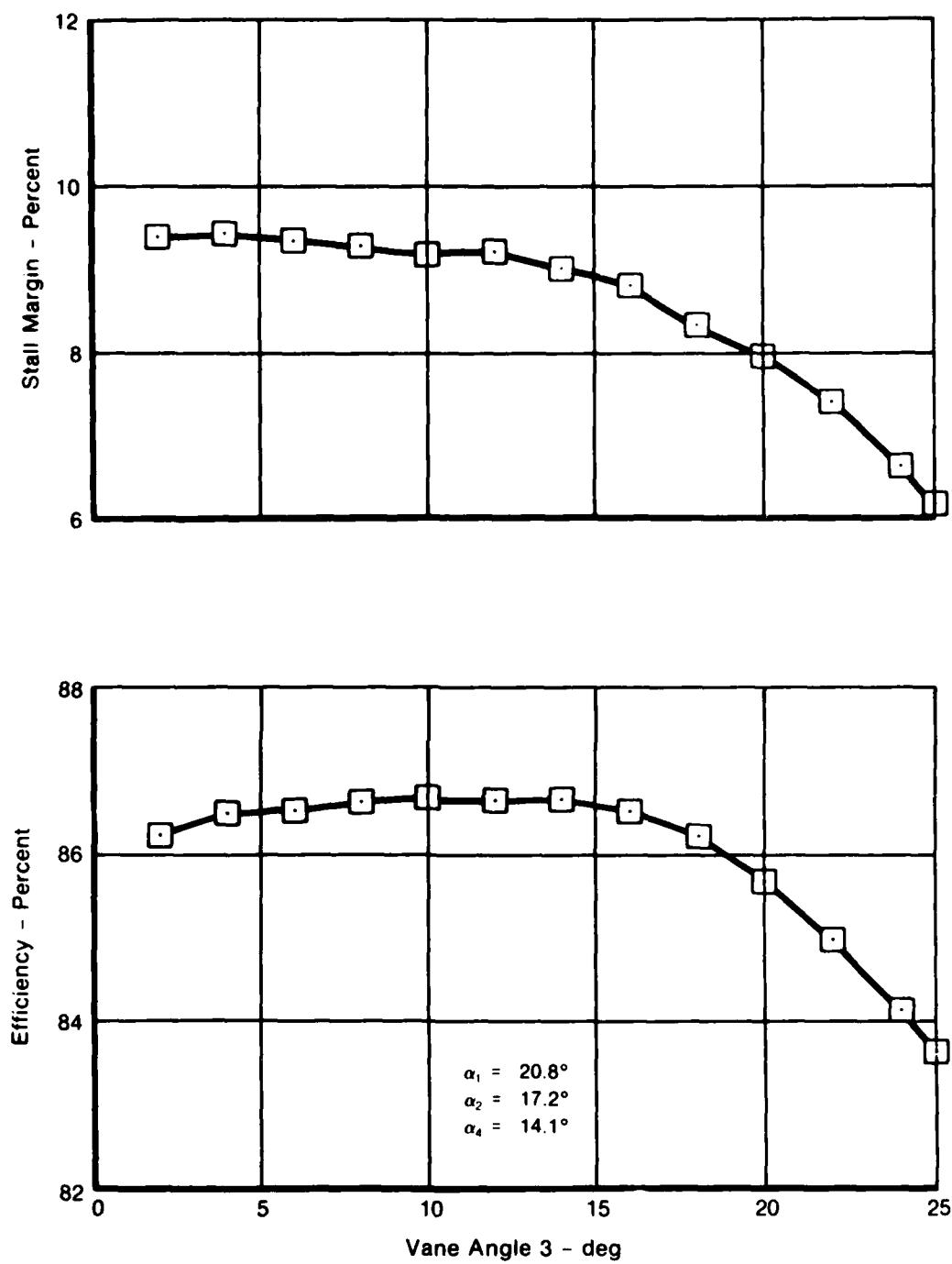
FD 161295

Figure 35. Efficiency and Stall Margin Variation with Variable Vane 1



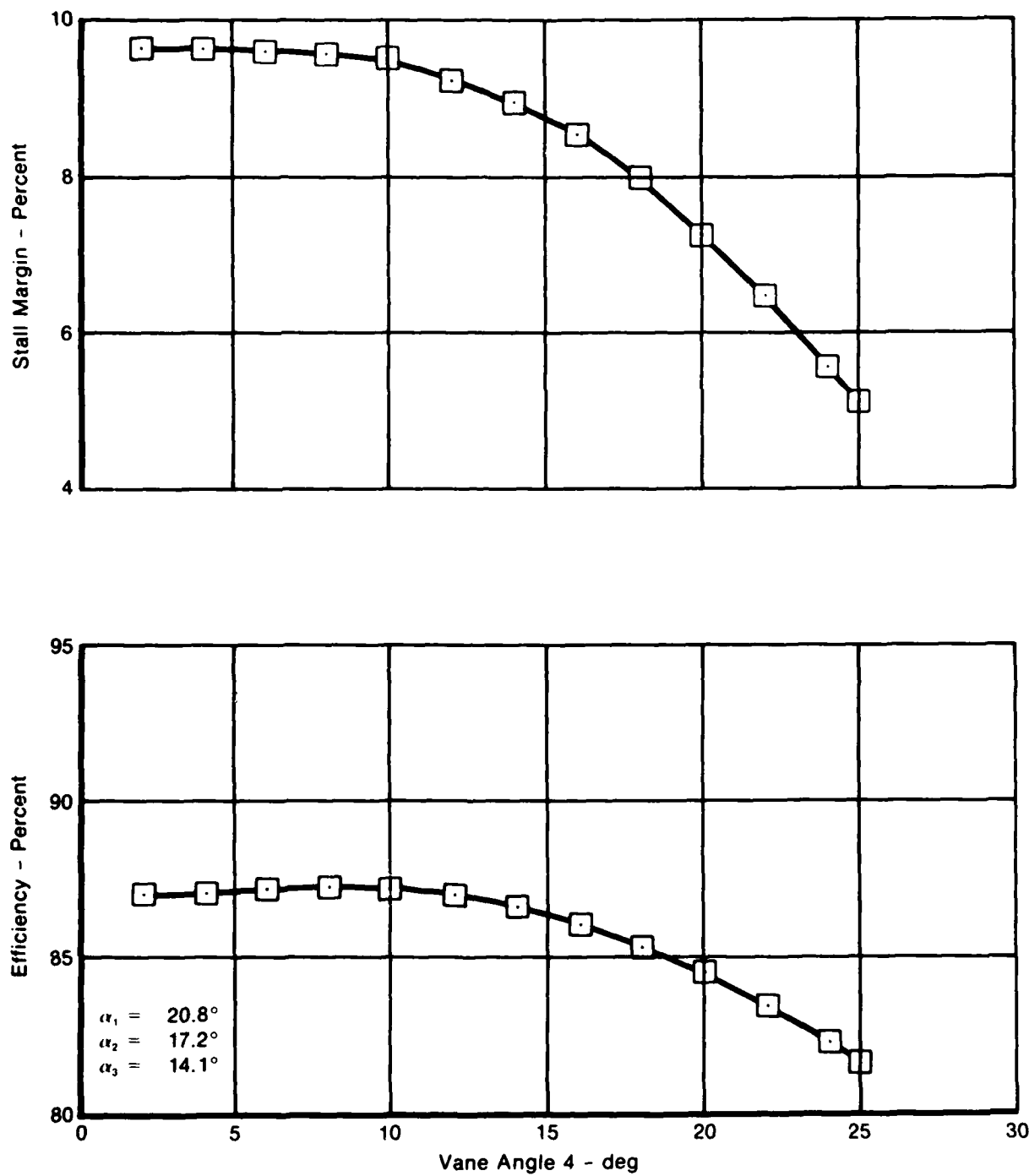
FD 181296

Figure 36. Efficiency and Stall Margin Variation with Variable Vane 2



FD 181297

Figure 37. Efficiency and Stall Margin Variation with Variable Vane 3



FD 181298

Figure 38. Efficiency and Stall Margin Variation with Variable Vane 4

Table 14. Summary of Optimization Examples Solved

Example Number	Optimization Goal	Vane Angle (deg)			Pressure Ratio	Corrected Flow (lbm/sec)	Efficiency (%)	Stall Margin (%)	Test Point Number at Optimum
		α_i	α_r	α_t					
1	Maximize η	25.59	17.99	12.17	7.47	—	87.53	9.32	15
2	Maximize η	24.55	17.78	11.68	7.76	—	87.52	9.45	15
3	Maximize SM	18.94	10.71	5.00	5.00	—	86.73	10.30	22
4	Maximize η with SM ≥ 10.0	23.73	15.58	7.29	5.37	—	87.39	10.00	10
5	Maximize η with SM ≥ 10.0	22.64	14.72	9.24	5.00	—	87.38	9.98	15
6	Maximize SM with $\eta \geq 87.3$	22.34	14.54	8.87	5.00	—	87.32	10.09	21
7	Maximize Wc with $\eta \geq 87.0$ and SM ≥ 8.5	20.08	10.31	5.85	5.00	84.39	86.81	10.19	14
8	Minimize Wc with $\eta \geq 87.0$ and SM ≥ 8.5	27.93	19.92	15.72	9.54	77.65	87.20	8.47	15
9	Maximize PR with $\eta \geq 87.0$ and SM ≥ 8.5	21.06	10.17	5.01	5.01	6.105	86.82	10.15	15

Table 15. Vane Travel Limits

	Vane Angle (deg)			
	α_1	α_2	α_3	α_4
Lower Bound	10	5	5	5
Upper Bound	35	25	25	25

With initial vane settings of $\alpha_1=29$ deg, $\alpha_2=18$ deg, $\alpha_3=15$ deg, and $\alpha_4=11$ deg, and initial efficiency of 87.14%, convergence to the optimum efficiency of 87.53% occurs in 15 tests (10 iterations). Optimum vane angle settings become $\alpha_1=25.59$ deg, $\alpha_2=17.99$ deg, $\alpha_3=12.17$ deg, and $\alpha_4=7.47$ deg. The incremental vane angle variation used for the initial sequence of 5 tests is -2 deg.

Example 2:

This problem duplicates Example 1, except that the initial sequence is modified. Design of the example evaluates the effect of randomly selecting the initial test points.

With initial vane angles set at $\alpha_1=18$ deg, $\alpha_2=10$ deg, $\alpha_3=5$ deg, and $\alpha_4=5$ deg, and efficiency (η) = 86.60%, convergence occurs in 19 tests, although optimization was reached at the fifteenth test point. Optimum vane angles become $\alpha_1=24.55$ deg, $\alpha_2=17.78$ deg, $\alpha_3=11.68$ deg, and $\alpha_4=7.76$ deg at an efficiency of 87.52%. A 2 deg incremental vane angle variation was used for the initial sequence of tests in this example.

The fact that the optimum efficiency duplicates that found in the first example indicates that the analysis is relatively insensitive to starting point. The optimum vane angle settings, however, are slightly different for the two examples, although they are within 1 deg of each other. The compressor model exhibits a very flat region near the optimum with little gain in efficiency. This fact also contributed to the additional tests required in the second example to meet the convergence criteria after the optimum was reached.

Example 3:

The objective of Example 3 is to maximize stall margin while holding speed and discharge area constant (Optimization Goal 7). The problem can be expressed as

$$\begin{aligned} &\max \text{ SM} \\ &\alpha_1, \alpha_2, \alpha_3, \alpha_4 \end{aligned}$$

With the same initial vane settings and initial test sequence as in Example 1, the optimum settings were obtained after 22 test points. The vane settings are $\alpha_1 = 18.94$ deg, $\alpha_2 = 10.71$ deg, $\alpha_3 = 5.00$ deg, and $\alpha_4 = 5.00$ deg with an optimum stall margin at 10.30%. The efficiency at these vane settings is 86.73%.

b. Constrained Optimization

Example 4:

The function maximized in Examples 1 and 2 is now solved with stall margin constrained above a given level (Optimization Goal 4). The stall margin at the optimum efficiency conditions in the previous examples are 9.32 and 9.45%, respectively. Mathematically, this problem can be stated as

$$\max \eta \text{ subject to } SM \geq 10.0\%$$

$$\alpha_1, \alpha_2, \alpha_3, \alpha_4$$

With the same initial vane settings and initial test conditions as Example 1, a converged solution results in 14 tests at $\alpha_1 = 23.73$ deg, $\alpha_2 = 15.58$ deg, $\alpha_3 = 7.29$ deg, and $\alpha_4 = 5.37$ deg with an efficiency at 87.39% and stall margin of 10.00%. Note that the optimization algorithm brought the efficiency down from the 87.5% values in Examples 1 and 2 to meet the stall margin constraint.

Example 5:

The same problem as Example 4 is considered, except that the influence of measurement error on convergence ability is examined. In addition to the $\pm 0.05\%$ noise in the stage-by-stage model, the random errors shown in table 16 are added to the performance values. The errors are normally distributed with a standard deviation of 0.05.

Table 16. Measurement Errors for Example 5

Test Point Number	Efficiency Error (%)	Stall Margin Error (%)
1	0.04	-0.04
2	-0.02	0.04
3	-0.03	0.09
4	0.03	-0.02
5	0.09	0.06
6	-0.02	-0.08
7	0.00	0.04
8	-0.06	0.00
9	0.01	0.01
10	0.02	0.00
11	0.06	0.08
12	0.02	0.00
13	-0.03	0.07
14	-0.04	-0.02
15	0.02	0.07
16	0.11	-0.01
17	0.01	-0.03
18	0.07	-0.02
19	-0.04	-0.06
20	0.05	-0.05
21	0.08	0.03
22	-0.03	0.04

The optimum was reached in 15 tests at $\alpha_1 = 22.64$ deg, $\alpha_2 = 14.72$ deg, $\alpha_3 = 9.24$ deg, and $\alpha_4 = 5.0$ deg with efficiency at 87.38% and stall margin at 9.98%. The efficiency and stall margin are essentially the same as the values obtained in Example 4 and the vane angles are within 2.0 deg.

Example 6:

This problem represents the constrained version of Example 3. Here, it is desired to maximize stall margin while maintaining efficiency above a given level (Optimization Goal 10). Mathematically, this can be represented as

$$\max SM \text{ subject to } \eta \geq 87.3\%$$

$$\alpha_1, \alpha_2, \alpha_3, \alpha_4$$

With start settings for vane angle as in Example 3, the optimum solution was reached after 21 tests at vane settings of $\alpha_1 = 22.34$ deg, $\alpha_2 = 14.54$ deg, $\alpha_3 = 8.87$ deg, and $\alpha_4 = 5.00$ deg with an optimum stall margin of 10.09% and an efficiency of 87.32%. Here, the optimization algorithm brought the stall margin down from 10.30% obtained in Example 3 to meet the efficiency constraint.

Example 7:

The next two examples establish the maximum and minimum flow points to provide the maximum flow range. In addition to airflow requirements, performance constraints of minimum acceptable efficiency and stall margin also define the flow range. Thus, their evaluations must be considered for each geometry setting. For this example, Optimization Goal 14 is defined as

$$\begin{aligned} &\max Wc \text{ with } \eta \geq 87.0\% \text{ and } SM \geq 8.5\% \\ &\alpha_1, \alpha_2, \alpha_3, \alpha_4 \end{aligned}$$

subject to the conditions of holding speed constant at 5567.5 rpm and discharge valve area at 76.779 in.².

For the initial test sequence used in Examples 1 and 3 through 6, the optimization algorithm converged to the maximum flow in 14 tests at a corrected flow of 84.39 lbm/sec with an efficiency of 86.81% and stall margin of 10.19%. Optimum vane settings are $\alpha_1 = 20.08$ deg, $\alpha_2 = 10.31$ deg, $\alpha_3 = 5.85$ deg, and $\alpha_4 = 5.0$ deg.

Example 8:

This example deals with minimizing corrected airflow (Optimization Goal 15), mathematically formulated as

$$\begin{aligned} &\min Wc \text{ with } \eta \geq 87.0\% \text{ and } SM \geq 8.5\% \\ &\alpha_1, \alpha_2, \alpha_3, \alpha_4 \end{aligned}$$

subject to holding speed and discharge area constant.

With the same initial test sequence as in Example 7, the minimum corrected airflow of 77.65 lbm/sec was reached in 15 tests at $\alpha_1 = 27.93$ deg, $\alpha_2 = 19.92$ deg, $\alpha_3 = 15.72$ deg, and $\alpha_4 = 9.54$ deg with an efficiency of 87.02% and stall margin of 8.47%.

Example 9:

As a final example, the pressure ratio is maximized at constant speed and discharge area while maintaining minimal acceptable values of efficiency and stall margin (Optimization Goal 17). The problem solution can be stated as

$$\begin{aligned} &\max PR \text{ with } \eta \geq 87.0\% \text{ and } SM \geq 8.5\% \\ &\alpha_1, \alpha_2, \alpha_3, \alpha_4 \end{aligned}$$

This example converged in 15 tests at a maximum pressure ratio of 6.105 with an efficiency of 86.82% and stall margin of 10.15%. The optimum vane settings are $\alpha_1 = 21.06$ deg, $\alpha_2 = 10.17$ deg, $\alpha_3 = 5.01$ deg, and $\alpha_4 = 5.01$ deg.

In summary, the various results obtained for the compressor simulation (table 14) are very satisfactory. In each case the number of test points is close to the estimated performance of the COPES/CONMIN approximate optimization algorithm. Thus, the technique can be expected to reduce the number of tests currently required to optimize multistage axial compressors.

SECTION IX CONCLUSIONS

A comparative evaluation of optimization techniques applied to the optimization of vane and bleed settings in multistage axial compressors has been performed. The prime considerations in the evaluation were: (1) the number of test points required to achieve an optimum performance goal, (2) the ability to handle performance and aeromechanical constraints, (3) the sensitivity to measurement errors, and (4) the effect of finite vane travel and bleed flow variations.

It is concluded that the COPES/CONMIN approximate optimization technique is capable of guiding the optimization of compressor vane and bleed settings. The approximate optimization approach works well on problems involving experimental measurements and finite step sizes of the independent variables. Minimum incremental vane angles of 0.5 degree, and efficiency and stall margin tolerances of $\pm 0.2\%$ were considered. Use of only up to the Hessian diagonal terms in the Taylor series expansion defining the design function surface has the potential to optimize a four-variable-vane compressor in about fifteen tests. Compared to current optimization procedures, the potential exists with this approach to significantly reduce the number of data points and test time required to perform the optimization.

The generally good agreement between analytic functions and compressor simulations with results from the optimization technique is very encouraging. However, the full range or reliability of the optimization technique can only be assessed after some experience with compressor tests.

REFERENCES

1. Garberoglio, J. E., J. O. Song, and W. L. Boudreaux, *Optimization of Compressor Vane and Bleed Settings — User's Manual*, Pratt & Whitney Aircraft, FR-13996, June 1981.
2. Fletcher, R., and C. M. Reeves, "Function Minimization by Conjugate Gradients," *Computer Journal*, Vol. 7, 1964.
3. Powell, M.J.D., "An Efficient Method for Finding the Minding Minimum of a Function of Several Variables Without Calculating Derivatives," *Computer Journal*, Vol. 7, pp. 155-162, 1964.
4. Brent, R. P., *Algorithms for Minimizing Without Derivatives*, Prentice-Hall, Inc., Englewood Cliffs, N. J., 1973.
5. Hooke, R., and T. A. Jeeves, "Direct Search Solution of Numerical and Statistical Problems," *Journal of the Association of Computing Machines*, Vol. 8, pp. 212-229, 1961.
6. Rosenbrock, H. H., "An Automatic Method for Finding the Greatest or Least Value of a Function," *Computer Journal*, Vol. 3, pp. 175-184, 1960.
7. Dahlquist, G., and A. Bjorck, *Numerical Methods*, p. 443, Prentice-Hall, Inc., Englewood Cliffs, N. J.
8. Zoutendijk, G., *Method of Feasible Direction*, Elsevier Publishing Company, Amsterdam, 1960.
9. Vanderplaats, G. N., *CONMIN-A FORTRAN Program for Constrained Function Minimization; User's Manual*, NASA TMX-62, 282, August 1973.
10. Aird, T. J., "Systematic Search in Higher Dimensional Sets," *SIAM Journal of Numerical Analysis*, Vol 14, pp. 296-312, 1977.
11. Box, G.P.E., and K. B. Wilson, "On the Experimental Attainment of Optimum Conditions," *Journal of Royal Statistical Society*, B13, p.1, 1951.
12. Myers, R. H., *Response Surface Methodology*, Allyn & Bacon, London, 1971.
13. Vanderplaats, G. N., and F. Moses, "Structural Optimization by Methods of Feasible Directions," *Journal of Computers and Structures*, Vol 3, Pergamon Press, July 1973.
14. Vanderplaats, G. N., *COPES — A FORTRAN Control Program for Engineering Synthesis*.
15. Vanderplaats, G. N., *Approximate Concepts for Numerical Airfoil Optimization*, NASA Technical Paper 1370, March 1979.

**DAT
FILM**